

11715



1995 -04- 18

# ANNALES

UNIVERSITATIS SCIENTIARUM  
BUDAPESTINENSIS  
DE ROLANDO EÖTVÖS  
NOMINATAE

SECTIO GEOPHYSICA ET METEOROLOGICA

TOMUS X.

BUDAPEST  
1994

P 90056-57/95



# ANNALES

UNIVERSITATIS SCIENTIARUM  
BUDAPESTINENSIS  
DE ROLANDO EÖTVÖS  
NOMINATAE

SECTIO GEOPHYSICA ET METEOROLOGICA

REDIGIT  
L. STEGENA

TOMUS X.  
1994

REDIGIT  
F. RÁKÓCZI

BUDAPEST  
1994

**ISSN 0237 2738**

**Készült az ELTE Sokszorosítóüzemében  
300 példányban**

**Felelős kiadó: Dr. Kiss Ádám**

**Felelős vezető: Arató Tamás**

**ELTE 94150**



## PROFESSOR G. BARTA

### 1915–1992

Professor György Barta, ordinary member of the Hungarian Academy of Sciences died on 21st of October, 1992 in Budapest, at the age of 77. His numerous contributions to Geophysics and to Earth Science, in general, as well as his organizational work and leading role in several international scientific bodies made him one of the internationally esteemed representatives of Hungarian science.

Professor Barta was born in Poprad (Slovakia) in 1915. After the First World War his family had to come to Hungary and he attended the University of Science in Budapest from 1934 to 1939. He studied to become a high school teacher in mathematics and physics.

In 1939 he joined the Hungarian Institute of Meteorology and Geomagnetism and worked from 1940 till 1945 in the Ógyalla Observatory of this Institute. In the academic year of 1941/42 he visited geomagnetic observatories in Germany and Denmark. He obtained his Ph. D. (summa cum laude) in Geography, Physics and Mathematics from the University of Debrecen in 1947.

Doctor Barta joined the Eötvös Loránd Geophysical Institute in 1947 and organized first the Geomagnetic Observatory in Budakeszi (1946), then the more complex Geophysical Observatory in Tihany (1953–54). He also directed the new detailed geomagnetic surveying of the country and did scientific research. In this very fruitful period of his life he published several papers and wrote two books on the geomagnetic field and its variation in the territory of Hungary.

He obtained his C.Sc. and D.Sc. degrees from the Hungarian Academy of Sciences in 1952 and 1956, respectively. He delivered lectures at various Hungarian Universities and in 1963 he was appointed a honorary professor of the Eötvös Loránd University.

Professor Barta's most outstanding contributions concern the magnetic and gravity field of the Earth. He pointed out that the secular change of the magnetic field contain a component with a period of about 50 years, emphasised and explained the asymmetric nature of the geomagnetic field and called attention to possible connections with the gravity field and the internal structure of the Earth. Later he postulated a global secular change of the gravity field and that of the geoid. In the 1955s he outlined the physical background of the figure of the Earth. Later on he dealt with the determination of the gravitational constant and tried to find new ways to improve the accuracy of the Eötvös' experiment. He published over 140 papers in various Hungarian and International periodicals, including such prominent journals as the *Zeitschrift für Geophysik*, *Boll. di Geofisica Teorica ed Applicata*, *Gerlands Beitrage zur Geophysik* and *Nature*.

Professor Barta delivered numerous lectures on his theory and his investigations at several Universities and scientific conferences: Prague, Warsaw, Moscow, Kiev, Vienna, Paris, Berlin, Florence, Genova, Barcelona, Uppsala, Seattle to mention but a few.

The Hungarian Academy of Sciences elected him a corresponding member in 1970 and in 1982 he became an ordinary member. Professor Barta was also elected a member of the International Academy of Astronautics (Paris). In 1971 he joined the Loránd Eötvös University and till 1985 he was the Head of the Geophysics Department. From that time till his death he worked as a scientific adviser of the research group of the department, mainly dealing with the Eötvös's experiment.

Professor Barta held leading posts in several Hungarian and International scientific organization, committees and councils. Some of his most important assignments include the seven-member Presidential Board of COSPAR (1971–1975) the chairmanship of working group six of the International Geodynamics Project (1971–1980) and the membership of the IAG Special Study Group No.4.21. He also served as chairman of the Geophysical Committee of the Hungarian Academy of Sciences, Chairman of the Hungarian COSPAR committee, vice-chairman of the Hungarian KAPG committee and several others. He was on the editorial boards of several scientific journals including the *Acta Geodaetica*, *Geophysica et Montanistica* and the *Geophysical Transaction*. Professor Barta played an active role in founding the Hungarian Geophysical Society and in 1966 he became an Honorary Member of the society.

In 1973 Professor Barta was awarded the State Prize, one of the highest distinctions in Hungary. In addition he was also given the Eötvös medal in 1966 by the Hungarian Geophysical Society, the Konkoly-Thege medal in 1973 by the Hungarian Meteorological Society, the Gauss and Humboldt medals in 1977 and in 1984, respectively, both by the Scientific Academy of the GDR, the Eötvös Loránd memorial medal in 1986 by the Eötvös Loránd University and the Einstein medal in 1990 by the International Academy Foundation (USA).

By his death we lost an outstanding scientist, a respected teacher and a warm-hearted colleague. His death is grieved by both the Hungarian as well as the International geophysical community. The results of his work and research such as the observations, the national geomagnetic surveys, his remarkable hypotheses about the structure of the gravity and magnetic fields of the Earth will long be remembered.

**Attila Meskó**





# A SUBJECTIVE MACROCIRCULATION CLASSIFICATION FOR THE WESTERN REGION OF THE UNITED STATES

JUDIT BARTHOLY and LUCIEN DUCKSTEIN

Department of Meteorology, Eötvös University H-1083 Budapest, Ludovika tér 2.  
Hungary

System and Industrial Engineering Department, University of Arizona,  
Tucson, USA

**Abstract.** In order to establish a stochastic linkage between types of daily macrosynoptic circulation patterns (MCP) and local or regional hydrologic parameters, a subjective or manual classification of MCP types is constructed. The case of Arizona (USA) is used to illustrate the methodology. A 35 point grid of daily pressure observations over the western USA for the 40-year period starting in 1949 is used in conjunction with precipitation and temperature data at 10 Arizona stations and further the daily output of the Global Circulation Model of the US National Center for Atmospheric Research. Four seasons of equal length are distinguished starting with winter from January to March. MCP's are developed for each season using the so-called anomaly field taken here as the normalized deviation pressure field. Relative frequencies of positive and negative anomaly centers are defined, leading to division of the entire area into three seasonally varying subareas, hence  $2^3 = 8$  types of MCP's (but actually this number is varying in each season between 6 and 8). The "turning points" of the circulation systems (cyclones, anticyclones) are then determined in time and space and with the seasonal pattern are defined. Next, each day of the 40 year historical, and the 10-10 year simulated record, the MCP is classified as one of the 8 types of patterns; the specifically pattern type that is the closest (in Euclidean distance sense) to the daily MCP is selected. The MCP time series (the historical and the two simulated) thus obtained is to be used for calibrating and validating the stochastic linkage with hydrologic time series, and then to investigate the effect of the climate change on extreme phenomena.

## Introduction

The general objective of this research is to develop and analyze the theoretical background of the impact of climate change on local or regional water resources and hydrological systems, such as lakes, rivers or drainage basins. The specific case of Arizona (USA) is used to illustrate the methodology. In order to evaluate local effects of various scenarios (for example  $\text{CO}_2$  - doubling) on hydroclimate, we are linking the daily macro scale circulation events to local or regional variables and parameters. For this specific reason we have studied the seasonality of the meteorological parameters for a regional network and identified macrocirculation types for each

season. This investigation involves two steps: first to identify reasonable seasons based on the yearly general circulation cycle of the region and also based on the precipitation and temperature phases for southern USA, in particular Arizona; second to identify the daily atmospheric macrosynoptic types for each season on the basis of the 500 hPa pressure height fields for the western USA.

The data base includes four time series of different climate parameters: 1–2./: a local network of daily precipitation and temperature data for 10 observation stations in Arizona; 3–4./: the 500 hPa observed pressure height data and General Circulation Model (GCM) output data for the northern hemisphere, which have been obtained from the National Center for Atmospheric Research (Boulder, Colorado).

The field analysis is based on daily values at 35 points on a diamond grid covering the western region of the USA. We have used for all observed parameters the daily data of the 40-year period between 1949 and 1989, and a simulated 10-year period of GCM output (for normal and doubled  $\text{CO}_2$  level). To give a reasonable good coverage of Arizona's unique climate (Sellers-Hill 1973) we are distinguishing four seasons of equal length starting with Winter: January, February, March. For each season we identify the main circulation action centers, their spatial distribution and relative frequencies. On the basis of these seasonal statistics, we divide the area into three subregions and select out the so-called "turning points" of the atmosphere, which are defined as the local maximas or minimas (in areal averages) of the 500 hPa height deviation time series (so called anomaly fields). After this selection further analysis and smoothing makes it possible to define the main seasonal macrocirculation pattern covering the western part of the USA. Theoretically eight patterns are obtained for each season, which reflect the more representative and characteristic condition of the atmosphere for each given season, and the typical geographical features of the region. (In the practice not in all season we found eight circulation type, as we will see below.)

Using those circulation patterns, we classify every daily 500 hPa height field into a characteristic type and create the catalogue of circulation patterns (CP) for the 40-year observed and the 10-year simulated ( $1\times\text{CO}_2$ ,  $2\times\text{CO}_2$ ) period. These catalogues will allow us to compare, possibly on the basis of a single index, the CP type, the observed daily and the simulated ( $2\times\text{CO}_2$ ) conditions of the atmospheric circulation (using the  $1\times\text{CO}_2$  catalogue for system calibration). On the basis of the three catalogues and using the daily average height of the 500 hPa field we will carry out our further investigations on the effect of climate changes on local hydrological parameters in Arizona.

After presenting the climatological and hydrometeorological background of the analysis, we describe the climatological data base of precipitation and temperature for Arizona, and the 500 hPa height field data base for the western US. We also pro-



vide an analysis of the precipitation and temperature data that is performed to identify the seasons. Later on we describe the process of identifying the 500 hPa height macrosynoptic types, discussing the way in which this data base will be used to investigate the impact of CO<sub>2</sub>-induced climate change on hydrological systems in Arizona.

## **Climatological and hydrometeorological basis of the analysis**

With very high probability future global climate changes will produce some changes of the atmospheric circulation processes. It means if we would like to predict the regional/local changes of some meteorological parameters in case of altering atmospheric circumstances, we should investigate first the expected changes of the circulation processes (Lamb 1972/a).

Well known that the atmospheric circulation varying in one respect on seasonal scale (yearly cycle), and on the other hand on some not regular scale occasionally (climate variability – and climate changes). As it happened for example in the 1950s and 1960s when an expansion and intensification of the Arctic high-pressure regime were observed (Lamb 1972/a), or in the middle of the 20th century when an exceptional predominance of the westerly winds in middle latitudes was found (Lamb 1972/a). A generally used method to follow the quasi-stationary circulation processes of the atmosphere in the medium and long wave frequency domain is to observe hemispherical and regional height pressure fields and define the so called "macrocirculation patterns" (MCP's). Define the MCP's for a larger region means: mapping the structure and location of the characteristic circulation phenomena over the geographical region (cyclones, anticyclones, ridges etc.). This pattern classification also could reveal climatic processes affecting the heat and moisture exchanges and transport. That is the main reason, why they can play so important roles in the downscaling processes of the climate variations and changes. Several methods (but mainly two big group of them) are available to get those patterns: a./ subjective (manual) approach: observation based selections [for example for the northern hemisphere Wangenheimer (1964), Dzerdzeevski (1968) and for the Atlantic European region Hess-Brezowsky (1952), Lamb (1972/b) gave MCP systems]; b./ objective (computation based) approach: cluster-, EOF (empirical orthogonal function) and teleconnection analysis (Namias 1981, Ambrózy et al. 1984, Richman 1985).

It is impossible and also useless to try to compare in general sense which method is better than the others, they all have advantages and disadvantages. Comparison between the different methods is just reasonable for a specific case study, when it is possible to introduce (define) quantities which will give the objective basis for the valuation of the results.

The purpose of this specific study is to obtain a reasonable good estimate for

macrosynoptical types, which will be used in the project on: Climate Change Effects on Regional and Local Hydrological Parameters with special emphasis on extremes. We intend to use in this project two methods to produce and evaluate a set of circulation patterns of types as representative as possible of the conditions in the western region of United States. The first, a subjective classification which is discussed in this study, gives valuable results in itself and also provides a foundation for the second one, in which we will use a combined objective or automated method, consisting of an empirical orthogonal function analysis with k-mean clustering technique (Richman 1985 and Bartholy 1989). To implement the second classification method k-mean clustering requires a good estimation of the cluster numbers and centers (Anderberg 1973), whose estimation will be also a result of the subjective classification constructed herein. The second purpose of this work is to identify macrocirculation types for the given area and for each day during a historical 40 year and the simulated 10 years (with double CO<sub>2</sub> level). This study involves two steps: 1./ to identify reasonable seasons based on precipitation and temperature data for Arizona; 2./ to identify the daily atmospheric macrosynoptic types for each season based on 500 hPa fields for the western USA.

### **Data base, seasonality**

The data base includes three time series of different climate parameters for the western part of US and Arizona. Since the primary task for this subjective classification is to forecast the behaviour of some hydrological parameters under climate change for Arizona. A local network including such daily precipitation and temperature data have been selected. Analyzing these data allows us to determine the seasonality of this unique climate.

#### ***a./ The 500 hPa height data:***

This observed (historical) and simulated (Global Circulation Model output) data base for the whole northern hemisphere are available from the National Center for Atmospheric Research (NCAR) in Boulder, Colorado. The field analysis of the historical data is based on daily values (12 a.m.) and we separated a net with 35 points on a diamond grid covering the western region of the US (Fig. 1.). We use the historical data base covering the 40 year period between 1949 and 1989, and the simulated (normal and doubled carbon-dioxid level) data series for a ten years period. First we define the seasonal macrosynoptical patterns on the base of the historical data series, and then we produce the daily catalog for all the three AT 500 database.



*b./ Precipitation and temperature, seasonality*

About 300 Arizona precipitation station are available for the analysis. Our goal is to choose a good representative set of 10 stations, which fulfill the following criteria: 1./ to provide broad geographical coverage and a faithful representation of the historical climate regions (Fig. 2 – source: Baker-McCleneghan 1966); 2./ to contain long time series of data without significant gaps; 3./ to have data available on other hydrological parameters for later research. The 10 stations selected are given in Table 1. and Fig. 2, in which we have computed the necessary climatological statis-

Table 1. List of ten Arizona observation stations

Numb.	Station	Latitude	Longitude	Elevation (ft)	Data reliability
1.	AGUILA	33° 57'	113° 11'	2170	93 %
2.	BETATAKIN	36° 41'	110° 32'	7290	97 %
3.	CLIFTON	33° 03'	109° 17'	3460	98 %
4.	FORT VALLEY	35° 16'	111° 44'	7350	99 %
5.	GRAND CANYON	36° 03'	112° 08'	6890	92 %
6.	KINGMAN	35° 11'	114° 03'	3360	95 %
7.	NOGALES	31° 21'	110° 55'	3810	97 %
8.	ROOSEVELT	33° 40'	111° 09'	2210	98 %
9.	TUCSON	32° 15'	110° 57'	2440	99 %
10.	YUMA	32° 37'	114° 39'	190	98 %

tics. On the basis of those quantities and a literature review, which primarily deals with the climate of Arizona from several points of view (temperature: Baker-McCleneghan 1966, Baldwin 1973, Green 1962; precipitation: Brysons-Lowry 1955, Hales 1974, Hirschboeck 1989, Roe-Vederman 1952, Sellers 1960; suggested seasonality: Bryson-Lowry 1955, Byers 1959, Hastings-Turner 1965) four seasons are distinguished, as follows:

- Winter: January, February, March
- Spring: April, May, June
- Summer: July, August, September
- Autumn: October, November, December

In Figs 3. and 4. we present for the 10 Arizona station the annual variations of the monthly average precipitation and the monthly average temperature. The figures verifies that seasonal choices are consistent with the climatological data and also reflect the broad variation between regions within the state.

**The structure of the subjective classification**

We separate the 500 hPa height series into four seasons, to develop the macrocirculation patterns for each season. The steps to create the seasonal macrosynoptical systems are as follows:

- 1./ The daily height fields are transformed into anomalies by subtracting the monthly averages, to make the identification of the circulation action centers easier.
- 2./ We determine for each season the spatial distribution and relative frequencies of the positive and negative anomaly centers. In Figs 5a and 5b we have the relative frequencies of the positive (+) and negative (-) anomaly centers for the winter season.
- 3./ From the maps of seasonal action centers it seems reasonable to divide the entire region into three areas (Fig. 6.). These areas show some variability from season to season which reflects the annual climatological variations within the region.
- 4./ To choose the most representative macrocirculation patterns for this region and for each season, we seek to determine the so called "turning points" of the atmospheric processes is defined as a local maximum or minimum in the areal average of the height anomaly time series. For this reason we produced the seasonal daily time series of 500 hPa average anomalies for the three areas, covering the 40 year period (1949–1989) of data.

Since each of these areas can be either positive or negative, there are 8 possible combination, based on the signs of the average anomalies for the areas. Choosing the maximum and minimum values from the area average anomaly time series, we determine the more representative and characteristic turning points of the atmospheric circulation.

In order to eliminate the extreme atmospheric states, we choose 10 case for each of the eight possible combinations, and take the average of these. These 500 hPa fields are the seasonal macrocirculation patterns (MCPs) – theoretically 8 patterns for each season (Fig. 7a and 7b).

5. Using the basic circulation patterns for each seasons we examine the observation record for the 40 year period of daily 500 hPa time series: each day is taken individually and then classified. Each day is labelled by a number between 1 and 8, corresponding to the nearest MCP, using the Euclidean distance between the MCPs and the daily 500 hPa fields.

## Acknowledgements

This research was supported in part by grants from the US National Science Foundation (BCS – 9016462/906556, EAR – 9217818/9205707 and INT 91 – 19295), NIGEC, the Hungarian Academy of Sciences (MTA), and the Hungarian National Science Research Foundation (OTKA/ T 4196). We thank Barbara Merrill and Bijaya Shrestha (University of Arizona), for their help to get and access the Arizona database and correct the manuscript.

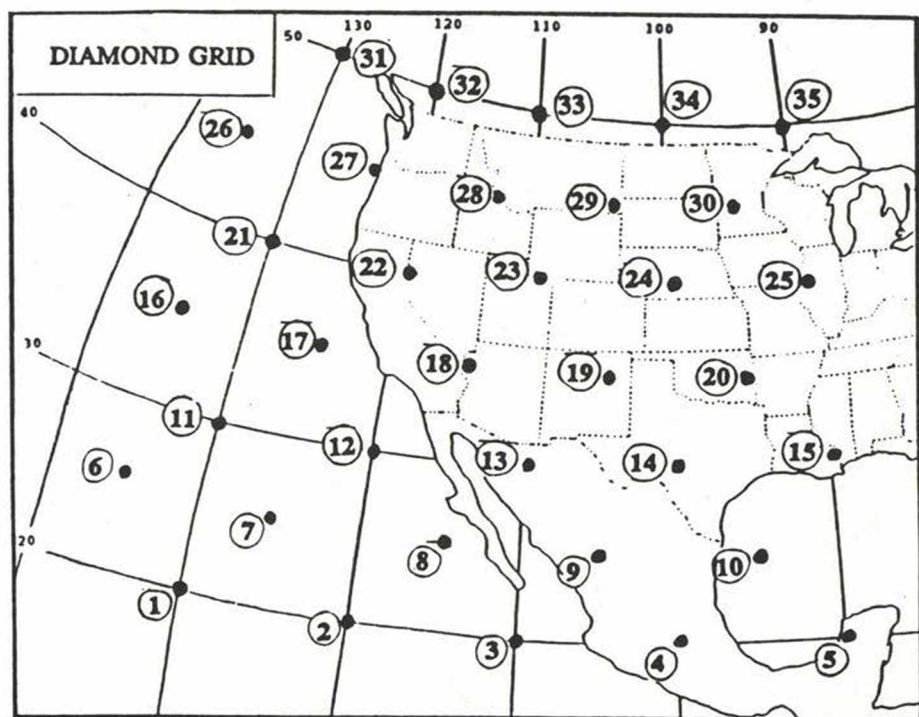


Fig. 1. Diamond grid (35 points) used for the representations of the 500 hPa pressure height fields



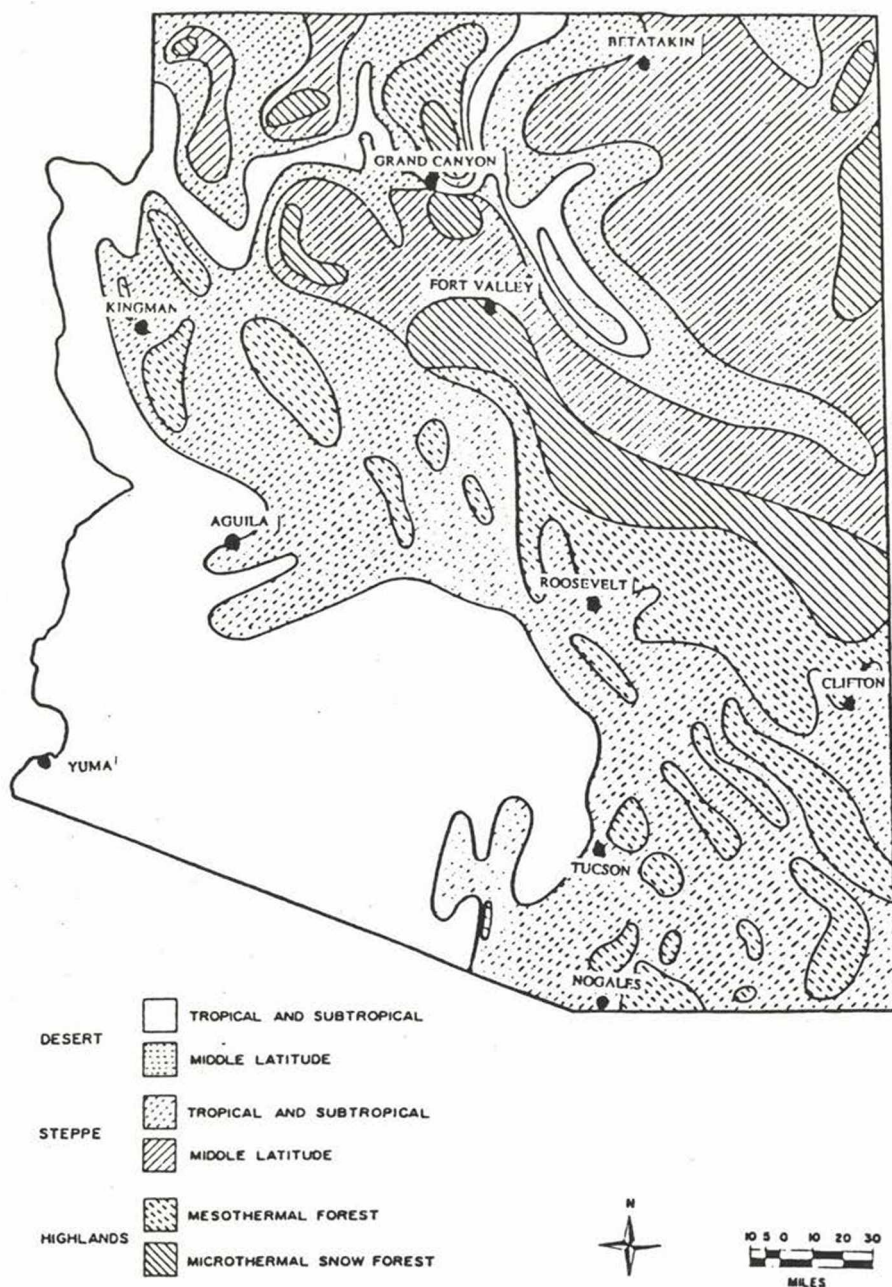


Fig. 2. Historical climate regions of Arizona, showing the 10 observation stations

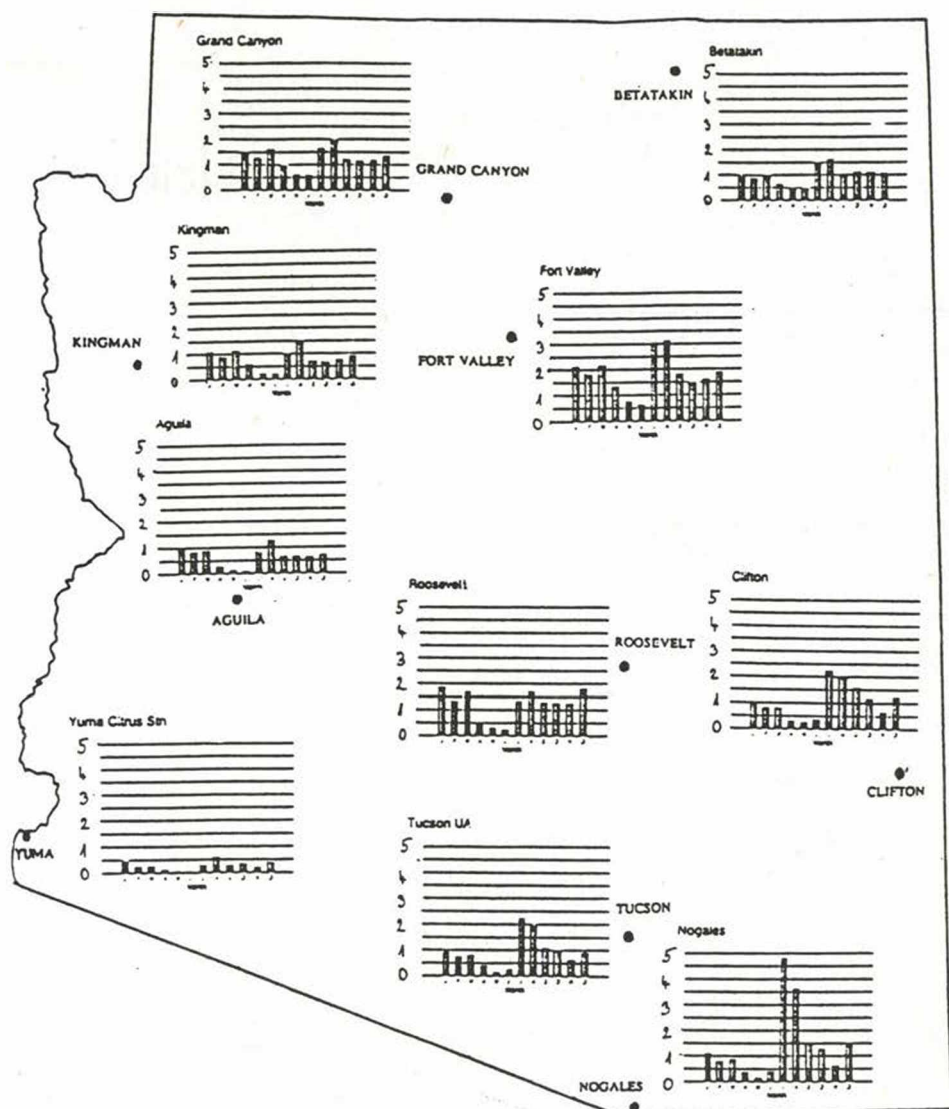


Fig. 3. Annual variation of the monthly average precipitation in Arizona (10 observation stations). Precipitations in 100 mm

Source: Atmospheric Physics Laboratory, U et A, Stephen Bahre

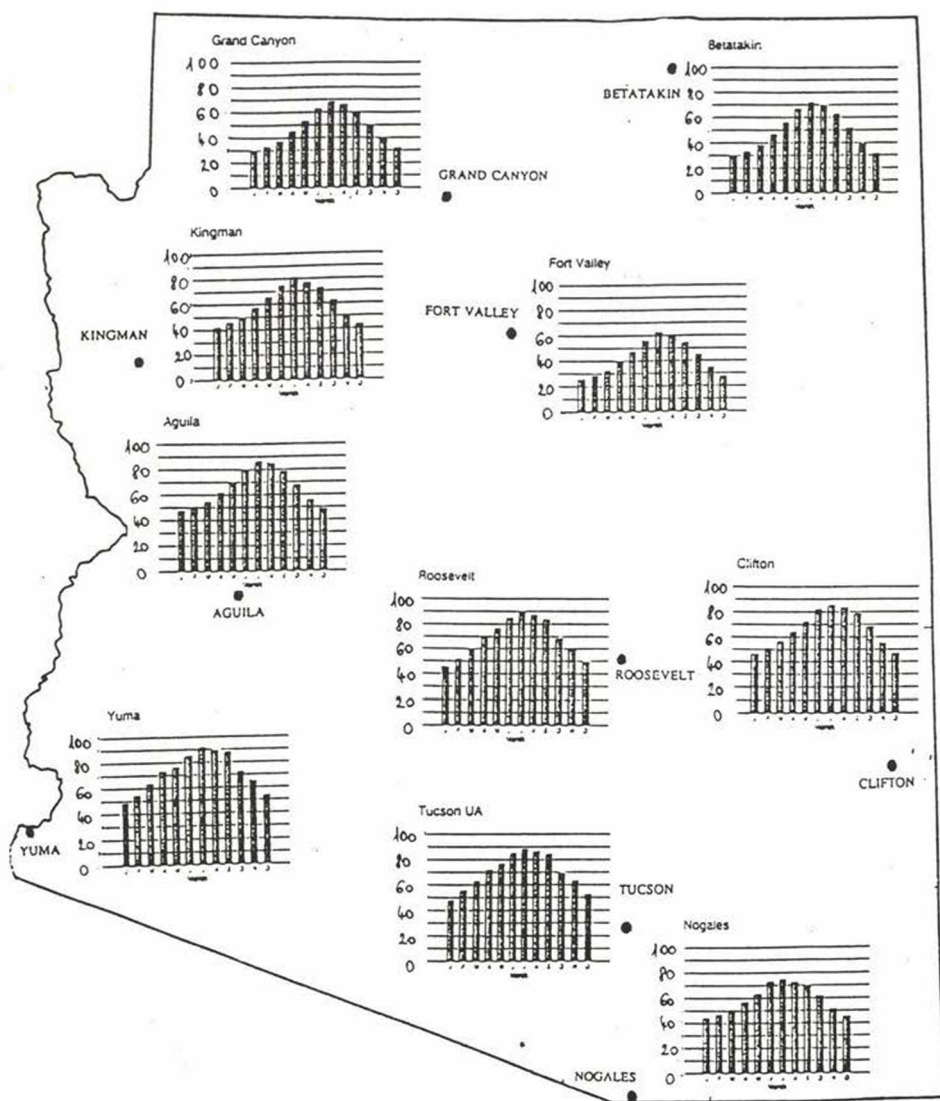


Fig. 4. Annual variation of the monthly average temperature in Arizona (10 observation stations). Temperature in °F

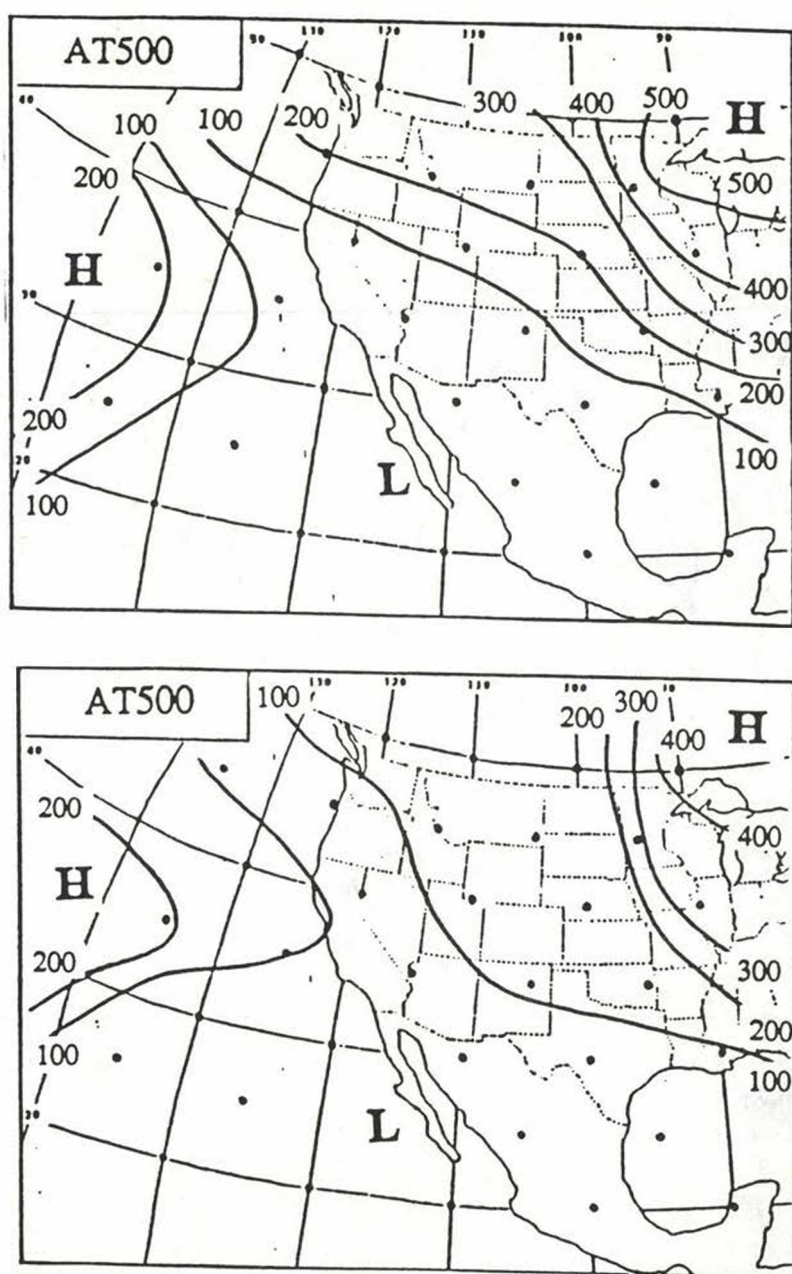


Fig. 5. Frequency contours of the positive (above) and negative (below) anomaly centers for the winter season



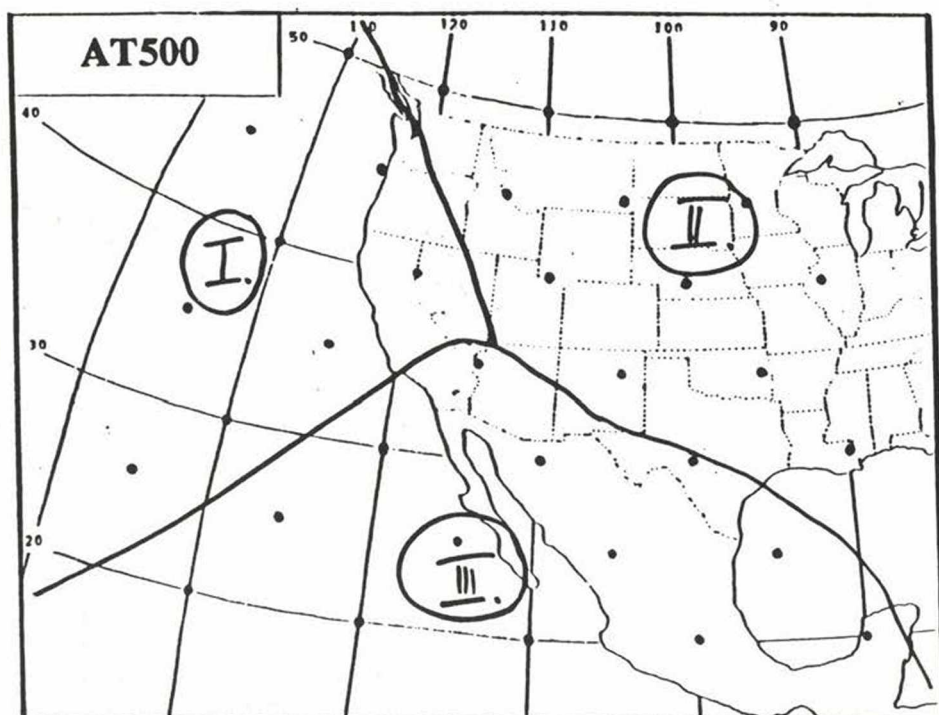


Fig. 6. The three subregions for the winter season



## DIAMOND GRID AT500

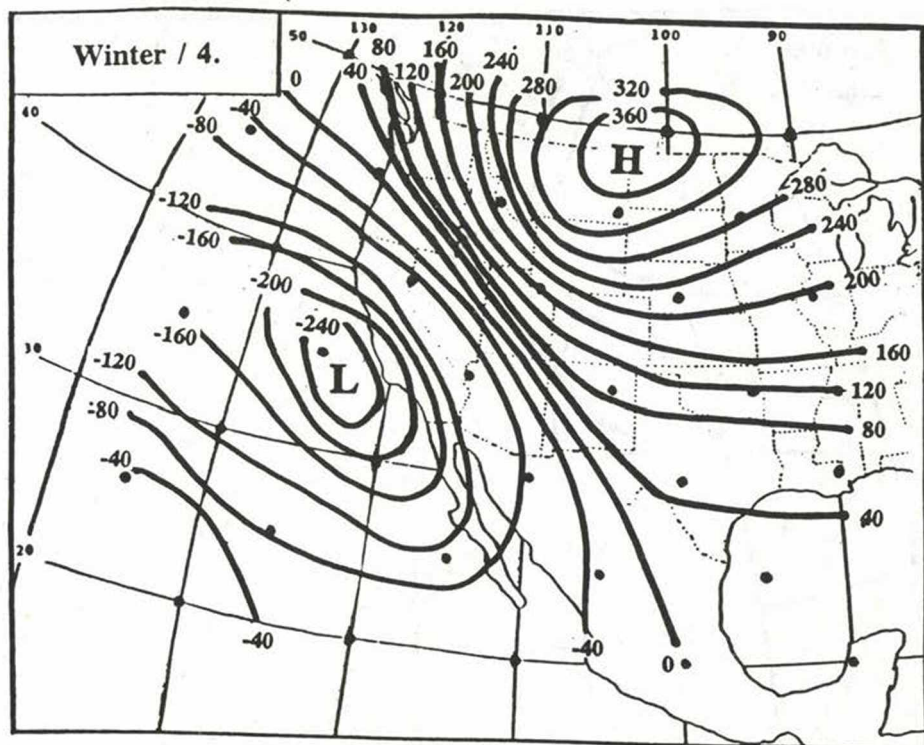


Fig. 7/a. The 4th macrocirculation pattern for the winter season

The numbers on the contour lines represent the anomaly (deviation from the seasonal mean) values in [gpm] units

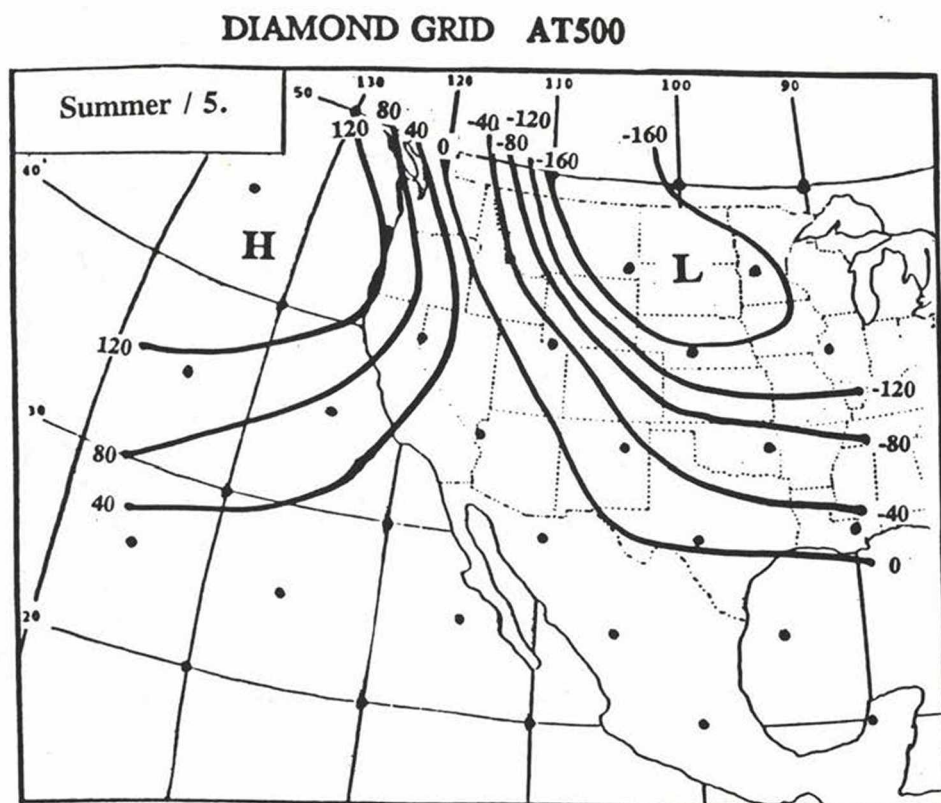


Fig. 7/b. The 5th macrocirculation pattern for the summer season

The numbers on the contour lines represent the anomaly (deviation from the seasonal mean) values in [gpm] units

## References

- Ambrózy P., Bartholy J., Gulyás O. 1984; A system of seasonal macrocirculation patterns for the Atlantic-European region. *Időjárás* 88, 3, 121—133
- Anderberg M. R. 1973; *Cluster Analysis of Applications*. Academic Press, London, p.237
- Baker S., McCleneghan T. J. 1966; an Arizona Economic and Historic Atlas. The Division of Economic and Buisness Research and The Department of geography and Area Development. The University of Arizona, Tucson, p. 41
- Baldwin J. L. 1973; *Climates of the United States*. U.S. Department of Commerce, National Oceanic and Atmospheric Administration, p. 113
- Bartholy J. 1989; Determination of Seasonal Macro Synoptical types Using Cluster Analysis and Rotated EOF Analysis. *Acta Climatologica*, XXI-XXIII, 1-4, 23-33
- Bryson R.A., Lowry W. P. 1955; Synoptic Climatology of the Arizona Summer Precipitation Singularity. *Bulletin American Society*, 36, 7, 329-339
- Byers H. R. 1959; *Physics of Winter in the Desert*. The Rossby Memorial Volume, 400-412
- Dziedziewicz B. L. 1986; Circulation Mechanism in the Atmosphere of the Northern Hemisphere in the 20th Century. (In Russian.) Moscow, Akad.Nauk., Inst. Georg.
- Green C. R. 1962; Probabilities of Temperature Occurrence in Arizona and New Mexico. The Institute of Atmospheric Science, University of Arizona, Tucson
- Hales J. E. Jr., 1974; Southwestern United States Summer Monsoon Source – Gulf of Mexico or Pacific Ocean? *Journal of Applied Meteorology*, 13, 3, 331-342
- Hastings J. R., Turner R. M. 1965; Seasonal Precipitation Regimes in Baja California, Mexico. *Geografiska Annaler*, 7, 204-223
- Hess P., Brezowsky H. 1952; *Katalog der Grosswetterlagen Europas*, Berichte des dt. Wetterdienst, US Zone, 33 Bad Kissingen
- Hirschboeck K.K. 1989; Hydrology of Floods and Droughts: Climate and Floods (from the volume of National Water Summary 1988-89: Hydrologic Perspectives on Water Issues 67-88).
- Lamb H. H. 1972/a; *Climate: Present, Past and Future*. Vol. 1., Methuen & Co Ltd., London, p. 613
- Lamb H. H. 1972/b; *British Isles Weather Types*. Geophys. Mem., 116. London (Met. Office) Meteorology Department, 1943, *Synoptic Weather Types of North America*, California Institute of Technology, Pasadena, p. 161
- Namias J. 1981; Teleconnections of 700 mb height anomalies for the Northern Hemisphere *Calcofi Atlas* No. 29

- Richman B. M. 1985; Rotation of Principal Components (Review paper), Illinois State Water Survey, Climate and Met. Sec. p. 73
- Roe C., Vederman J. 1952; September Rains in the Southwestern United States. *Monthly Weather Review*, 156–160
- Sellers W. D., Hill R. H. 1973; Arizona Climate 1931–1972. University of Arizona, Tucson, 1–28
- Sellers W. D. 1960; Precipitation Trends in Arizona and Western New Mexico. Institute of Atmospheric Science, University of Arizona, Tucson, 81–94
- Wangengejm G. J. 1964; Catalogue of Macroscopic Processes, According to the Classification of Wangengejm, 1891–1962 (ed. by M. S. Bolotinskaya and L. J. Ryzakov). (In Russian), Leningrad, *Arkt. i Antarkt. Nauk. Issled. Inst.*



# PRECIPITATION VARIABILITY AND CHANGES IN HUNGARY PAST AND FUTURE

JUDIT BARTHOLY and ISTVÁN MATYASOVSKY

Department of Meteorology, Eötvös University, Budapest, Ludovika tér 2. Hungary

ISTVÁN BOGÁRDI

Department of Civil Engineering, University of Nebraska-Lincoln,  
Lincoln, Nebraska, USA

**Abstract.** Precipitation averages and extremes are examined using two station networks: one for Hungary (162 stations, 1901–1990 time period, monthly data) and one for the region of the Lake Balaton (28 stations, 1951–1990 time period, daily data). The Hess–Brezowsky (1969) macrocirculation types were examined for the period 1881–1990, in order to detect whether a significant change in the circulation structure of the Atlantic-European region has occurred. Also we analyzed the probability of Hess–Brezowsky macrocirculation types and the occurrence of precipitation (areal averages, individual stations) associated to these types. Small altering was found on the Atlantic European region: some anticyclonic types have less, while some cyclonic ones have higher probability of occurring nowadays, than they had in earlier decades of this century. Changes in the statistical properties of circulation types are analyzed for the last century and an estimation in case of doubling of atmospheric  $\text{CO}_2$  concentration is given.

A method is suggested and applied to estimate the space-time distribution of daily precipitation under climate change for the western part of Hungary. The estimation technique is based on the analysis of semi-Markovian properties of atmospheric macrocirculation pattern (MCP) types, and a stochastic linkage between daily macrocirculation types and daily precipitation events. Historical data and General Circulation Model (GCM) outputs of daily MCP corresponding to  $1\times\text{CO}_2$  and  $2\times\text{CO}_2$  are considered. Under the temperate continental climate of western Hungary a moderate variable spatial response to climate change has been obtained. The local average precipitation reflects mostly, under  $2\times\text{CO}_2$  a somewhat dryer precipitation regime in western Hungary.

## Introduction

The purpose of this study includes: 1./ to give an overview and show some statistical results on the circulation patterns and precipitation relationships and changes over a subregion (western Hungary); and 2./ to develop a stochastic space-time model to estimate the effects of climate change scenarios on regional/local precipitation. The method is applied to the temperate continental climate of western Hungary, in particular the region of Lake Balaton and its drainage basin.

The magnitude and consequences of regional response to anticipated climatic changes are uncertain. Sustained regional droughts, excessive floods, multiyear shortage of water in reservoirs, excessive water levels in natural lakes, and other hydrological events pose considerable economic and social concerns. A typical question to be answered is: can time series of hydrological events be conditioned on future climate change scenarios and, if so, how can this conditional event-estimation process be implemented?

The proposed approach is an extension of the usual analysis of regional hydrological impact of climate change. Often, the quite uncertain hydrological output of atmospheric general circulation models (GCMs) are segregated to estimate regional hydrological events. This study proposes to examine a time series of daily GCM-produced atmospheric macrocirculation patterns (MCPs) to estimate regional and local precipitation. The approach is based on a classification of daily MCPs of the Atlantic European region, where the patterns are mainly defined using the 700 hPa geopotential pressure field. The classified types consist of a reduced version of the Hess-Brezowsky (1969) macrosynoptic system (HBms), which is based on the motions of air masses and the average location of the circulation phenomena (as cyclones, anticyclones). The analysis was done using this classification system and trend forecast was made for the territory of the Lake Balaton and for its drainage basin.

After a short discussion on the Atlantic European circulation fluctuations and the Hungarian precipitation variability of this century the space-time precipitation model will be described. Then, daily MCP classification will be analyzed statistically, first for historical, and then for GCM-produced data. Next, the height of the 700 hPa pressure field will be introduced as an additional variable influencing daily precipitation within each MCP type. The  $1\times\text{CO}_2$  and  $2\times\text{CO}_2$  scenarios have resulted in similar MCP types and frequencies but, as expected, in different average pressure heights. This fact will be utilized to estimate the regional/local effect of climate change.

## Past

We carried out a trend analysis with linear and quadratic approaches on the precipitation data set, for the individual stations and areal averages for Hungary (162 precipitation stations, 1901–1990 period). We couldn't find any real significant changes in the precipitation amounts on monthly and yearly time scales during this period.

We also examined the Hess and Brezowsky (1969) macrocirculation classification and the catalog of the types for the period 1881–1990 (110 years) to find out fluctuations or changes in the circulation patterns in the last century. Fig. 1. shows the fluctuation of the frequencies of the 30 Hess-Brezowsky macrocirculation types (HBms) in the last 110 years [box diagram: vertical axis – absolute frequencies of



the types in decades; horizontal axis – abbreviations of the HB macrocirculation types (more about this circulation system in Hess and Brezowsky (1969)); The boxes show the medians, quartiles, and outliers of the frequency values]. As it can be seen, most of the types are stable, only with slightly fluctuations, but there exist 6 weather types which did change definitely during this period: SWz (6th), NWa (7th), HM (9th), BM (10th), HNa (14th), TrW (29th). Three of them have decreasing, three of them have increasing frequency distributions, see Figs 2 and 3. The circulation patterns with decreasing frequencies are: a./ Northwestern anticyclonic (NWa), b./ Central European high (HM) and c./ North flow with Iceland high, anticyclonic (HNa); each of them has very small precipitation probability (10, 11 and 29% respectively), and if it is raining daily amounts are very low (0.2, 0.2 and 1.1 mm respectively). The circulation patterns with increasing frequencies are a./ Southwest cyclonic (SWz) b./ Central European ridge (BM) and c./ Western European trough; all have much higher chance for rain (25, 32 and 35% respectively), and if it is raining also the amount will be higher (0.6, 1.3 and 1.8 mm). This means that few anticyclonic dry types have smaller, and some cyclonic wet types have higher probability to occur. Could we then predict more precipitation for this area? Definitely not. For example, in this case we could observe even less precipitation amount, if some more frequent types occurrences would change just a slightly bit. We don't have to prove the importance of a precipitation model, which will give us a higher chance to avoid misleading forecast. We will try to follow the processes with a time-space precipitation model in order to be able to give an estimate, a prediction for the next future for this local area (for the drainage basin of Lake Balaton).

### **Future: Precipitation model with space-time approach**

For meteorological application, precipitation is usually modeled as a stochastic process. These point-process models describe precipitation occurrence, amount (Chang et al. 1984, Bogárdi et al. 1988) at selected locations. Spatial characteristics of precipitation are usually analyzed for selected events (Chua and Bras 1982). Space-time models for the spatial and time distribution of precipitation over a region are usually models for single events, are based on some general physical considerations and several stochastic assumptions (Rodríguez-Iturbe and Eagleson 1987). A model for simultaneous multisite generation of daily precipitation was developed in Bárdossy and Plate (1990) will be used.

Univariate autoregressive (AR) processes represent a well developed and commonly used technique to model time series. In our case, the time series of daily precipitation at spatially correlated location, would need to be modeled as a multivariate AR process that is a natural generalization to vector time series.

The main difficulty of modeling the precipitation is its space-time intermittence. The precipitation occurrence at a given location must be conditioned on pre-

precipitation at other locations; then the precipitation amount is conditioned on occurrence and amount at other locations. This approach requires the estimation of many parameters. Another difficulty is that time series models have been developed principally for Gaussian processes but conditional probability distributions of precipitation are far from normality. Therefore, there is a need to develop a transformation that establishes a relationship between precipitation and the normal distribution [(Bárdossy and Plate (1990), Bogárdi et al. (1993) and Matyasovszky et al. (1993)].

The difficulty in using the above mentioned stochastic model is that the process cannot be observed. As a consequence, the correlation matrices must be estimated indirectly from the observed precipitation time series. Specifically, indicator series defined by precipitation quantiles are used to estimate the correlations among the indicator series. Then the required correlations can be calculated from the indicator series correlations. For further details see Bárdossy and Plate (1990) or Matyasovszky et al. (1993).

### **Linkage: Circulation patterns – precipitation**

Daily circulation patterns for the Atlantic-European region are characterized by the daily spatial distribution of sea level pressure (Hess-Brezowsky microcirculation system – 1969) and middle tropospheric pressure height. The regional/local hydrological variables at a given time and location are strongly influenced by atmospheric circulation patterns, hence climatic variability may be related to changes in atmospheric circulation (Lamb 1977).

The task here is to extend the mathematical model described in the previous section by conditioning on daily MCP types. As proposed in Bárdossy and Plate (1992) this can be done by considering each circulation type separately and define the multivariate normal process.

### **Circulation patterns – climate change scenarios**

Three types of daily MCP data are used.

- 1./ Historical data are represented by the National Meteorological Center (NMC) grid point analyses of the height of 700 hPa pressure fields available from the National Center for Atmospheric Research (NCAR). The analysis is based on daily values (12UT) at 51 points on a diamond grid covering the Atlantic European region (Fig. 4.) for the period January 1950 – June 1989.
- 2-3./ Two 10-year long data series for the same pressure level has been obtained from the outputs of the Max Planck Institute corresponding to the  $1\times\text{CO}_2$  and  $2\times\text{CO}_2$  scenarios.

There are several possibilities combined with considerable experience for classifying daily MCPs. A brief review of classification techniques for precipitation model-



ing purpose can be found in Bartholy (1992). In the present work, the three data sets are classified with the above described MCP system. The periods from April to September 30 (Summer half year) and from October to March 31 (Winter half year) have been examined separately. Defining 10–10 types (MCPs) for both periods seem to be a good compromise between the increasing number of types and decreasing distances of pressure fields within types.

One MCP pattern example are given for the winter and summer season, respectively (Fig. 5). Given the set of MCP types, the next step is to develop a stochastic model in order to describe the sequence of these patterns, which is done here by using Markov chains. This Markov model is used to calculate the distribution of MCP type duration as well as to develop simulated time series of space-time local climatological quantities conditioned on MCP types (Bogárdi et al. 1992). Originally, it was intended to use this approach to simulate space-time series of regional/local precipitation reflecting climate change. But the difference between the frequencies of the  $1xCO_2$  and  $2xCO_2$  cases is relatively small as compared to the difference between the frequencies of the  $1xCO_2$  case and historical data. Therefore, we included the spatially averaged 700 hPa pressure height into the analysis; and the annual cycle of the pressure height is considered as an analogy of the difference between present and  $2xCO_2$  climates. The relationship between the two quantities can then be used to estimate the effect of climate change on regional/local precipitation (Matyasovszky et al. 1992).

### Case study for western Hungary

The geographical region to be investigated is located in western Hungary (the drainage basin of the Lake Balaton) and is represented by 28 precipitation stations (Fig. 6, and Table 1). Daily precipitation data at 28 stations in western Hungary between 1950 and 1989 are used. The precipitation model was checked using a split sampling approach, that is, parameters are estimated from the first 20 years of data (model calibration) and the simulated precipitation series is compared to the second 20 years of data (model validation). Regional precipitation climate reflecting  $2xCO_2$  scenario is estimated by the same simulation technique, but using parameters (Fourier coefficients) corresponding to the  $2xCO_2$  case. The winter and summer half years are analyzed separately.

Probability distribution functions estimated from the historical data and simulated data corresponding to the historical and  $2xCO_2$  cases are calculated. Fig. 7 shows examples for two precipitation stations, one from the northern region (station 5) and one from the southern region (station 7), for the summer half year. An important conclusion is that, as expected, the regional response to a global climate change is variable in space.

Fig. 8 summarizes the results of the probability (8/a) and the average amount (8/b) of daily precipitation respectively for the summer season (growing season). The diagrams show that in case of  $2\times\text{CO}_2$  on the whole area the precipitation probability will be lower and the average daily precipitation amount will be definitely less (four station exceptional) than in the last 50 years. In the winter season the area is divided into two parts: subregions with decreasing and increasing precipitation amounts. We can find on the Fig. 9 the spatial distribution of the mean daily precipitation anomalies in case of  $\text{CO}_2$  doubling. The southern part will be slightly more wet, while the other area somewhat dryer than it was recently.

## Summary

A space-time precipitation model has been coupled with stochastic simulation of daily MCPs in order to generate time series of point or areal daily precipitation reflecting regional/ local effect of a global climate change. To this end, in addition to historical data daily large-scale atmospheric pressure output of the GCM model for the  $1\times\text{CO}_2$  and  $2\times\text{CO}_2$  cases has been used. The approach is based on the statistical relationship between daily MCP types and daily precipitation. Classification method of daily MCPs cannot be used alone to measure changing spatial distribution of pressure heights obtained from GCMs and related to climate change. For this reason an additional variable, the average pressure height, is introduced into the analysis. The methodology may be sensitive to choice of GCM.

## Acknowledgements

Research leading to this paper has been supported by grants from U. S. National Science Foundation and the Hungarian Academy of Sciences, INT 91-19295, Nos. BCS- 9016462/9016556, and EAR-9217818/9205717. The additional support of Eastern European Program, the Hungarian Academy of Sciences and OTKA/T 4196 is also acknowledged. We wish to thank András Bárdossy for providing us the 35 years observation NCAR diamond grid dataset of the 700 hPa height fields, the ECHAM-1 General Circulation Model outputs (10 years, daily data) for  $1\times\text{CO}_2$  and  $2\times\text{CO}_2$  runs (700 hPa height), and for the stochastic downscaling of the Hess-Brezowsky MCP's with fuzzy rule.

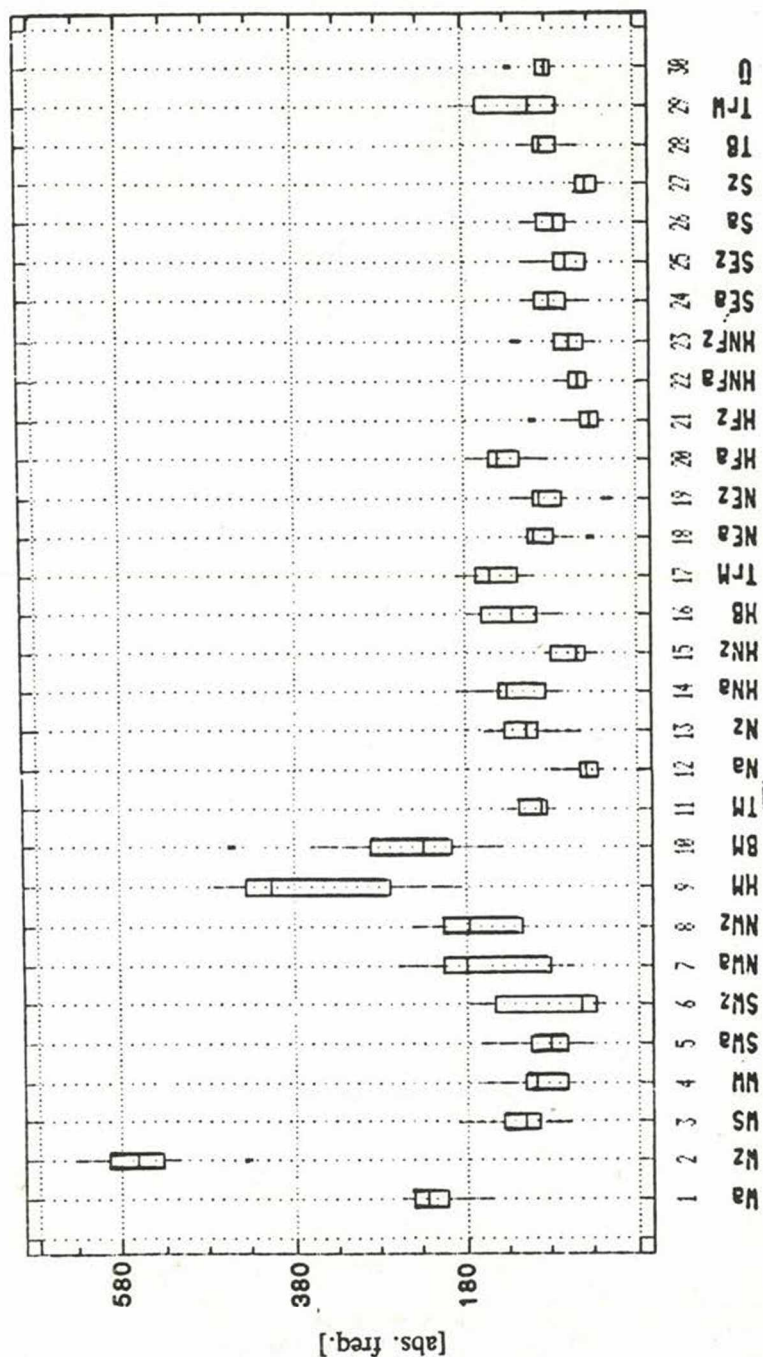


Fig. 1. The frequency fluctuation of Hess-Brezowsky MCP's (box diagram for the decades of the 1881-1990 period)



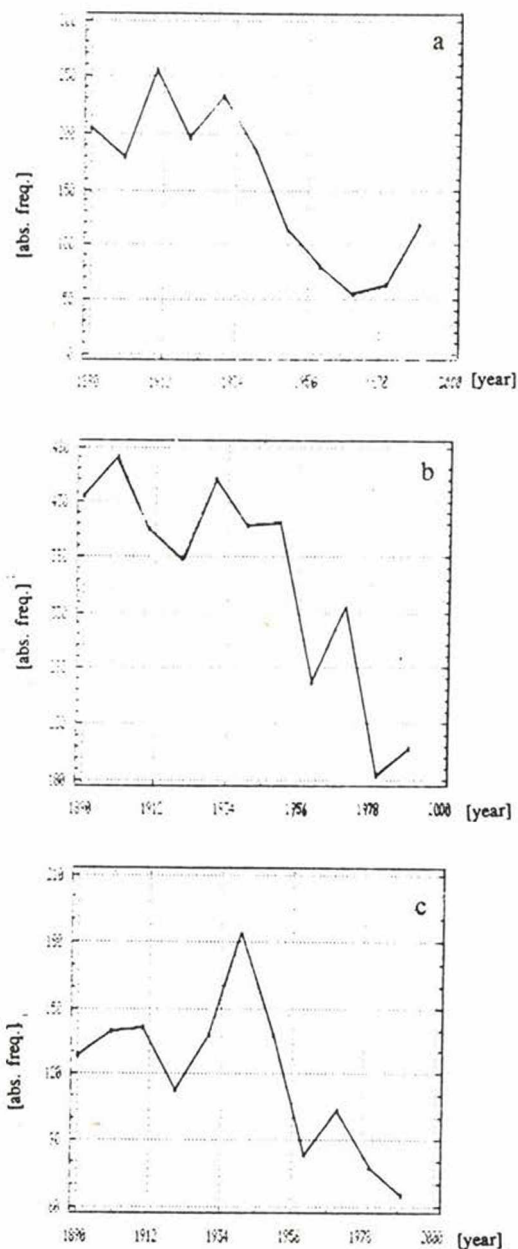


Fig. 2. Decreasing frequencies at the HBms's  
a./ 7th pattern – NWa: Northwest anticyclonic  
b./ 9th pattern – Hm: Central European high  
c./ 14th pattern – HNn North, Iceland high, anticyclonic

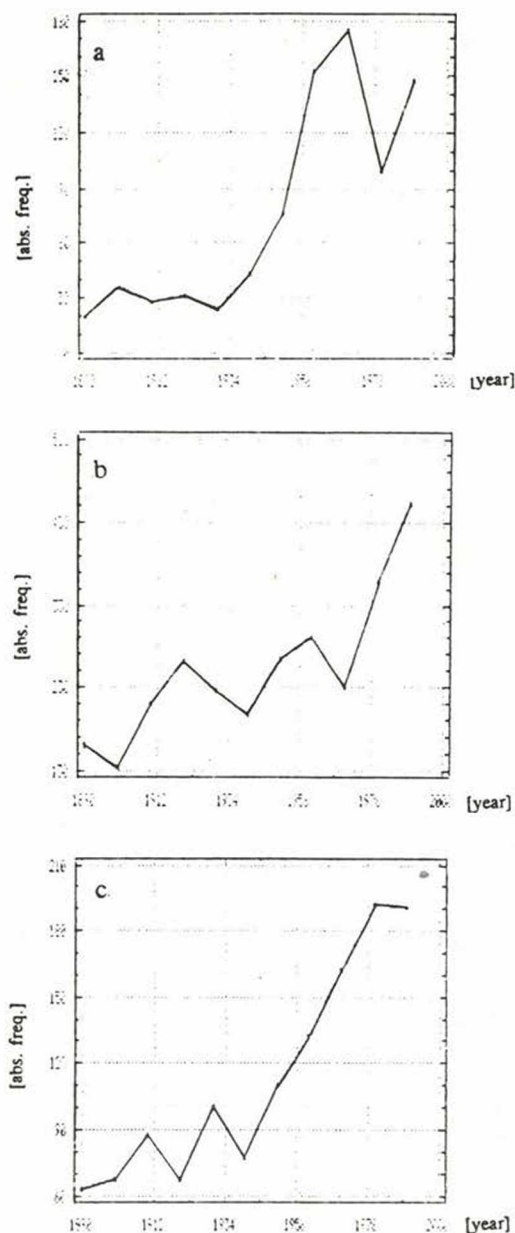


Fig. 3. Increasing frequencies at the HBms's  
a./ 6th pattern – SWz: Southwest cyclonic  
b./ 10th pattern – BM: Central European ridge  
C./ 29th pattern – TrW Western European trough

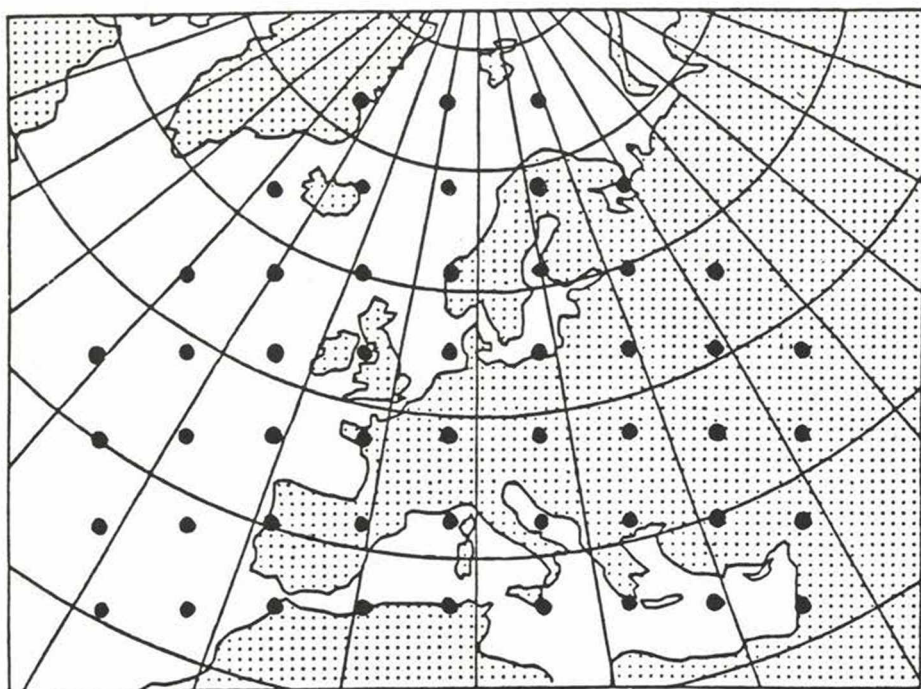


Fig. 4. Diamond grid covering the Atlantic European region AT 700 geopotential field – 51 gridpoints

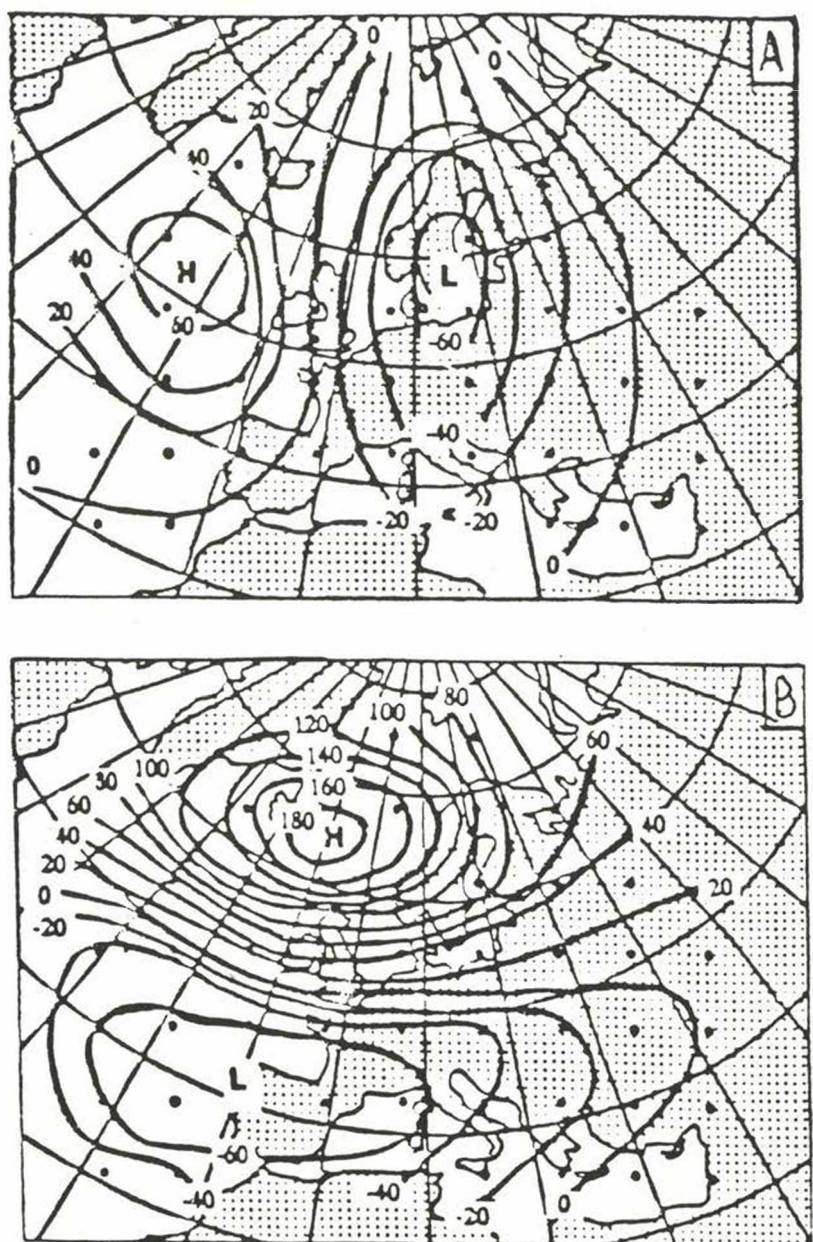


Fig. 5. One characteristic MCP for the Summer (A map) and for the Winter (B map) seasons on 700 hPa height level

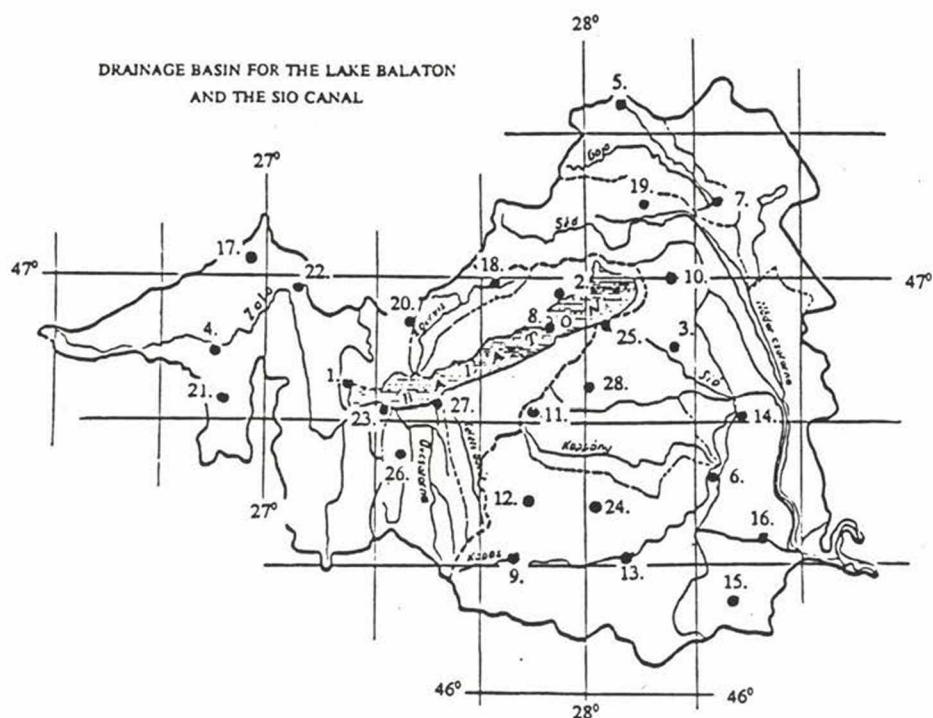


Fig. 6. 28 precipitation stations covering the drainage basin of the Lake Balaton



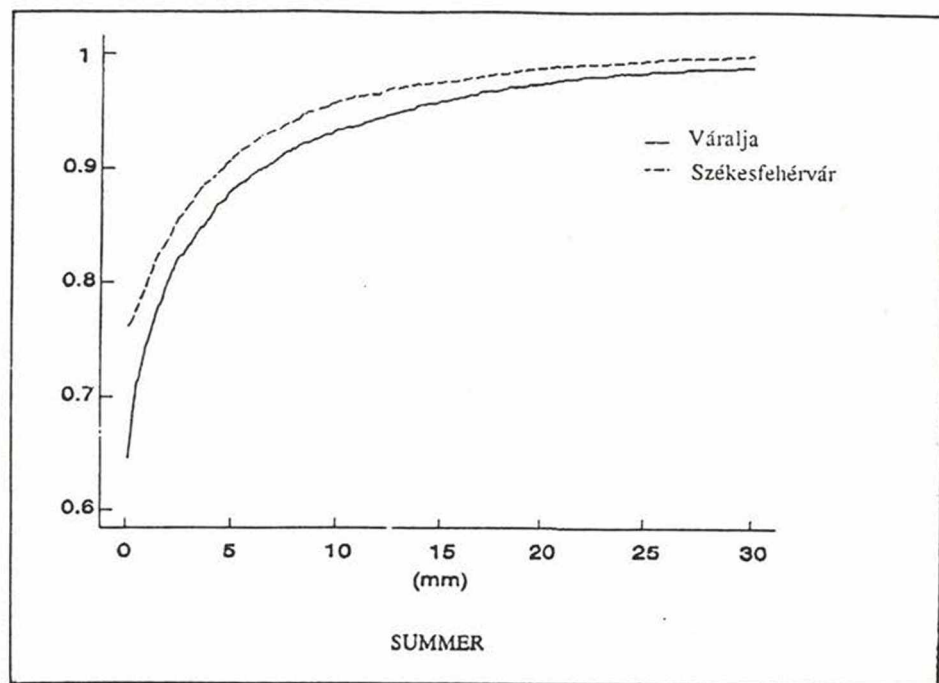


Fig. 7. Probability distribution function of daily precipitation amount estimated from simulated data (summer half year, station 5 and 7)

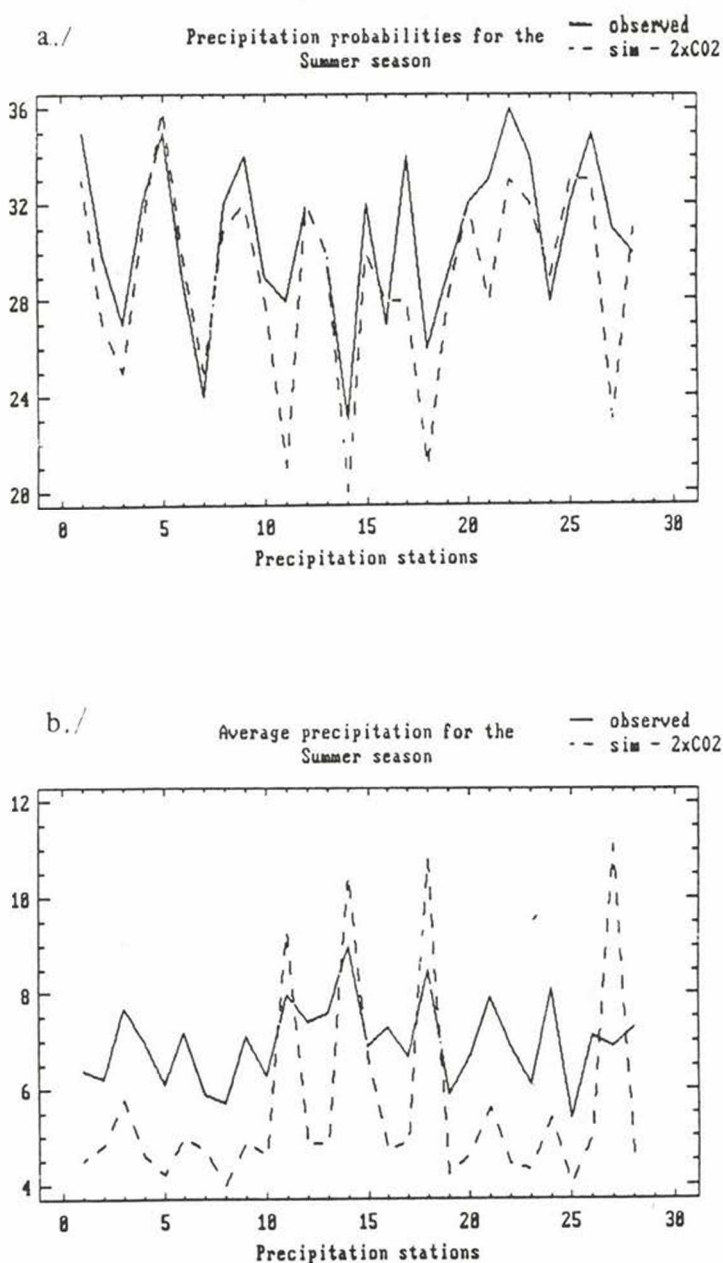


Fig. 8. Comparison between the observed and simulated probabilities (a.) and average precipitation (b.) in summer (28 stations)

## DRAINAGE BASIN FOR LAKE BALATON AND THE SIO CANAL

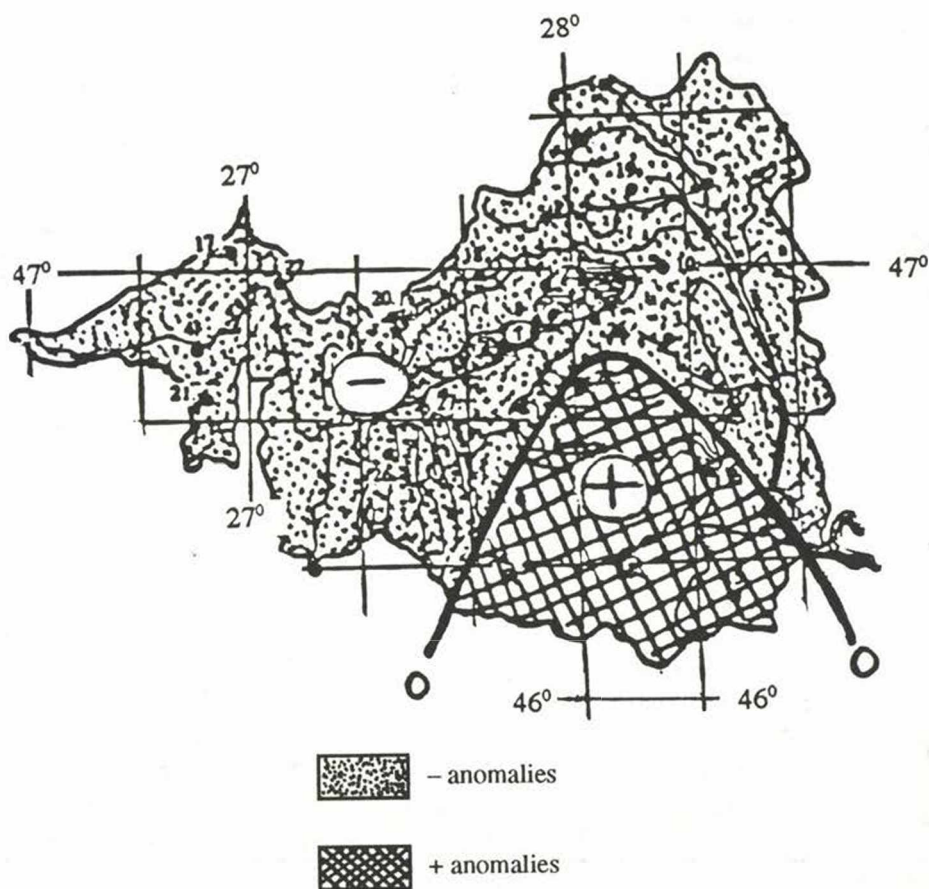


Fig. 9. Spatial distribution of daily precipitation in case of  $\text{CO}_2$  doubling (winter season)

Table 1. The list of the 28 observation stations

Numb	Station	Country	Degree		Height
			$\lambda$	$\delta$	
1.	Keszthely	Zala	17° 15'	46° 45'	115 m
2.	Balatonfüred	Veszprém	17° 55'	46° 58'	130 m
3.	Mezőkomárom	Fejér	18° 18'	46° 50'	12 m
4.	Zalaegerszeg	Zala	16° 51'	46° 50'	162 m
5.	Mór	Fejér	18° 12'	47° 23'	203 m
6.	Szakály	Tolna	18° 23'	46° 32'	116 m
7.	Székesfehérvár	Fejér	18° 25'	47° 12'	111 m
8.	Tihany	Veszprém	17° 54'	46° 55'	150 m
9.	Kaposvár	Somogy	17° 50'	46° 22'	152 m
10.	Lepsény	Fejér	18° 15'	47° 00'	119 m
11.	Karád	Somogy	17° 51'	46° 42'	210 m
12.	Memye	Somogy	17° 49'	46° 30'	168 m
13.	Dombóvár	Tolna	18° 08'	46° 22'	133 m
14.	Pincehely	Tolna	18° 26'	46° 41'	114 m
15.	Váralja	Tolna	18° 26'	46° 16'	164 m
16.	Zomba	Tolna	18° 34'	46° 23'	130 m
17.	Csehimindszent	Vas	16° 57'	47° 03'	175 m
18.	Nagyvázsony	Veszprém	17° 42'	46° 59'	268 m
19.	Osi	Veszprém	18° 11'	47° 09'	113 m
20.	Tapolca	Veszprém	17° 27'	46° 53'	125 m
21.	Bak	Zala	16° 51'	46° 44'	174 m
22.	Türje	Zala	17° 06'	46° 59'	152 m
23.	Balatonkeresztúr	Somogy	17° 22'	46° 42'	120 m
24.	Gölle	Somogy	18° 01'	46° 27'	147 m
25.	Siófok	Somogy	18° 02'	46° 55'	108 m
26.	Marcali	Somogy	17° 25'	46° 35'	129 m
27.	Fonyód	Somogy	17° 33'	46° 44'	166 m
28.	Tab	Somogy	18° 01'	46° 44'	177 m



## References

- Bárdossy A., Plate E. 1990; Modeling daily rainfall using a semi-Markov representation of circulation pattern occurrence. *J. Hydrol.* 66, 33–47
- Bartholy J. 1992; Methodological choices to clustering precipitation dataseries and a case study for Hungary, Proceeding, 5th International Meeting on Statistical Climatology, Toronto, Canada
- Binark A. M., Duckstein L., Plate E. 1976; Multisite rainfall generation for multisite flod simulation. Fall Annual Meeting, AGU, San Francisco, CA.
- Bogárdi I., Matyasovszky I., Bárdossy A., Duckstein L. 1993; Application of a Space-Time Stochastic Model of Daily Precipitation Using Atmospheric Circulation Patterns. *J. Geoph. Res.* To appear.
- Bogárdi J., Duckstein L., Rumambo O. 1988; Practical generation of synthetic rian-fall event time series in a semiarid climatic zone. *J. Hydrol.* 103, 357–363
- Chang T. J., Kavvas M. L., Delleur J. W. 1984; Daily precipitation modelling by discrete autoregressive moving average, *Water Resour. Res.* 20, 565–580
- Chua S. H., Bras R. L. 1982; Optimal estimators of mean areal precipitation in regions of orographic influence. *J. Hydrol.* 57, 23–48
- Hess P., Brezowsky H. 1969; Katalog der Grosswetterlagen Europas. *Berichte des Deutschen Wetterdienst*, 15. 113. Offenbach am Main.
- Lamb H. H. 1977; Climate, present, past and future. Vol. 2: Climatic history and the future. Methuen & Co Ltd, London.
- Matyasovszky I., Bogárdi I., Bárdossy A., Duckstein L. 1992; Evaluation of historical and GCM produced atmospheric circulation patterns, Working Paper, Department of Civil Engineering, University of Nebraska-Lincoln, Lincoln, NE68588, USA.
- Matyasovszky I., Bogárdi I., Bárdossy A., Duckstein L. 1993; Examination of local precipitation statistic reflecting climate change. *Water Resour. Res.* 29, 3955–3968
- Rodriguez-Itrube I., Eagleson P. S. 1987; Mathematical models of rainstorm events in space and time. *Water Resour. Res.* 23, 11–190



# SHORT-RANGE FORECAST USING A LINEAR BALANCED MODEL OF ATMOSPHERE

GYÖRGY GYURÓ

Department of Meteorology, Eötvös University

H-1083 Budapest, Ludovika tér 2. Hungary

**Abstract.** The paper presents 24-hour forecast of the surface pressure and the geopotential height of the 500 and 300 hPa surface computed by a linear balanced model. The prognosticated area consists of a belt of the Northern Hemisphere between 20N and 70N. Effect of the orography, the turbulent vertical mass transport and the sensible heat exchange are parameterized in the model. Finite difference form of the prognostic equations is solved by the aid of the pseudo-spectral method. Geopotential data of 22 days from the period between July 17 and August 16, 1989 are used. Detailed verification of the forecast are also discussed. From the results it emerges that in 69% of the gridpoints on the surface pressure chart, 86% of the gridpoints on the 500hPa and 89% on the 300 hPa contour charts correlation coefficients of the ensemble forecast are higher than the critical value calculated from the formula of the statistical hypothesis tests on a significance level of 95%.

## Introduction

A linear balanced model was used for short-range forecasts. The first activities in the numerical weather prediction at the Department of Meteorology of the Eötvös Loránd University were made by Práger et al. (1985). A three-parameter baroclinic quasi-geostrophic model was used for multiple aims, as for short-range prediction experiments, long term integrations of the model equations and investigation of wave solutions. (Gyuró 1987, Gyuró and Práger 1988). Both short- and long-term integration of the equation of the limited area model version showed the effect of improper boundary values. For further experiments channel version of the model was elaborated (Gyuró 1990). Results of long-term integration of the channel version allowed to conclude in the usefulness of the modifications. Considering the results and the computer facilities it seemed to be possible to use a more complex model of the model hierarchy for operative aims. For short-range forecasting experiments the linear balance equation is used in place of the geostrophic adjustment. The aim of this paper is to present prognostic formulae and verification results of the forecasts produced by the linear balanced model.

## Basic equations

Prognostic equation of the model are the vorticity, balance, continuity and thermodynamic equations using politropic approximation. It gives the following energy-consistent system of equations:

$$(1) \quad \frac{\partial \zeta}{\partial t} + v_{-y} \nabla \zeta + v_{-x} \nabla f + v_{-x} \nabla f + f D = 0 \quad ,$$

$$(2) \quad f \nabla^2 \Psi + \nabla f \nabla \Psi = \nabla^2 \Phi \quad ,$$

$$(3) \quad D + \frac{\partial \omega}{\partial p} = 0 \quad ,$$

$$(4) \quad \frac{\partial \Phi}{\partial t} \frac{\partial \Phi}{\partial p} + v_{-y} \nabla \frac{\partial \Phi}{\partial p} + v_{-x} \nabla \frac{\partial \Phi}{\partial p} + \frac{R}{P} \Gamma \omega = - \frac{R}{p} \frac{g}{c_p} \frac{\delta Q}{\delta t} \quad ,$$

Where  $\Gamma$  is statistic stability parameter. The other symbols used here and further in the text have their usual meaning (see e.g. Haltiner and Williams 1980).

Dependent variables of the model are the streamfunction for the nondivergent wind component, the velocity potential for the nonrotational wind component, the geopotential and the vertical velocity. The latter is a diagnostic variable while the others are prognostic ones. To obtain a diagnostic equation for the vertical velocity, the time derivatives between the vorticity and the thermodynamic equation must be eliminated. First it is necessary to differentiate the balance equation with respect to time and to subtract the result from the vorticity equation. The equation resulting after this operations must be differentiated with respect to pressure. Finally, applying the Laplace-operator on the thermodynamic equation and subtracting it from the foregoing equation yields the omega equation:

$$(5) \quad \frac{R}{p} \Gamma \nabla^2 \omega + f^2 \frac{\partial^2 \omega}{\partial p^2} = f \frac{\partial v_{-y}}{\partial p} \nabla (\zeta + f) + f v_{-y} \nabla \frac{\partial \zeta}{\partial p} + f \frac{\partial v_{-x}}{\partial p} \nabla f - \frac{Rg}{pc_p} \nabla^2 \frac{\partial Q}{\partial t} - \nabla^2 \left[ (v_{-y} + v_{-x}) \nabla \frac{\partial \Phi}{\partial p} \right] - \nabla f \nabla \frac{\partial^2 \Psi}{\partial p \partial t}$$

The above equation is not strictly diagnostic, since a time derivative appears in the last term. Moreover, the nonrotational wind component appears in the third and fifth terms on the right side of the equation, which is not known from the initial data. Consequently, the system must be solved iteratively as follows:

*Step 1:* The balance equation is solved using the initial geopotential data to give the streamfunction, the vorticity and the nondivergent wind component.

*Step 2:* The omega equation is solved omitting the last term and the terms containing the nonrotational wind component to give a first estimate of the vertical velocity.



- Step 3:* The continuity equation is solved using the first estimate of the vertical velocity to give a first estimate of the velocity potential and the nonrotational wind.
- Step 4:* The vorticity equation is solved to give a first estimate of the unknown streamfunction tendency in the last term of the omega equation.
- Step 5:* Returning to *Step 2* a second estimate of the vertical velocity can be computed using first estimates of nonrotational wind component and streamfunction tendency.
- Step 6:* The iterations of *Step 3*, *4* and *5* have to be repeated until convergence is obtained, i.e., until the changes in the estimated variables (vertical velocity, velocity potential and streamfunction tendency) are within a preassigned error limit.
- Step 7:* The actual prediction of the streamfunction is made using a finite difference scheme in time.
- Step 8:* The balance equation is solved using the new streamfunction to give the predicted geopotential values.

Vertical structure of the model is analogous to the structure of the quasi-geostrophic model. The atmosphere is divided into three layers: two tropospheric layers, separating by the atmosphere and one layer above the tropopause. Prognostic values of the model variables refer to four different levels: the Earth's surface, the quasi-nondivergent level, the tropopause and finally the upper boundary of the atmosphere, which is well-determined using quasistatic approximation. Similarly to the quasi-geostrophic model, vertical profile of the nondivergent and the nonrotational wind is given by fractionally linear function, i.e. we suppose that the wind field changes linearly with the pressure inside the significant layers. These simple function of the wind components are substituted into the prognostic equation and the latter are integrated over the three significant layer of the model with respect to pressure. In that way second order partial differential equations in the variables  $x$  and  $y$  are gained. In order to get the canonic form of the balance equation, a simple transformation is applied. A general solution of the equation can be written in the following form:

$$(6) \quad P = \Psi \exp \left\{ \frac{\beta_0}{2 f_0} (x+y) \right\}$$

Putting this into the balance equation, one obtain second order partial differetial equation for the new variable  $P$ :

$$(7) \quad \nabla^2 P - \frac{\beta_0}{2 f_0^2} P = \frac{1}{f_0} (\nabla^2 \Phi) \exp \left\{ \frac{\beta_0}{2 f_0} (x + y) \right\}$$

Detailed description of integration of the equation and differentiation of prognostic formulae is given in Gyuró (1990). As it was pointed out earlier, all formulae of the model are second order elliptic differential equations. Knowing the initial values of the variables and using appropriate boundary conditions the prognostic equations can be uniquely solved.

## Prognostic area

For the channel version of the model a rectangular prognostic area is chosen on the beta plane covering a 6600 km times 30 000 km belt of the Northern Hemisphere. Finite difference version of the equations is given on an equidistant rectangular grid with a grid interval of 600 km. Map magnification parameter is supposed to be zonally constant. Values of the parameter for each row of gridpoints in the meridional direction are shown in Table 1. Space derivatives are taken in finite difference form using the nine-point scheme of Arakawa (1966). Predicted values of prognostic variables are computed from the tendencies using the leapfrog scheme (first order forward scheme in the first step) with a time step of 1 hour. Some numerical experiments with the Adams-Bashforth scheme did not show any significant change in numerical solutions.

The use of a finite difference scheme for the space derivatives converts the original differential equations into system of algebraic equations, each consisting of  $p-2$  times  $q-2$  equation and  $p$  times  $q$  variables, where  $p$  and  $q$  are number of gridpoints in zonal and meridional directions respectively. A closure of the system can be achieved by specifying boundary values. In accordance with the channel structure of the prognostic domain, disappearance of the gradient normal to the boundary is demanded on the northern and southern boundaries (Neumann problem), while a periodic solution is required on the eastern and western boundaries. Algebraic system of finite difference equation is solved by the pseudo-spectral method (Práger et al. 1985), i.e. a finite Fourier method is used for discrete value functions. This method seems to be more efficient than iterative methods or Liebmann's successive overrelaxation. Ihász (1989) reduced computational time for solving algebraic equations using the fast Fourier transformation with factorization.

Effect of orography forcing, turbulent vertical transport of mass and sensible heat exchange between the atmosphere and the Earth's surface are taken into consideration using simple parameterization formulae. Presence of orography modifies the lower boundary value of the vertical velocity as follows:

$$(8) \quad \omega_{L1} = J(\Psi_s, P_s)$$

where the right side is Jacobian of the streamfunction and the pressure at the altitude of the orography. Dispersion of the orography is shown in Fig. 1.

Turbulent vertical mass transport gives further modification in the vertical velocity at the lower boundary:

$$(9) \quad \omega_{L2} = k \zeta_s$$

where the coefficient of the vorticity is an empirical constant. Its value is  $-1.688 \text{ m}^3$  according to Bengtsson and Moen (1971).

Third parameterization applied in the model refers to the sensible heat exchange between the lower troposphere and the sea surface. Heat exchange pro-



cesses between the atmosphere and the continental surface are negligible for the time scales of the prediction. Transport of heat from below is proportional to the temperature gradient between the ocean and the atmosphere. Non-adiabatic term in the thermodynamic equation (4) is given by the following expression:

$$(10) \quad \frac{\delta Q}{\delta t} = \begin{cases} 10^{-9} |\underline{V}| (T_s - T_0), & \text{if } T_s > T_0 \\ 0, & \text{if } T_s < T_0 \end{cases}$$

Where  $|\underline{V}|$  is the wind speed at the Earth's surface,  $T_0$  is the corresponding air temperature and  $T_s$  is the sea surface temperature. Heat capacity of the of the ocean is assumed to be infinite for the period of the forecast. Because of the missing sea surface temperature data a constant meridional temperature gradient is assumed with a value of  $2^\circ\text{C}/1000 \text{ km}$ . Temperature difference between the ocean and the atmosphere in the middle zonal row of gridpoints is supposed to be zero. For the vertical integration of the thermodynamic equation vertical profile of the non-adiabatic term is necessary. It is given by a simple linear function as show in Fig. 2.

## Results of the forecast and conclusions

As an initial data basis the NMC Washington 00 UTC objective analysis of the 1000, 500 and 300 hPa geopotential field were used from the period between July 17 and August 16, 1989. The initial geopotential values on the equidistant grid of the model were interpolated from the 5 degree resolution spherical grid of the objective analysis by a simple bilinear interpolation formula. Because of some troubles in the telecommunication network, data of 22 days are preset only for the entire Northern Hemisphere. Computer code was written in Fortran programming language. Computations were carried out in the Computer Centre of the Hungarian Meteorological Service by the aid of a BASF 7/61 high speed computer. In order to get verification scores of the forecast root mean square error was calculated from gridpoint to gridpoint. Root mean square error of the 24 hour forecast is shown in Fig. 3. for the surface pressure, and Fig. 4. for the 500 and 300 hPa geopotential field. Geopotential height  $z$  of the 1000 hPa isobaric surface was transformed to surface pressure values  $p$  using the following truncated Taylor series:

$$(11) \quad p = 1000 + z/8.41.$$

According to Fig. 3. and 4. best verification scores can be seen on July 21, August 16 and 15. Highest root mean square error was received from the forecast for August 13, 6 and 11. Mean absolute error for the 22 forecast are Table 2.

Another possibility to get verification scores of numerical predictions is, to calculate the correlation coefficient between the forecasted and the analysed fields. Random variable in our case is the geopotential height ( the surface pressure at the

lower boundary of the model). Length of the sample is 22 in every gridpoint. Isocorrelation field of the forecast is shown in Fig. 5. The assumption, whether the correlation coefficient represents real connections between the forecast and the analysis can be checked with the aid of the statistical hypothesis test. The following expression containing the correlation coefficient ( $r$ ) and the length of the sample ( $n$ ) has Student or  $t$ -distribution:

$$(12) \quad t = \sqrt{n-2} \frac{r}{\sqrt{1-r^2}}$$

From tables of the Student distribution the value of  $t$  can be given for different levels of significance. Knowing  $t$  the correlation coefficient can be checked using the following relation:

$$(13) \quad |r| > \frac{t}{(t^2 + n - 2)^{1/2}}$$

In Table 3. number of such gridpoints is given, where the correlation coefficient is higher than the limit calculated from (13). Distribution of the gridpoints with higher correlation than the limit is shown in Fig. 6. A significant difference can be seen between the main levels of the model. Statistical connection between the forecast and the analysis is stronger on the 500 and 300 hPa level than on the lower boundary of the model. That indicates the problem of the lower boundary conditions. A significant improvement can be expected from a use of a finer grid and finer orographical contour. Also, the used parameterization method has to be corrected and completed with the parameterization of latent heat release.

### Acknowledgement

The author is thankful to the staff of the Computer Centre and the Telecommunication Department of the Hungarian Meteorological service for their valuable help.





Fig. 1. Orography used in the model. (Contours represent 75 meter distance in altitude.)

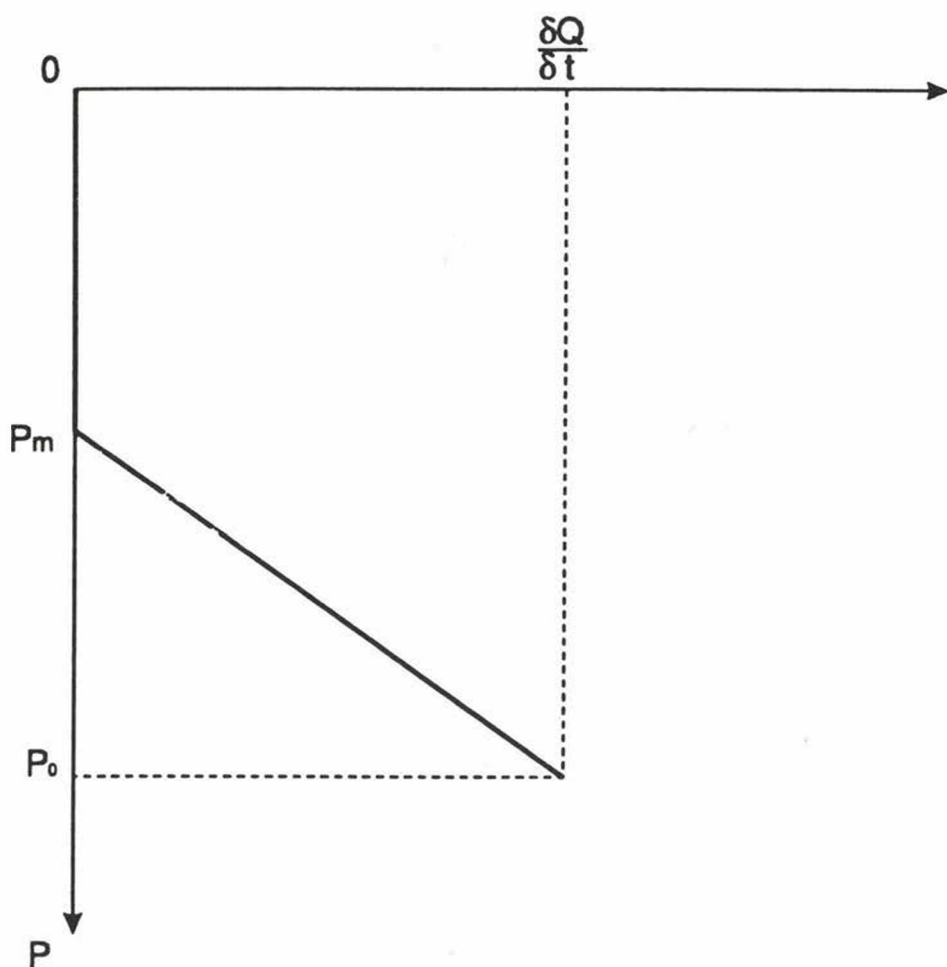


Fig. 2. Vertical profile of the non-adiabatic term in the thermodynamic equation between the Earth's surface ( $P_0$ ) and the middle troposphere ( $P_m$ )

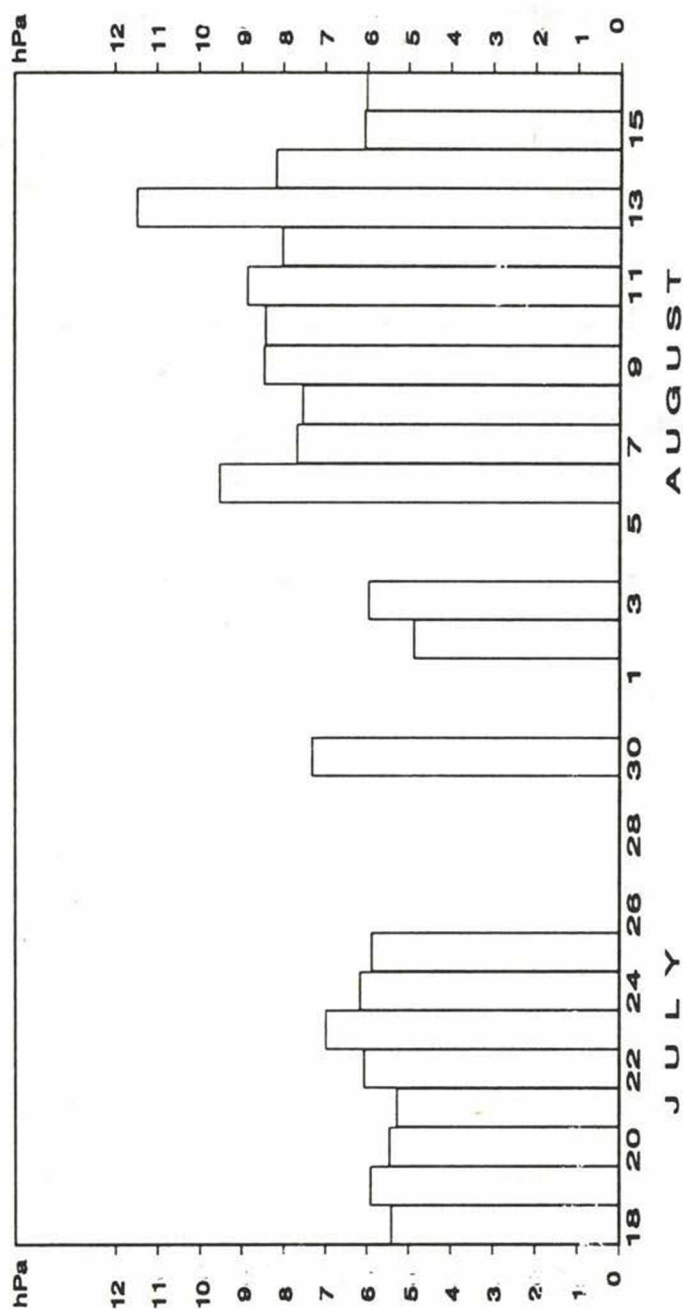


Fig. 3. Root mean square error of forecasts of the surface pressure

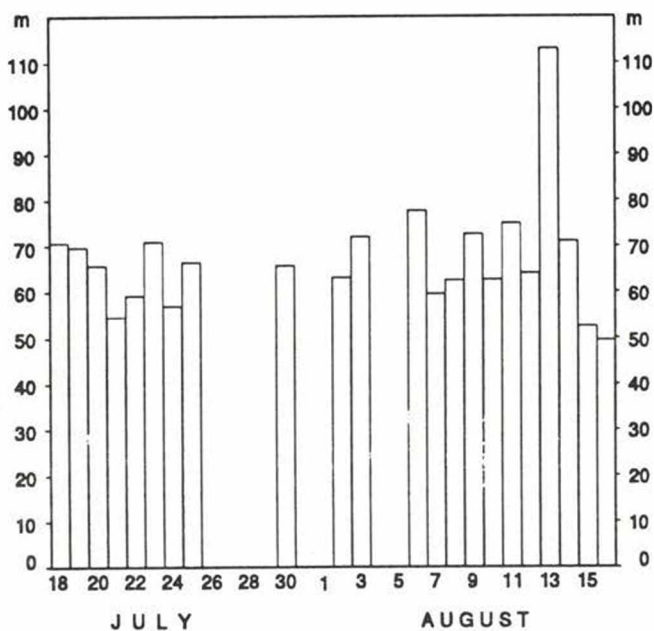
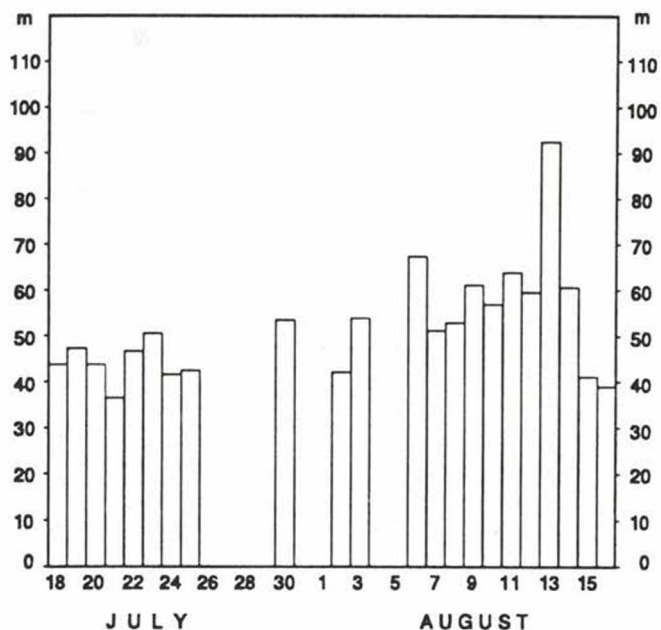


Fig 4. Root mean square error of forecasts of the 500 hPa (upper) and the 300 hPa (lower) field







Fig. 5. Isocorrelation field of the forecasts for the surface pressure (upper), the 500 hPa and the 300 hPa (lower) field

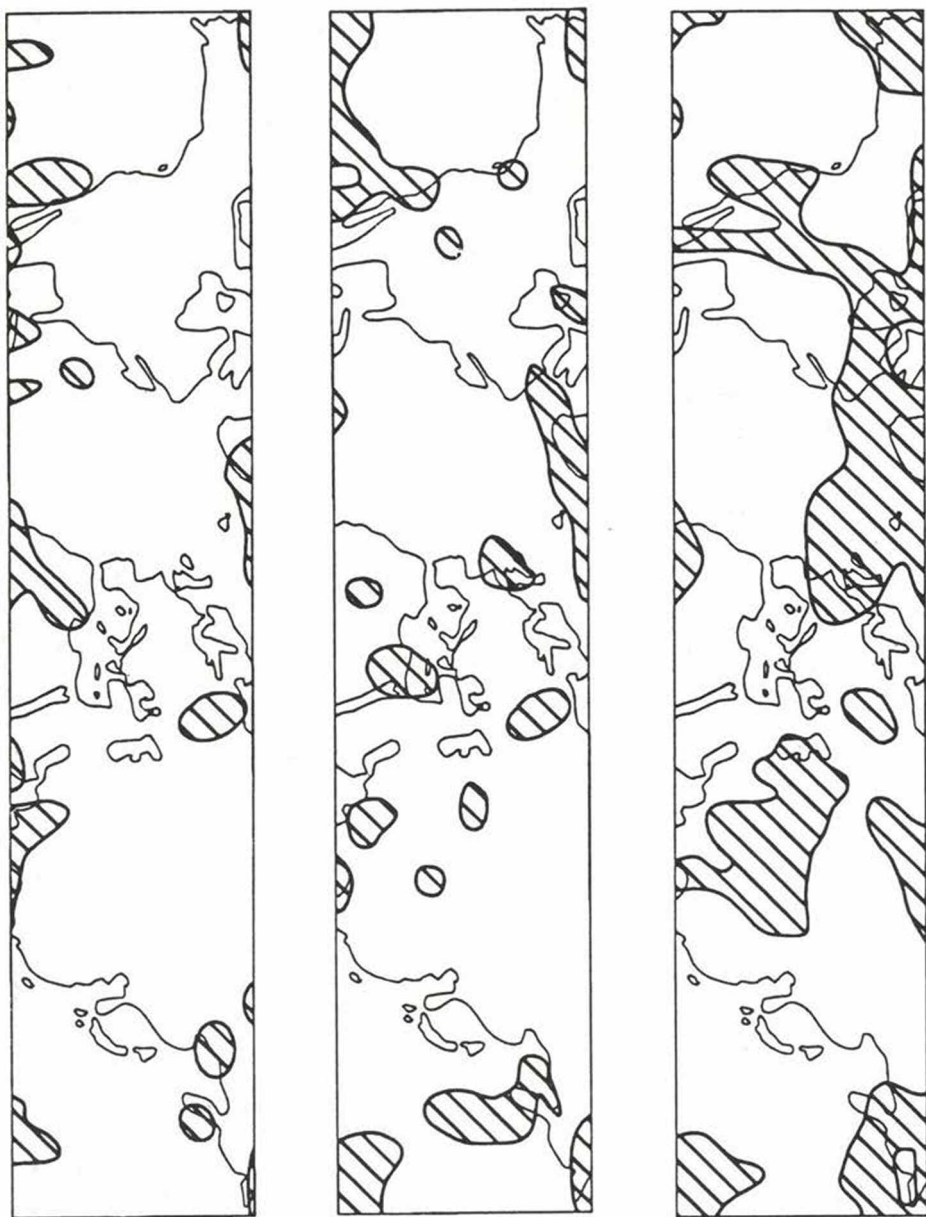


Fig. 6. Distribution of the gridpoints (unstriped area) with higher correlation than the limit at 95% significance

**Table 1.** Map magnification parameter from gridpoint 12 (70 N) to gridpoint 1 (20 N)

12: 2.0291	6: 0.8379
11: 1.4546	5: 0.7967
10: 1.2045	4: 0.7640
9: 1.0584	3: 0.7376
8: 0.9609	2: 0.7162
7: 0.8906	1: 0.6988

**Table 2.** Mean (m) and standard deviation (s) of absolute error and root mean square error of the forecast

Level	Absolute error	Root mean square error
Surface	m = 4.16 hPa s = 0.84 hPa	m = 6.00 hPa s = 1.38 hPa
500 hPa	m = 34.6 gpm s = 7.6 gpm	m = 51.7 gpm s = 12.4 gpm
300 hPa	m = 44.1 gpm s = 6.6 gpm	m = 66.8 gpm s = 12.6 gpm

**Table 3.** Limit of the correlation coefficient, number and ratio of gridpoints with correlation higher than the limit at different levels of significance. (Total number of gridpoint is 624.)

Level of significance	Limit of correlation	Number and ratio of gridpoints		
		Surface	500 hPa	300 hPa
95 %	0.42	433 (69 %)	538 (86 %)	557 (89 %)
99 %	0.53	352 (56 %)	478 (77 %)	505 (81 %)
99,9 %	0.65	233 (37 %)	369 (59 %)	411 (66 %)

## References

- Arakawa A. 1966., Computational design for long-term numerical integration of the equations of fluid motion. Part 1: Two-dimensional incompressible flow. *Journal of Computational Physics* 1, 119–143
- Bengtsson L., Moen L. 1971., An operational system for numerical weather prediction. *WMO* 283, 65–88
- Gyuró Gy. 1987., Short-range forecast attempts with a limited area quasi-geostrophic model. In: Boer G. J. Ed., *Research Activities in Atmospheric and Oceanic Modelling*, WMO/TD. 200, 5.11–5.14
- Gyuró Gy. 1990 Short-range forecasts with a three-parameter model-hierarchy (in Hungarian). *Egyetemi Meteorológiai Füzetek* 3. Department of Meteorology, Eötvös University, Budapest
- Gyuró Gy., Práger T. 1988., Short-range forecast experiments with a limited area quasi-geostrophic model. *Időjárás* 92, 17–29
- Haltiner G. J., Williams R. T. 1980., *Numerical prediction and dynamic meteorology*. Second edition. John Wiley and Sons, New York
- Ihász I. 1989., Computationally efficient method for solving the barotropic vorticity equation with orographic forcing (in Hungarian). *Időjárás* 93, 351–362
- Práger T., Kovács E., Gyuró Gy. 1985., Numerical experiments with a three-parameter baroclinic quasi-geostrophic model of the atmosphere. *Annales Uni. Sci. Budapestinensis de Rolando Eötvös nominatae. Sectio Geographica et Meteorologica* I–II, 212–280



# MEASUREMENT OF NITRIC OXIDE, OZONE AND SULFUR DIOXIDE FLUX BY GRADIENT METHOD OVER SHORT VEGETATION DURING THE TRACT EXPERIMENT, SEPTEMBER 1992

LÁSZLÓ HORVÁTH, ZOLTÁN NAGY

Hungarian Meteorological Service, Institute for Atmospheric Physics  
H-1675 Budapest, P. O. Box 39, Hungary

TAMÁS WEIDINGER

Department of Meteorology, Eötvös University,  
H-1083 Budapest, Ludovika tér 2., Hungary

## Introduction

The Hungarian EUROTRAC/ BIATEX group was invited to join in the extensive EUROTRAC/ TRACT campaign carried out between 10–22 September, 1992, in Germany, Switzerland and France. Measuring program of TRACT covered many kinds of meteorological and chemical observations. The task for Hungarian group was to monitor the concentrations of nitrogen oxides, ozone and sulfur dioxide and to determine the surface resistance of these gases. The gradient method was used to determine the deposition velocity (reciprocal surface resistance) of gases.

## Experimental

Measuring site was selected in Rhine valley in the nested area (TRACT, 1992) about 3 km south of Lichtenau and 1 km south-east from Scherzheim villages, over a flat field covered by short wheat. Location of measurement can be seen in Fig. 1. The homogeneity of the surface (fetch) was satisfactory between the azimuths of 15–70 degrees, while between 340–15 and 70–115 degrees poor fetch was considered. Between the azimuths 115 and 340 degrees the surface characteristics did not meet the requirements of surface homogeneity.

For the meteorological and chemical measurements a 6.4 meter long mast was used (see Fig. 2.). Radiation balance and wind direction sensors were settled at the top of the mast. Vertical temperature and wind velocity profile were determined by four sensors arranged in logarithmic scale (0.5, 1.0, 2.0 and 4.0 meters). The air inlet and teflon tubing for gas monitors were at the same levels. A computer controlled solenoid valve system switched the air inlet from one level to the next one in every five minutes. Result of the first minute was omitted to avoid the mixing air

samples from different levels and to eliminate the delay of response of monitors. Concentration profiles were determined according to a 20 minutes period.

A data acquisition system and a computer collected and stored the data for each of 5 minute period. For wind direction the most frequent direction was considered in the five minute time interval.

## Preliminary results

By the use of gradient method the dry flux of a given trace gas (D) can be derived as:

$$D = K_T \frac{dc}{dz},$$

where  $K_T$  is the eddy-diffusivity for turbulent heat flux,  $dc/dz$  is the concentration gradient of the given gas, respectively.

$K_T$  was calculated according to Monin-Obukhov's semi-empirical similarity theory (Horváth et al. 1992) using the wind and temperature profile. Typical  $K_T$  values varied between the interval of 0–0.3 m<sup>2</sup>s<sup>-1</sup>, with a peak at noon (Fig. 4.). During night (between sunset and sunrise) rate of diffusivity was generally one order of magnitude lower than at day-time.

Richardson's number was also computed to distinguish between unstable and stable cases (Fig. 3. and 4.). Stable stratification was observed generally between 7 a. m. and 8 p. m. As we can see from Figs. 3. and 4. unstable stratification dominates during day-time.

Concentration of nitric oxide varied between 0 and 55 ppb. Daily peak values can be observed in early afternoon (Figs. 5. and 8. ). Average concentration of NO during the experiment was 6.3 ppb. It is surprisingly high in rural air because NO reacts with ozone rapidly, producing nitrogen dioxide. The high level of nitric oxide in day-time suggests that soil may be a substantial source of NO. Probably the bacterial activity in the soil, depending on the temperature, produces the nitric oxide from the decomposition of the fertilizer used. We should know more about the quality and quantity of fertilizer applied around the monitoring site.

Ozone concentration was monitored between 5–60 ppb (Fig. 6. and 8.) with expressed late afternoon peaks. Photochemically produced ozone reaches its concentration maxima usually afternoon according to many observations. Average ozone concentration is around 18 ppb.

The daily variation of sulfur dioxide concentration has the same pattern as ozone (Figs. 7. and 8.). Concentration varied between 0 and 9 ppb with an average of 1.9 ppb. The daily variation of sulfur dioxide concentration as well the source of SO<sub>2</sub> at the measuring site is an open question.

Average concentration gradients can be seen in Fig. 9. Concentration of sulfur dioxide and ozone are increasing with height indicating deposition processes for these compounds. For NO the soil and vegetation can be source and sink parallelly. Fig. 9. suggests that the soil was a source for NO during the campaign. It should be noted here that ozone and nitric oxide profile can be modified by photochemical reactions of NO/NO<sub>2</sub>/O<sub>3</sub> triade (Kramm et al. 1991). For precise interpretation a so-called chemical correction is needed for the calculation of concentration profiles and deposition.

Dry deposition velocity can be defined as  $v = D/C$ , where C is the concentration, measured at the upper level. Calculated deposition velocity figures are seen in Figs. 10–13.

From these figures the following preliminary conclusion can be drawn:

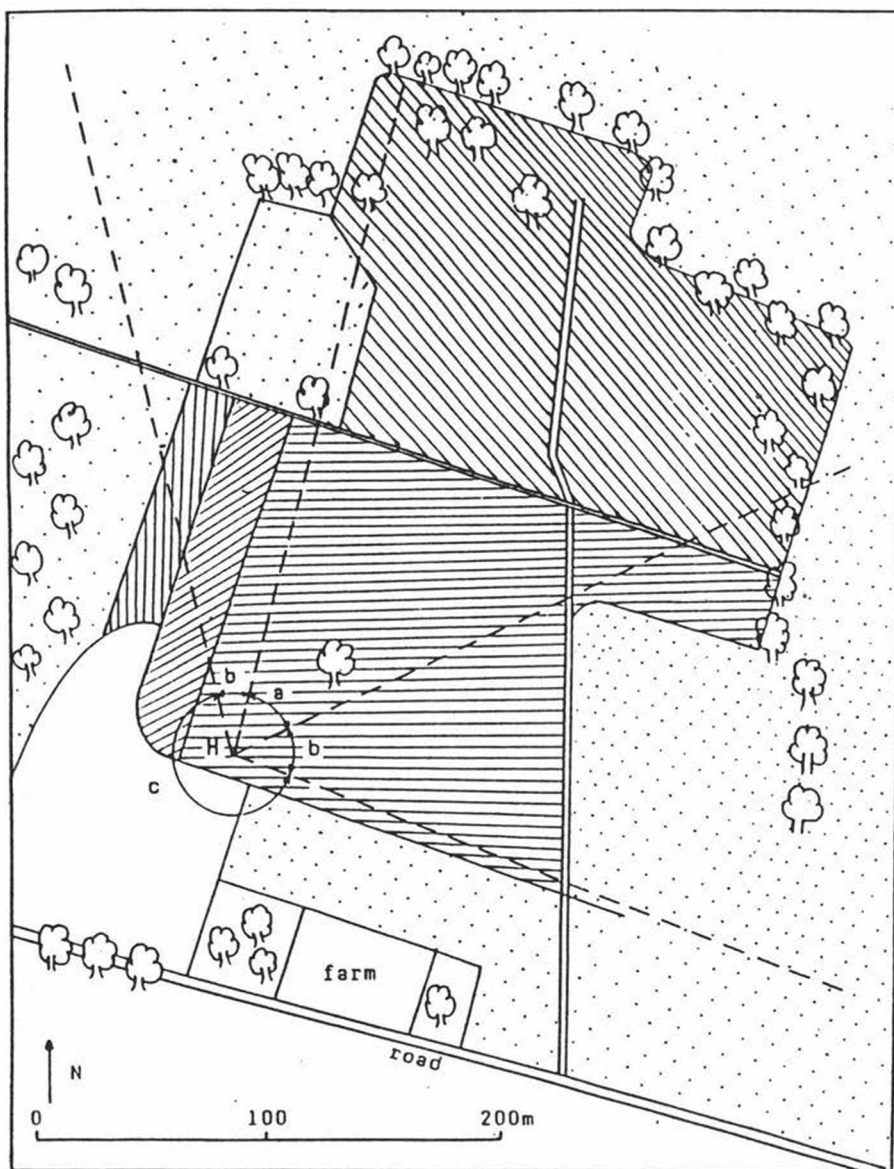
Average deposition velocity for nitric oxide (Fig. 13a) is negative which supports the soil source theory. Ozone deposition velocity (Fig. 13b) is generally positive however in many cases inverse deposition can be observed. Being the inverse deposition (emission) of ozone from the soil impossible the reason of the observed phenomena may be attributed to three reasons:

- 1) lack of surface homogeneity condition (no fetch or poor fetch),
- 2) rapid increase or decrease of concentrations due to advection during the 20 minute long measuring period of gradient,
- 3) standard error of sampling and analysis of gases.

To eliminate these errors we have different possibilities. For example we can select between "good fetch" and "poor or no fetch" cases, taking only the data when surface homogeneity conditions are fulfilled. In this case we loose the majority of data because of the narrow sector for good fetch (Fig. 1.).

Other possibility is to separate the "true" and "false" cases. When we see the frequency distribution of ozone (Fig. 14.) let's suppose that the distribution of deposition velocity is a superposition of "true" values (log normal distribution having zero limit). Let's suppose moreover that the left negative area of the bulk distribution is caused only by the errors. Because the normal distribution of error we can subtract the negative cases from both the negative and the positive side of distribution. In this manner we have a long normal distribution of "true" values (Fig. 14., corrected distribution).





- |                |              |             |
|----------------|--------------|-------------|
| H : mast       | : meadow     | : mustard   |
| a : good fetch | : corn       | : bare soil |
| b : poor fetch | : wheat (I)  | : trees     |
| c : no fetch   | : wheat (II) | : path      |

Fig. 1. Location of Hungarian measuring point during TRACT campaign in the nested area



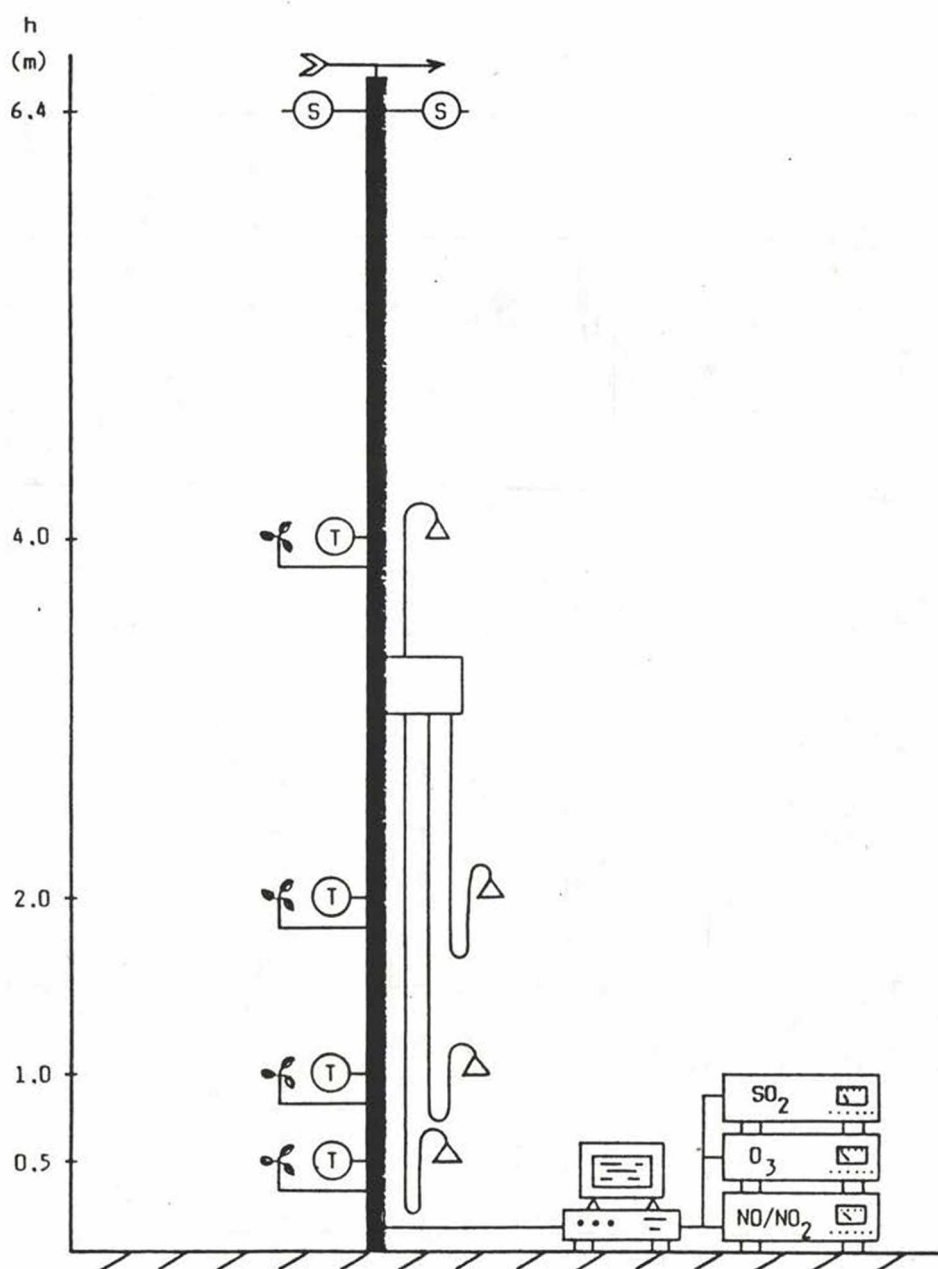


Fig. 2. Measuring mast during the TRACT campaign

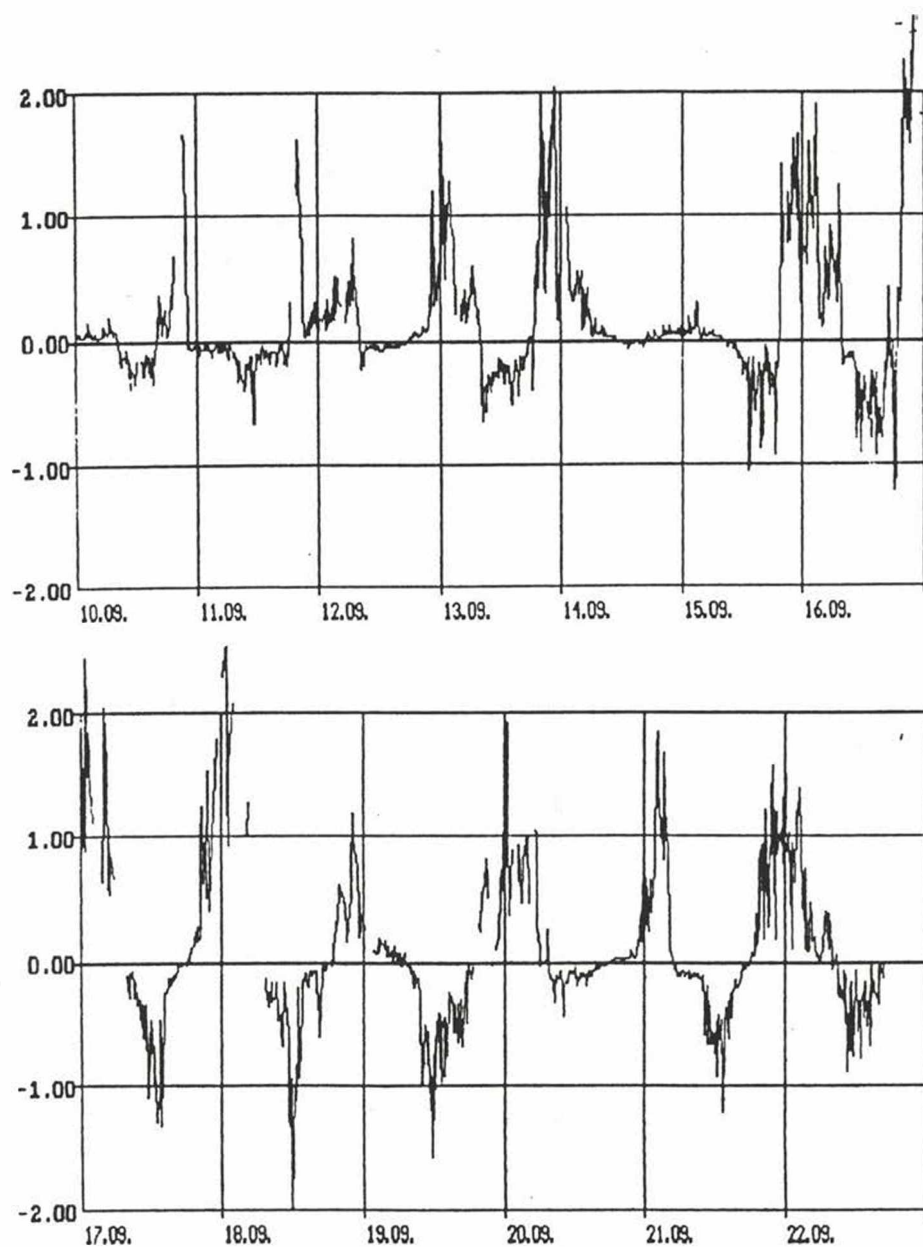


Fig. 3. Variation of the Richardson's number (10–22 September)

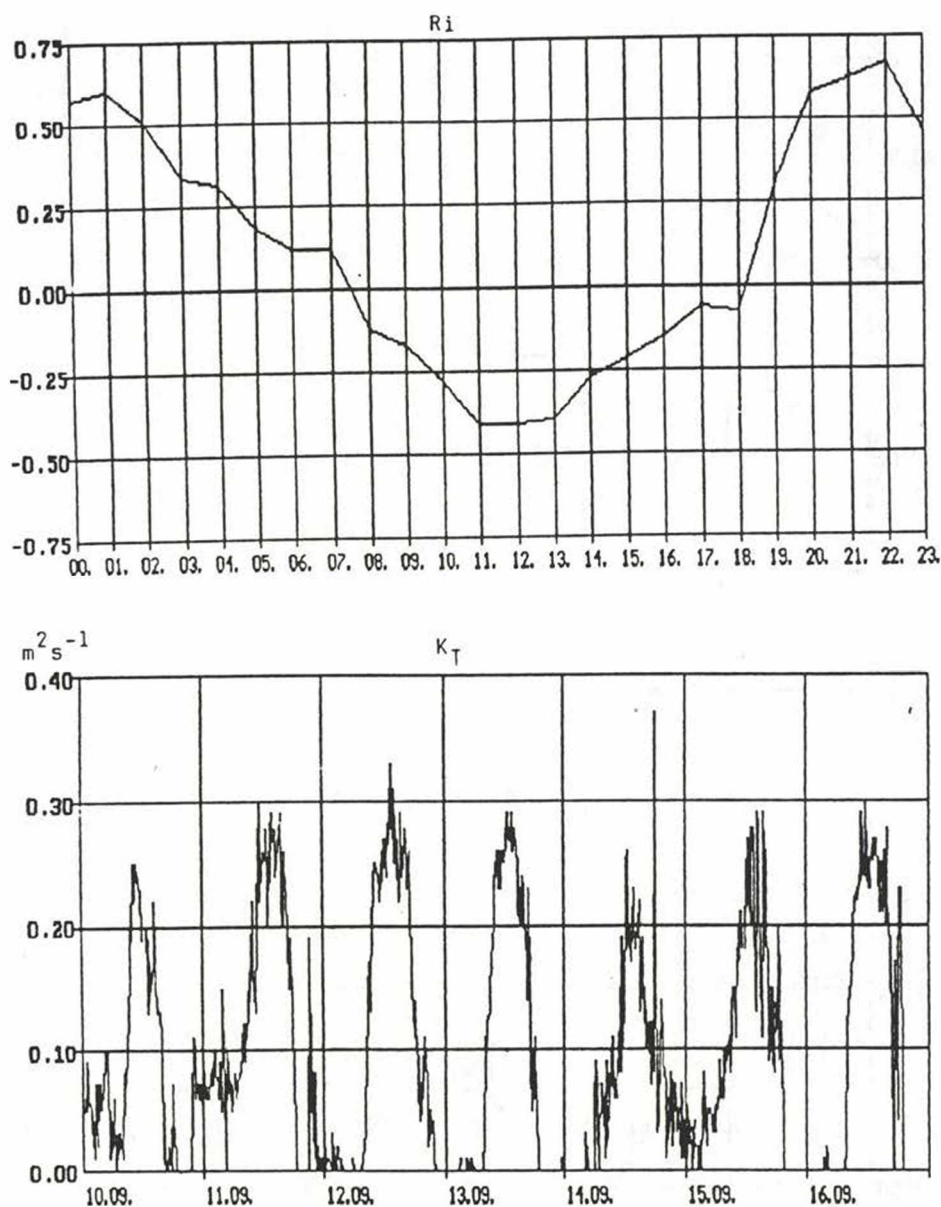


Fig. 4. Average daily variation of the Richardson's number (upper figure, 10-22 September) and variation of eddy-diffusivity (lower figure, 10-16 September)

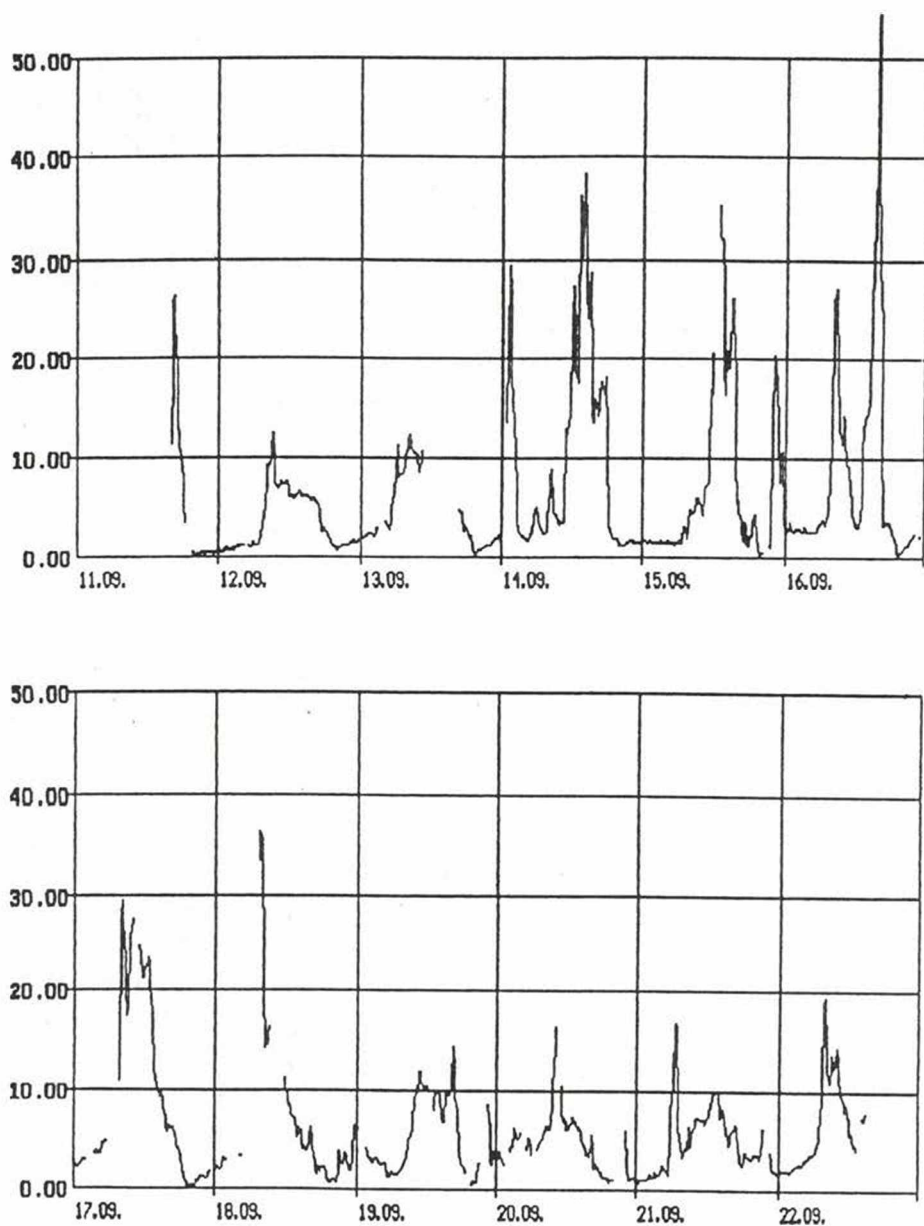


Fig. 5. Variation of nitric oxide cocentration in ppb (10-22 September)



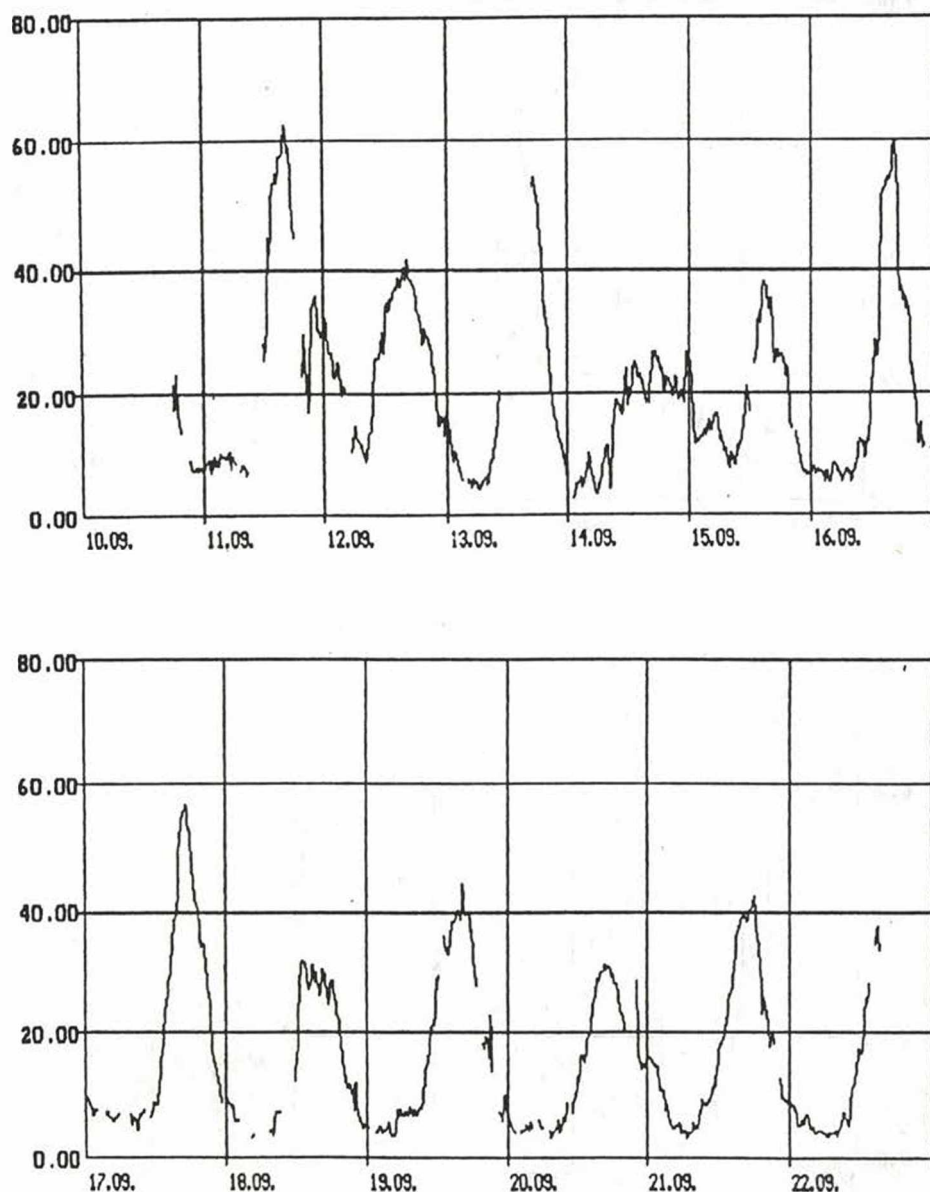


Fig. 6. Variation of ozone concentration in ppb (10-22 September)

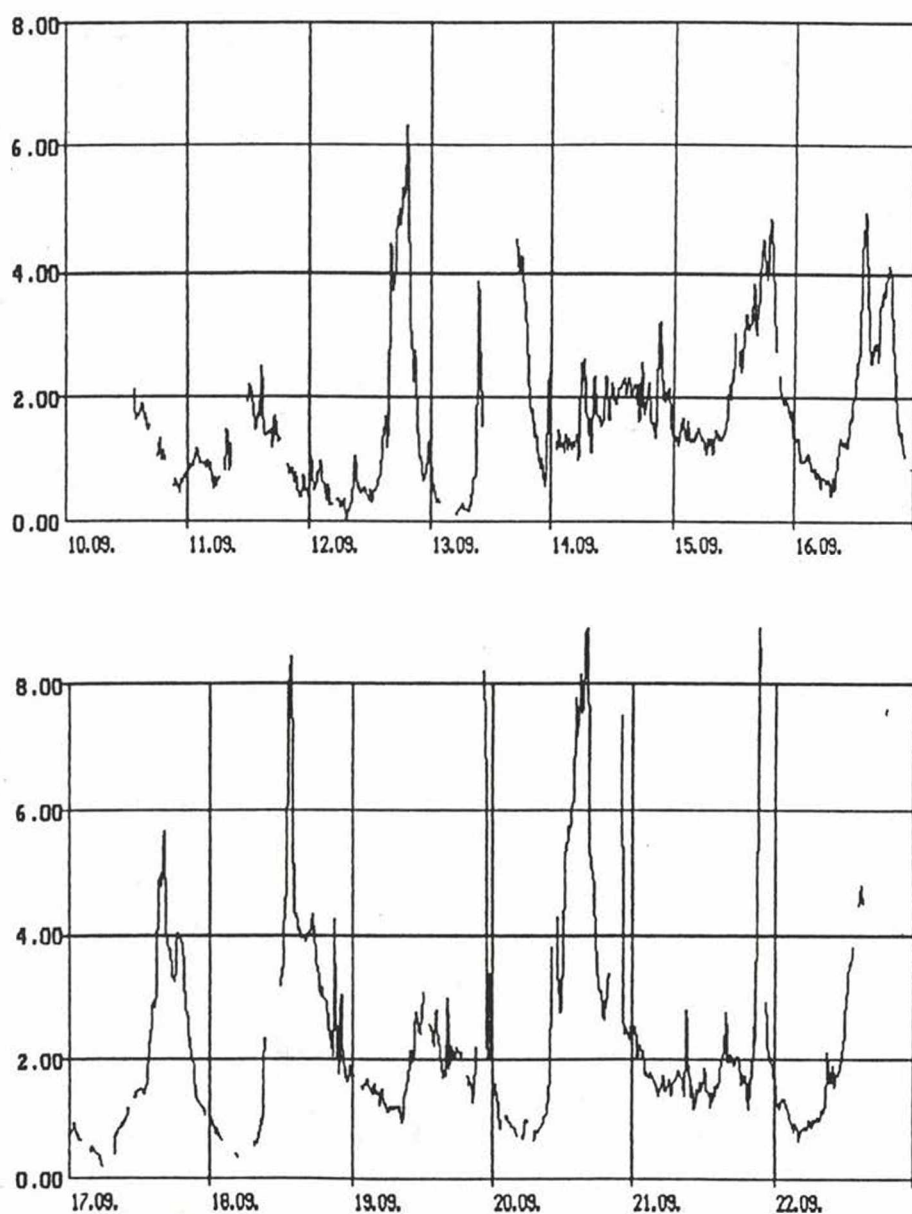


Fig. 7. Variation of sulfur dioxide concentration in ppb (10–22 September)

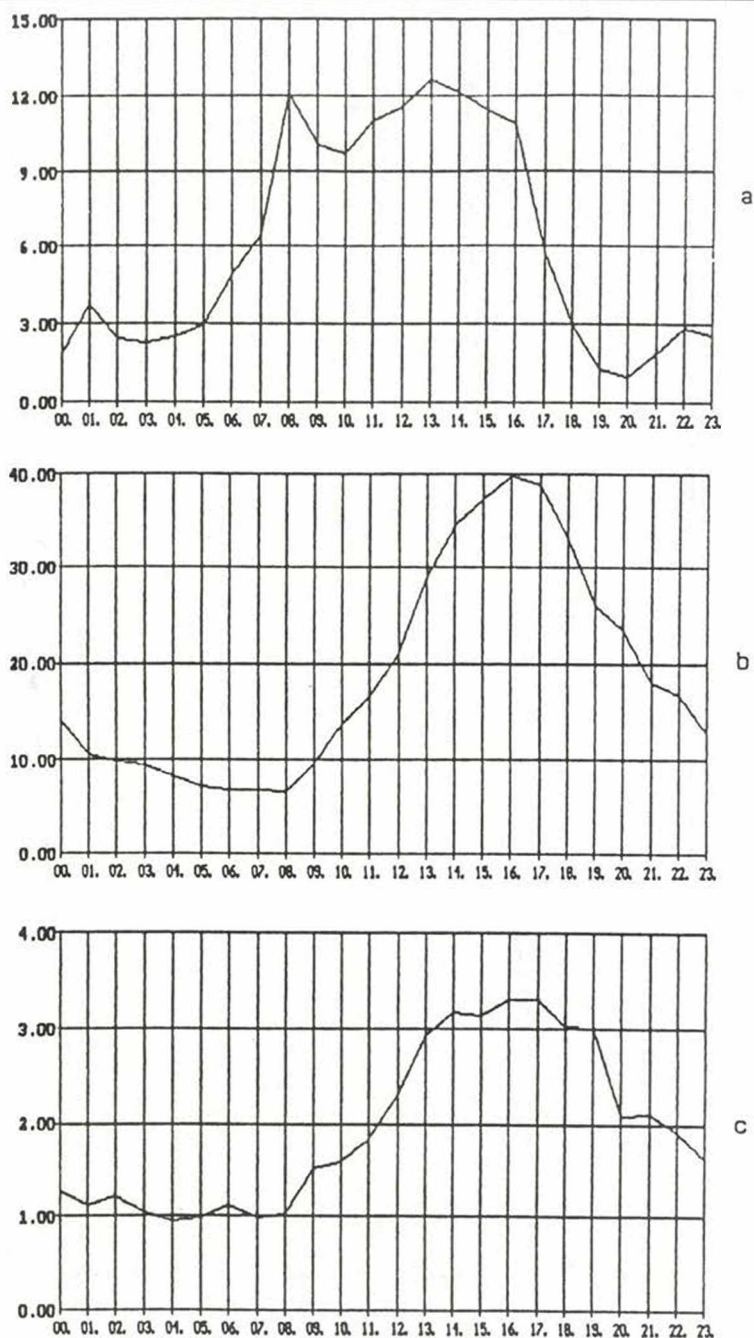


Fig. 8. Average daily variation of nitric oxide (a), ozone (b) and sulfur dioxide (c) concentration in ppb (10–22 September)

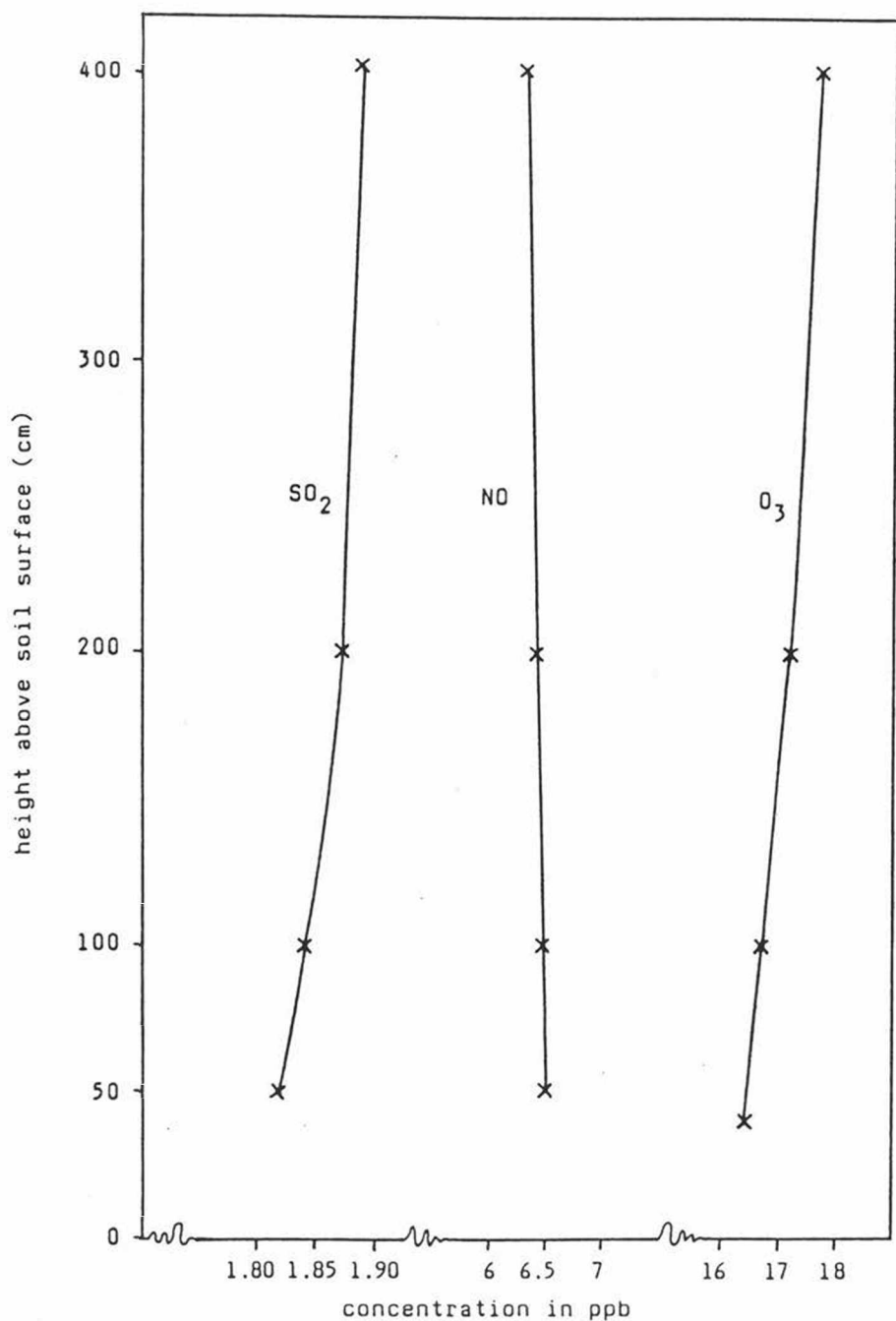


Fig. 9. Average concentration gradient of sulfur dioxide, nitric oxide and ozone



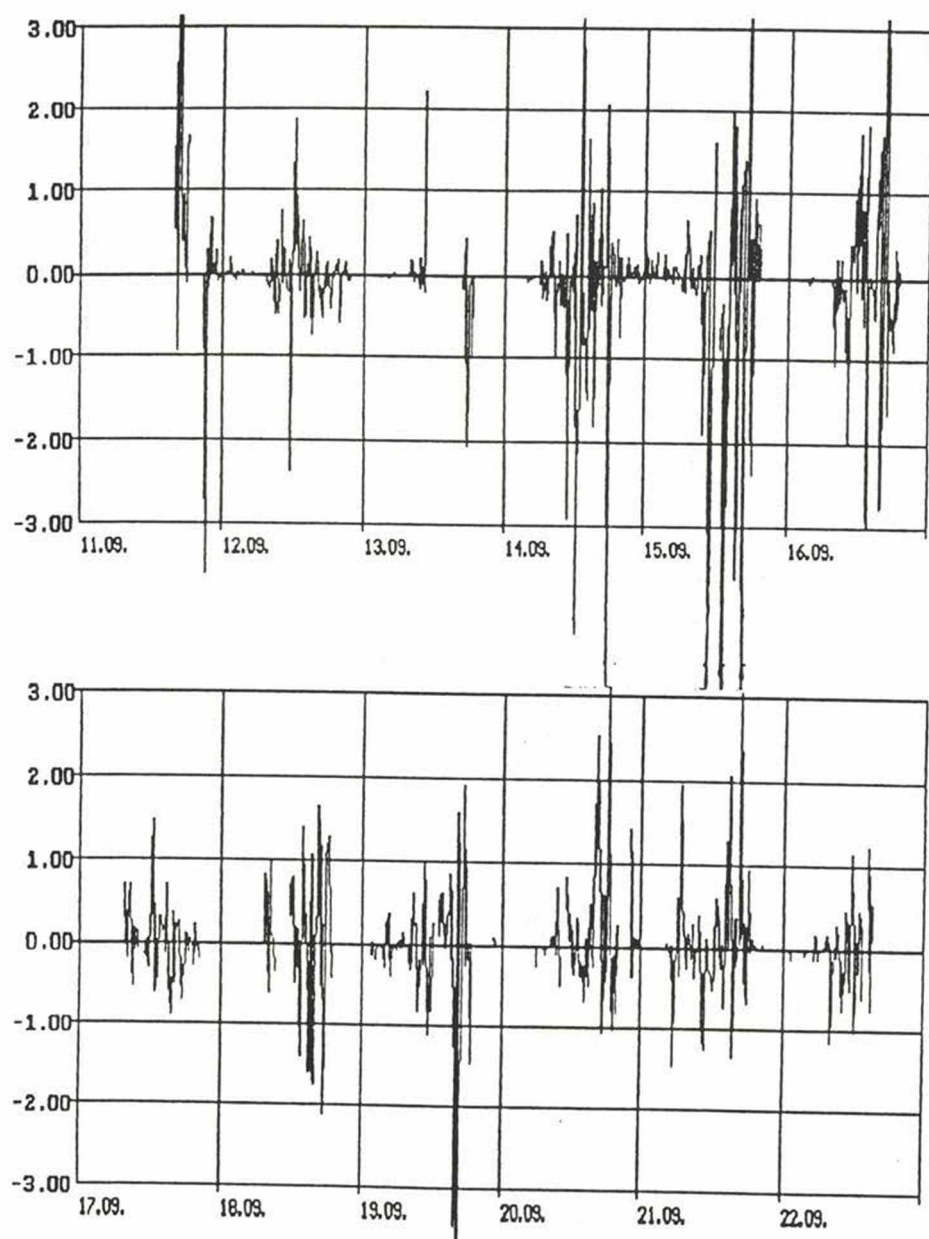


Fig. 10. Deposition velocity of nitric oxide in  $\text{cm s}^{-1}$  (10-22 September)

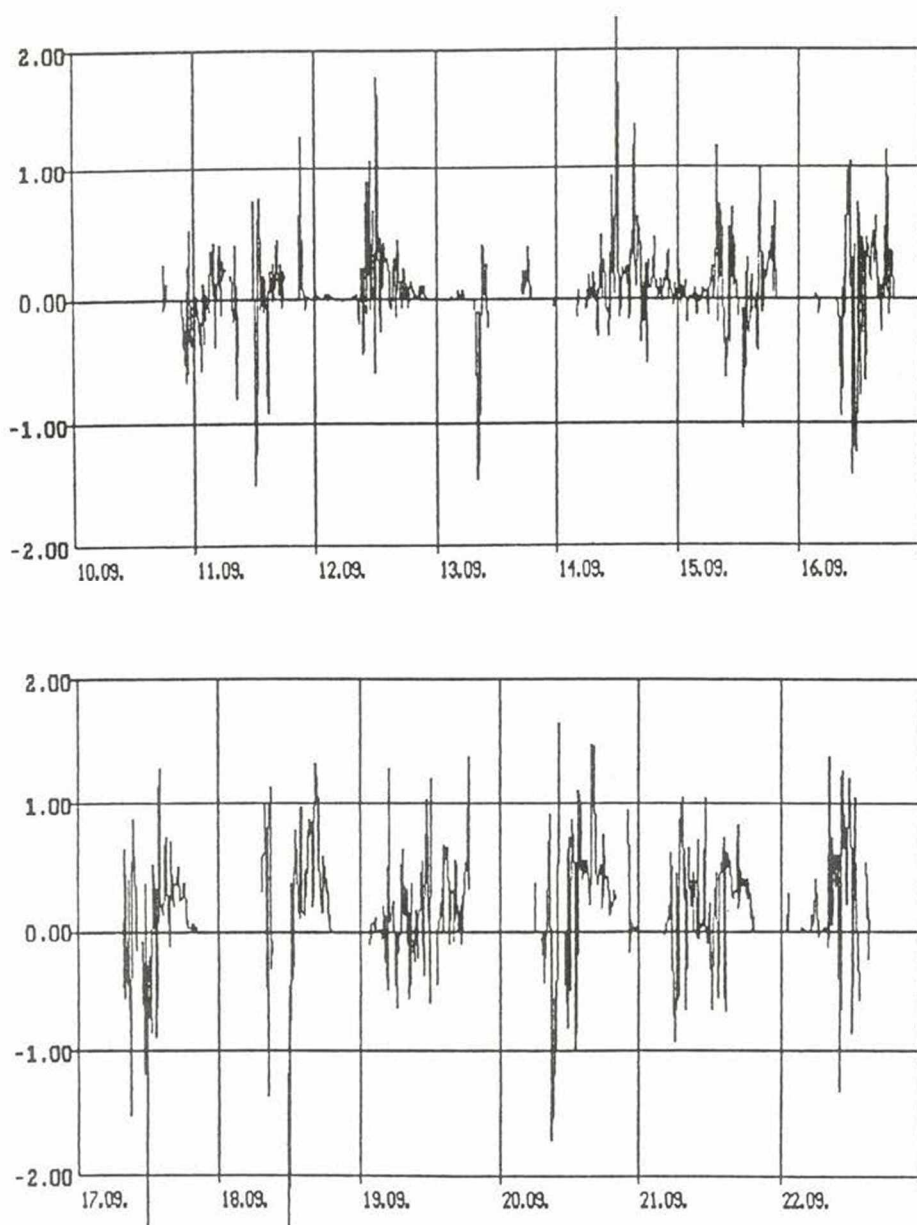


Fig.11. Deposition velocity of ozone in  $\text{cm s}^{-1}$  (10–22 September)

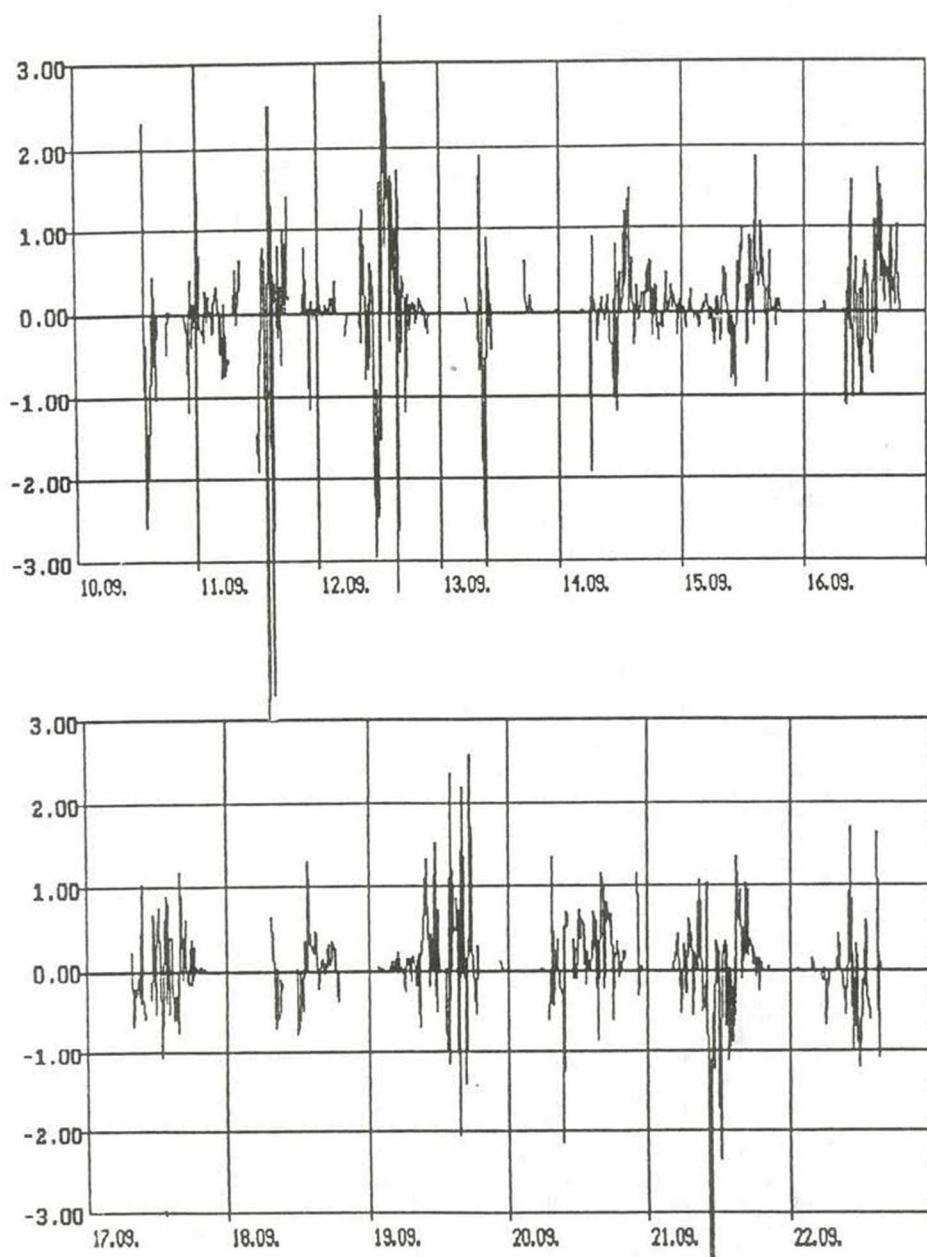


Fig. 12. Deposition velocity of sulfur dioxide in  $\text{cm s}^{-1}$  (10–22 September)

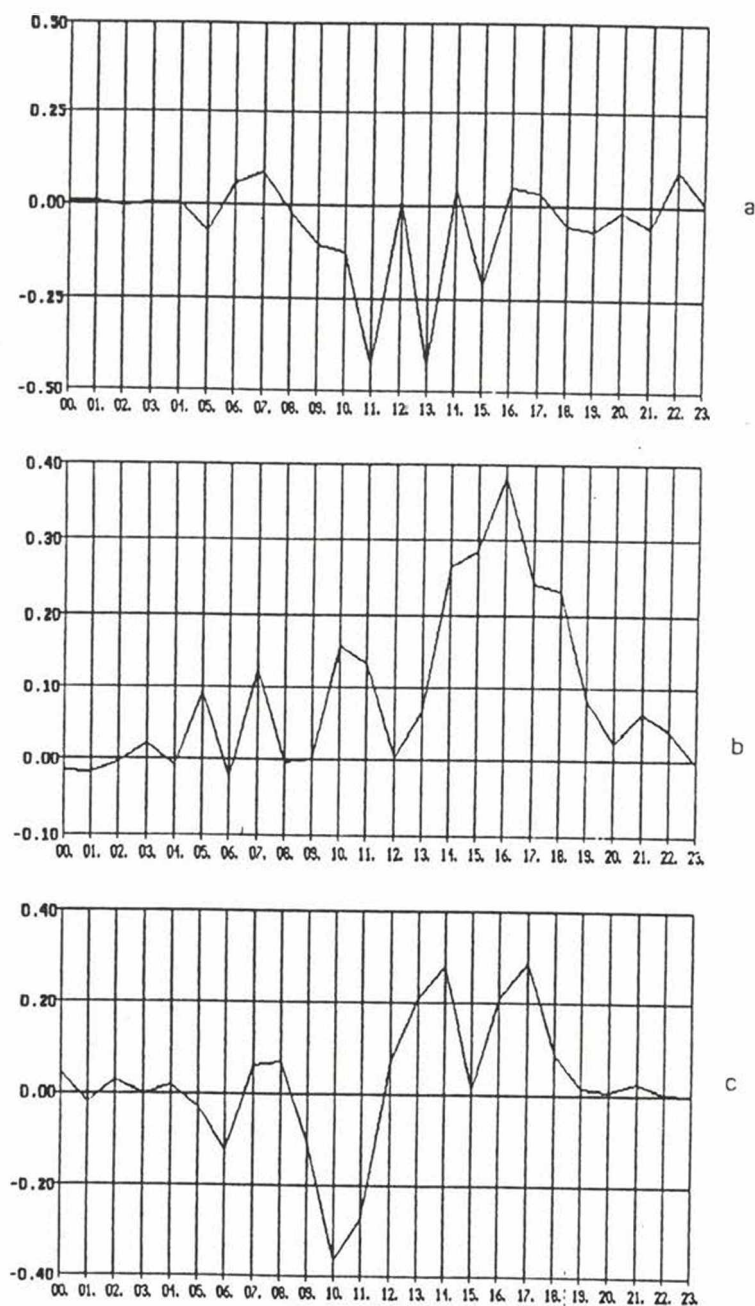


Fig. 13. Average daily variation of deposition velocity of nitric oxide (a), ozone (b) and sulfur dioxide(c) in  $\text{cm s}^{-1}$  (10–22 September)



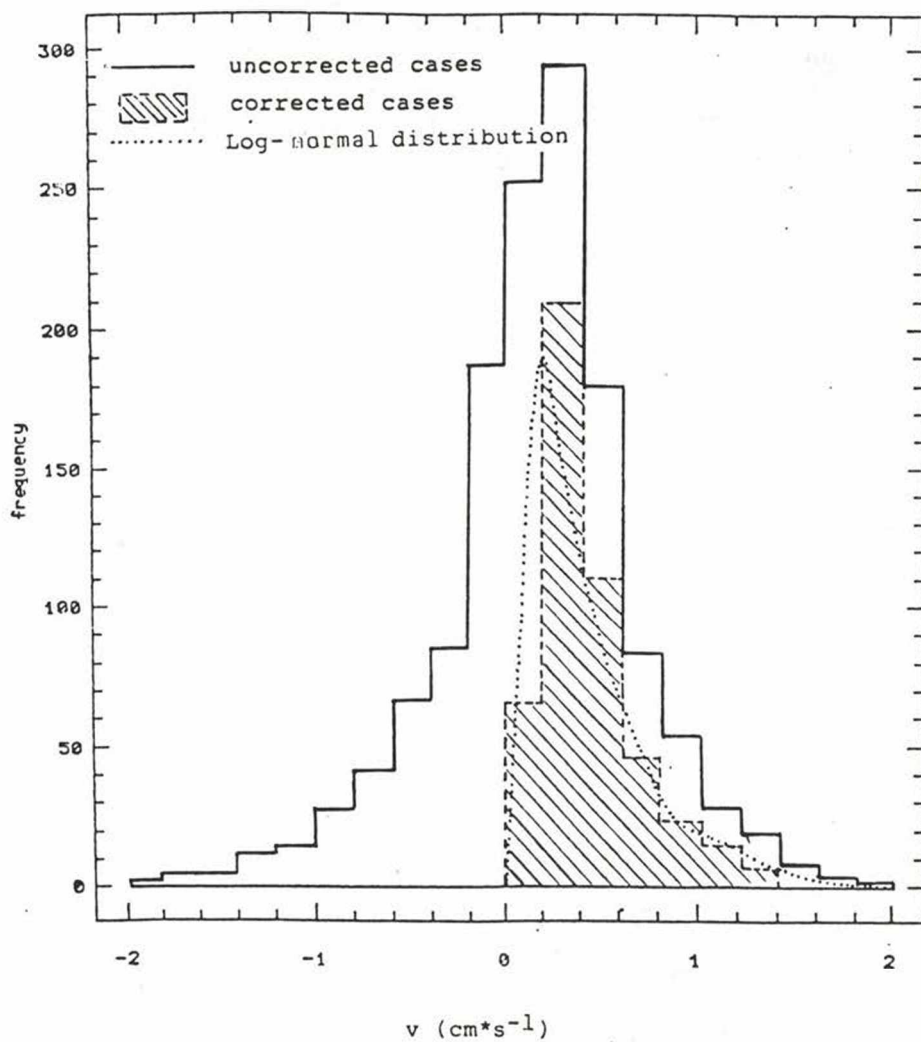


Fig. 14. Frequency distribution of the deposition velocity of ozone (unstable cases)

## References

- Horváth L., Bozó I., Haszpra L., Kopacz J., Molnár Á., Práger T., Weidinger T. 1992. Gradient measurement of air-soil exchange of gases. In: Precipitation scavenging and atmosphere-surface exchange. Hemisphere Publishing Co, Washington, Philadelphia, London 2, 637-647
- Kramm G., Müller H., Fowler D., Höfken K. D., Meixner F. X., Schaller E. 1991. A modified profile method for determining the vertical fluxes of NO, NO<sub>2</sub>, ozone and HNO<sub>3</sub> in the atmospheric surface layer. *J. Atmos. Chem.* 13, 265-288
- TRACT 1992. EUOROTRAC subproject TRACT, operational plan. Institute für Meteorologie und Klimaforschung, Karlsruhe.

# STATISTICAL CHARACTERISTICS OF LOCAL WEATHER WITHIN PÉCZELY'S MACROSYNOPTIC CLASSIFICATION AND ITS MODIFIED VERSION

JÁNOS MIKA\* AND PÉTER DOMONKOS\*\*

\*Hungarian Meteorological Service, Institute for Atmospheric Physics  
H-1675 Budapest, P.O. Box 39, Hungary

\*\*University of Agricultural Sciences H-2103 Gödöllő

**Abstract.** Traditional macrosynoptic classification by Péczely (1957), separating 13 classes, and its alternative (20 classes) are presented and characterized by their relative frequencies and conditional distributions of local weather elements. The alternative classification is derived from the original one by splitting 7 types to low- and high-index realizations with respect to the number of groups formed according to significantly frequent transitions between the original types. Conditional mean anomalies and also standard deviations of temperature, relative sunshine duration and daily precipitation are presented for both classifications in comparison with (unconditional) interdiurnal standard deviations. Conditional mean anomalies for both classifications amount just 30–50%, in annual mean, relative to the interdiurnal standard deviations. The proportion of days with at least a 10 percent decrease of estimation error, achieved by knowing the actual macrosynoptic code is only 40–60%. Thus, the original classification can not separate local weather effectively, but its modification, introduced in this study, does not perform much better, either.

## Introduction

Climatic variables at a given time and location are strongly influenced by the atmospheric circulation. Atmospheric circulation patterns are considered to play a major role in precipitation occurrence, amount and spatial distribution, especially in temperate zones. Determining role of thermal characteristics might be less unequivocal, as they also have some physical "memory", concerning weather in the previous days.

*Macrosynoptic typization* is a description of spatial distribution of the sea level pressure or mid-tropospheric height by subjective or objective methods. Since its first appearance in the literature, probably connected with the names of van Bebbber and Köppen (1895), macrosynoptic types often meet application in diagnostic and sometimes in prognostic tasks of descriptive or applied climatology, weather forecasting (e.g. Barry and Perry 1973), and recently in the environmental meteorology.

Recently, a new stream of definition and application of macrosynoptic classification can be registered. An additional reason to this is the need for regional climate scenarios related to the expected global warming. Most appreciated tools in this concern are the general circulation models producing computer-generated pres-

sure patterns with a resolution which might be adequate to simulate large-scale vortices of atmospheric circulation, but not enough to resolve the regional distribution of meteorological elements, and hence, their changes, with confidence.

There are two ways in the literature to solve the problem of *downscaling* ie. to relate large-scale patterns of macrosynoptic fields to local climate variations. The first is the use of a limited area model, nested into the original GCM with a one-way-coupling (Giorgi et al. 1990). The second way is to combine larger scale averages, or main components of the model-generated fields with empirical relationship, learned on really measured data sets, between the large scale characteristics and targeted regional climate elements (see eg. Mika 1993, for references). In terminology of forecasters, this combination of model generated fields with empirical connections is a "perfect prognosis" approach. That is, a statistical model is developed between dynamic and prognostic quantities in the observed atmosphere, and it is applied to the simulated atmosphere unchanged.

Coupling to this new wave of using macrosynoptic types, the aim of the present study is to quantify the connections between the traditional macrosynoptic types, introduced by Péczely (1957) and local weather. As this connection appears to be not very close, a modification of this classification is also suggested and characterized parallel to the original one. After describing the original classification, the modified version to it is presented. Statistical characteristics, related to the original and modified typization, namely the relative frequencies, the averages and standard deviations are also presented.

## The original Péczely's classification and its modification

### *The original classification (13 types)*

Péczely (1957) defined a macrosynoptic classification, based on the position of the cyclones and anticyclones on the sea-level pressure maps, relative to Hungary. Thirteen types are defined, and grouped according to the direction of the prevailing current:

Types connected with northerly current:

mCc – Hungary is in the rear of an East-European cyclone

Ab – anticyclone over the British Isles

CMc – Hungary is in the rear of a Mediterranean cyclone

Types connected with southerly current:

mCw – Hungary is the fore part of a West-European cyclone

Ae – anticyclone to the east from Hungary

CMw – Hungary is in the fore part of a Mediterranean cyclone

Types connected with westerly current:

zC – zonal, cyclonic

Aw – anticyclone extending from the west

As – anticyclone to the south from Hungary



Types connected with easterly current:

An – anticyclone to the north from Hungary

AF – anticyclone over the Fenno-Scandinavian region

Types of pressure centres:

A – anticyclone centre over Hungary

C – cyclone centre over Hungary

Péczely (1983) also published the transition-matrices and other statistical characteristics of the code-series for 1881–1983. Since his death, Károssy (1987) continues the tradition, determining the actual codes. Makra (1980) published and analyzed time series of half-yearly mean frequencies of the macrotypes.

Péczely's classification has been widely used for diagnostic purpose (eg. Kiss and Károssy 1973, Koppány and Kiss 1985, Maller et al. 1990) to understand connection between the circulation and local weather, sometimes including its variability, too. In air-pollution meteorology, where relatively short series of measurements often obstacle final conclusions, macrotypes can be interfaces between the concentrations and local weather (e.g. Lakatos and Ferenczi 1993).

Subjective identification of discrete categories from pressure patterns, however involves several problems. First, atmospheric modes are continuous, so that the definition of any boundary between classes is arbitrary. Second, atmospheric circulation patterns sometimes switch abruptly, but on other occasions a gradual evolution takes place. Therefore the decision of any two meteorologists may well differ, so no unequivocal classification can be obtained. In the latter concern, related to the original Péczely's macrotypes Kapitány and Maller (1989) quantified the similarity between the original classes by averaging subjective categorization of experienced synopticians. The collected similarity matrix suggests that there are classes in the original classification, which are quite similar to each other. The authors of the study found these similarities enough to aggregate the original 13 classes into 9 for verification of pressure fields, operatively issued by numerical forecast centers.

Bartholy and Gulyás (1980) investigated the connections between subjective codes, determined by Péczely from the surface pressure patterns and objective codes yielded by an objective algorithm, using 500 hPa fields, creating in this way the mid-tropospheric version of the original types. Although the authors establish (below their Table 1.), that "The code determined by the synoptician ... is in surprisingly good agreement with the code determined on the basis of the AT<sub>500</sub> field ...", the Table 1 of the quoted study indicates that the coincidence is far not so unequivocal. That is, for at least 6 types from the 13, there are two or more objective AT<sub>500</sub> configurations with equivalent frequency, and several objective AT<sub>500</sub> patterns correspond to different Péczely's types with large frequency. This questionable correspondence does not mean, that the synoptic coding is bad, as the correspondence between surface pressure patterns and mid-tropospheric fields is just stochastic,

since they both are horizontal cuts of the real atmospheric processes being rather three-dimensional, especially in such a mountainous area, like the Carpathian Basin and its surroundings.

On the other hand,  $AT_{500}$  patterns cover the whole Atlantic-European region, so they represent larger scales, than the original classification is based on. The importance of this difference can also be proven applying the seasonal objective typization, (Ambrózy et al. 1984), which is a generalization of European macrotypes by Hess and Brezowsky (1969). Applying calculations of Péczely (1983, Tables 8–11), the similarity in averaged 500 hPa fields of the European macrotypes, appearing parallel to any fixed Hungarian macrotype with a significant frequency (at 90% level) is frequently weak or medium (Table 1). Using scoring values, scaled from 1 to 9 (Ambrózy et al. 1984), 54% of comparisons yield values 3–5 in annual average.

This difference, ie. that macrotypes defined in a "window" around Hungary, can frequently be formed by different continental-scale processes is a possible reason of the shortcoming of the original macrotypes, experienced in the practical work with them and also suggested by the figures and tables of the above mentioned studies. This is, that local weather elements can not be determined exactly enough knowing just the actual macrosynoptic code. This is considered to be a limit of using stratified samples to estimate climatic means from small samples, based on Péczely's classes (Mika et al. 1993).

Whether or not this is the reason, we try to determine after deriving a new classification described in the next section, based on the sequence of consecutive macrotypes investigating the frequent transitions from one type to another.

#### *The modified typization (20 types)*

Facing the above mentioned shortcomings, it is decided to registrate pairs of macrotypes following each other with a significant frequency, as compared to the frequency of unconditional occurrence (according to chi-square test at 80% level). Unconditional and conditional probabilities are taken from Péczely (1983, Table 3, in combination with Tables 4 and 6). The transition from any type into the other, has been established to be significantly frequent for the season, if

- I. the relative frequency of transition from the preceeding type into the investigated one is significantly higher than the unconditional appearance of the latter one in at least two months of the season, and
- II. the average from the three monthly relative frequencies is also higher than the significance threshold.

The results of applying this two parallel criteria is demonstrated in Fig. 1, where the arrows between appropriate macrotypes indicate significantly frequent transitions in the given direction in any season of the year. Such transition into one fixed type can be seen from rather different types, in some cases.



Sorting these transitions into groups promises the answer to the question, whether the set of significant transitions form one or more groups? (To illustrate this, somewhat complicated algorithm of sorting the macrotypes into subgroups 1 or 2, see Table 2).

First, it is investigated relative to a given, fixed type, whether the macrotypes preceeding it with significant frequency, can be organized into a chain (open, closed or having more than one side-branch) in any way, or not. In the latter case two subgroups (1 and 2) are defined, relative to the original type, as different versions of the original type. In the first case the macrotype remains unchanged. (No more than two chains could be formed relative to any fixed type.)

In this first step of sorting only 1-5 types, preceeding the fixed original types can be sorted into subgroups 1 or 2. For the remainder it has been determined, that members of which newly formed group (completed already by those which frequently preceed the fixed ones) can follow them with a significant frequency.

If this step is still not resultative, a new iteration has been done on the same basis. For types, being connected to both groups (relative to the fixed type), the following decision has been made: The preceeding macrotype has been attributed to the group from which these connections repeated themselves more frequently.

The above described splitting of the macrotypes, introduced completely by a mathematical algorithm, can also be interpreted in terms of large-scale circulatory patterns. Transitions forming group 1 correspond to zonal ("high-index") processes, while those from group 2 represent blocking-type ("low index") patterns at larger scales. However, this is just a consequence of the applied algorithm, not a preliminarily followed distinction.

## Conditional climatology for the classification

In the following we characterize features of both classifications separately for relative frequencies, conditional averages and standard deviations, because the usefulness of any macrosynoptic classification can be considered or compared to another one only in connection with the practical task, they are applied in. Some of these tasks rely on short samples and need as little number of individual types, as possible, while others operate on long series where more types, giving better separation of the local weather, are allowed. Importance of shape differences in the average deviations between the classes, as compared to the remained uncertainty (after recognizing the actual macrosynoptic codes), as measures of skill related to the classification, also depend on the decision function, characterizing the problem. Having these decision function, the following three characteristics can be combined into one criterium, qualifying the typizations, in question.

## FREQUENCY STATISTICS OF THE TWO CLASSIFICATIONS

Monthly mean relative frequencies of all individual types are documented in Table 3, according to the recent 1961–1990 climate normal period. Its descriptive analysis would fall out of the scope of this study, but a comparison of these numbers with those from the previous decades might be of interest.

## BASIC STATISTIC OF THE CONDITIONAL DISTRIBUTIONS

We analyzed the efficiency of the classifications on daily data of temperature, sunshine duration and precipitation, registered in Debrecen CLINO Station for 1961–1990. In order to filter out the annual course of the elements, a specially derived anomaly of temperature is introduced. This is the difference between actual temperature and the thirty years average of the surrounding 5 days (2 before and 2 after). For the sunshine duration, the proportion of the actual values compared to the maximum possible value is applied, and named as relative sunshine duration. (for daily precipitation totals no transformation has been applied.)

These two operations cause very different decreases in the standard deviations of the elements. For temperature this fine account of the annual course, even within the months could decrease the standard deviation by as much as 6% in the average of 12 months, with maxima in the transient seasons (14% in March, 10, 12 and 10% in September, October and November). At the same time, for sunshine duration the effect of day-by-day smoothing of the annual course is only 0.3%. This means, that interdiurnal variation of the latter element is much more irregular as compared to its annual course, as in case of temperature.

Monthly standard deviations of the three elements are represented in Fig. 2 as reference values for conditional averages and standard deviations within both classifications in the following.

### *1. Average anomalies*

Our classifications are related only to one single station. A detailed presentation of conditional mean anomalies within each individual macrotype would not be too informative, but rather extensive. On the other hand conditional averages for different stations, months and elements are published by Péczely (1961) and in other applications. Difference in the reference periods, compared to that in the present study, can cause changes, that are minor relative to the interdiurnal variability of the elements.

In Fig. 3, therefore, the behaviour of a more integrated characteristic can be investigated for both the original and the new classifications. This is the mean deviation of conditional anomalies from zero ( $\overline{M^2}$ ), normalized by the appropriate unconditional standard deviations (see Fig. 2), yielded by squared averaging from the absolute values of means from each macrotype.



Not any squared mean monthly anomaly is higher, than 70 % for the three weather elements in the Fig. 2. No definite annual course can be established, although values in the neighbouring months are not without any regularity, especially if separating them into summer and winter half-years, only. In this case, the macrosynoptic types specify local weather somewhat more successfully in the winter half-year for the temperature and precipitation, but with less skill for the sunshine duration.

Annual mean values of these normalized average deviations are presented in Table 4, as completed by their values ( $\overline{|M|}$ ) calculated with not squared, but linear averaging. Besides the trivial mathematical consequence of differences in averaging, that ( $\overline{|M|}$ ) is always less than ( $\overline{M^2}$ ), one can establish, that higher number of classes do not mean higher normalized average differences of the conditional averages in all cases.

General values for the latter classifications are only 30–50 % in rounded numbers. The degrading sequence between the 3 investigated elements in this concern is temperature, relative sunshine duration and precipitation, where information about the actual macrosynoptic code gives the less deviation from zero anomaly, in average.

## 2. Standard deviations

Comparing the standard deviation of a weather element in an individual group to the (unconditional) standard deviation in the whole sample (see Fig. 2), we get information about the similarity of weather inside the given group. In a more pragmatic interpretation, conditional standard deviation is a measure of the error caused by the operation of using conditional averages, instead of the measured values. So, the proportion of conditional standard deviations to their unconditional values is a measure of information, gained by using (perfectly identified) macrotypes.

Investigating monthly standard deviations averaged for all macrotypes of the original classifications and the new one (Tables 5, 6 and 7), we can see that majority of the numbers are below 100, especially for precipitation with those, related to the new one, it can be concluded, that in the majority of cases the former ones are between the values of the splitted types. Several cases for temperature, and some for sunshine duration are exceptions, where our trial to narrow the uncertainty by splitting perform well.

Standard deviations with higher than 100 % are distributed rather unevenly between the types and season for the temperature, while a more common picture can be investigated for the other two elements. For the sunshine duration high standard deviations are concentrated mainly in anticyclonic classes in the winter half-year, but for precipitation they are specific features of the cyclonic types, practically in the whole year. The latter means that 'wet' types have bigger standard deviations than 'dry' ones.

Comparing standard deviations in the splitted groups 1 vs. 2, no considerable differences can be established: Values in group 1 (high index) are higher than in the opposite one in 54, 49 and 53 % of all months and types for temperature, sunshine duration and precipitation, respectively.

Annual characteristics of distributions for high and low relative standard deviations are presented in Table 8. Relative frequency of macrotypes with  $> 100$  % and  $< 71$  % values (ie. 50 % in relative variance) represent a minority of all cases, except for precipitation. Between the original and new classifications one can not make a significant difference, because even for the same element the conclusion on the basis of  $> 100$  % cases is sometimes contradictory comparing to that from  $< 71$  % cases.

However, if one wants to decide, whether the information about the actual macrosynoptic code can yield a substantial narrowing of uncertainty in local wether, relative frequencies of the classes should also be considered. This has been done before preparing Fig. 4, where the proportion of days with more than 10 % narrowing the uncertainty (ie. falling into individual types, with normalized standard deviation, less than 90 % according to Tables 5, 6 or 7), relative to the whole 30 years period is represented.

Annual course of these proportions is somewhat hectic, because this criterium is rather nonlinear, ie. dramatic difference exists between 89.9 and 90.1 % of normalized standard deviations. This can cause fluctuations, that are more random, than regular. This hectic feature might also be a reason of the impression, that there is no serious annual course in the diagrams.

Proportion of days with this rather modest gain of information (ie. 10 %) is rarely higher than 70, but sometimes less than 30 %. Comparing the original classification to the new one, we can establish that for temperature and sunshine duration the increased number of classes can cause some gain in the proportion of narrowed uncertainty, but for precipitation there are months with both higher and lower propotions, too. Annual mean frequencies of the 10 % gain by knowing the actual codes of the classifications are 61 and 50 % for temperature, 44 and 40 % for sunshine duration and 63 and 61 % for precipitation, respectively.

## Discussion

Our results generally show, that the Péczely's widely used macrosynoptic classification is suprisingly ineffective in narrowing the uncertatinty (natural interdiurnal variation) of the local weather. Unfortunately the presented attempt of the better classification by splitting a part of them, does not promise substantially better results, either.

The question arising after this, can be argued as which one is true from the three possible statements, i.e.

- a) macroscale circulation itself can determine local weather only with moderate efficiency,
- b) classification, and especially coding, of macrotypes subjectively is rather imperfect, or
- c) the only problem is, that surface pressure patterns alone, even using just as snapshots to characterize weather processes for 24 hours (especially with a 12 hours shift, in average) are not enough to characterize significant events of circulation, and our first trial (leading to 20 types) to eliminate this two sources of errors in one step, performed unsuccessfully, too.

Not excluding the theoretical possibility of a) and b) as general conclusions, our next attempt will follow the working hypothesis, that eliminating c) must lead much better macrosynoptic types, as practical tools. To realize this objective and to be able to choose between statements a), b) and c), combinations of Péczely's types from 2-3 consecutive days with codes of mid-tropospheric types by Hess and Brezowsky (1969) will be tested.

\* \* \*

**Acknowledgements:** The authors thank Prof. C Károssy at Berzsenyi College, Szombathely for making the updated sequence of original macrotypes available. Our study was partly supported by the contract OTKA-268 with the Hungarian Academy of Sciences.

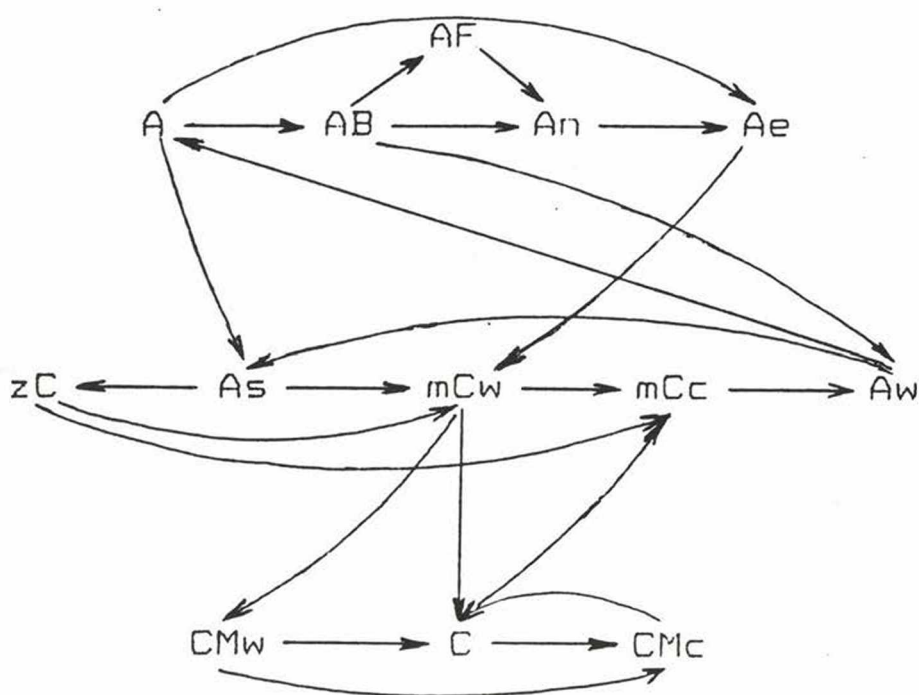


Fig. 1. Significantly frequent transitions between the original Pécze's classes in at least one season



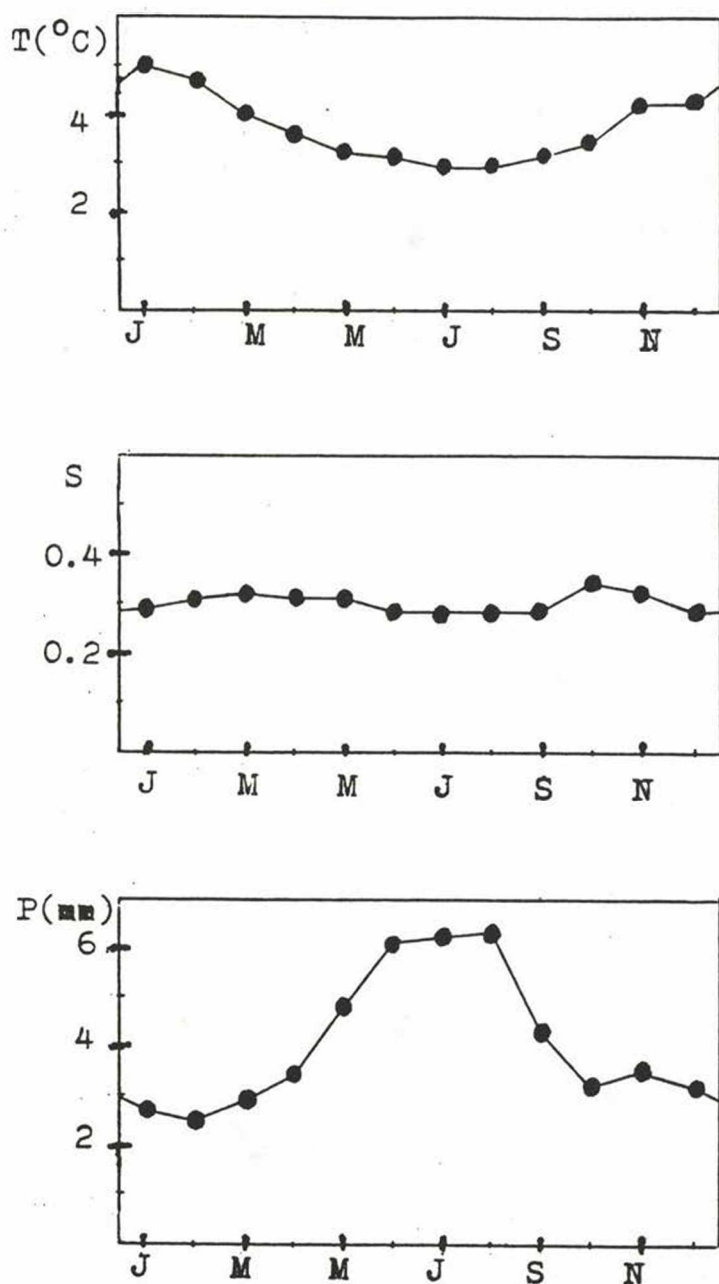


Fig. 2. (Unconditional) standard deviations of daily temperature (T), relative sunshine duration (S) and precipitation (P) anomalies for Debrecen in 1961–1990

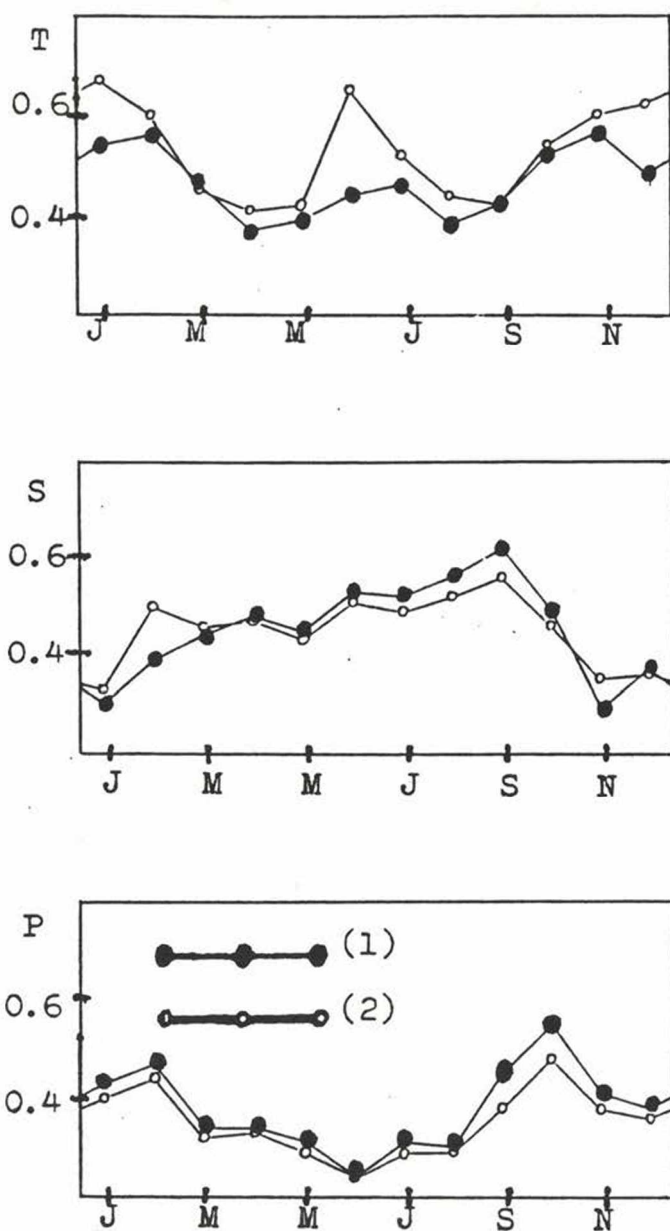


Fig. 3. Proportion of conditional mean anomalies, relative to the interdiurnal standard deviation in the original (1) and newly derived (2) classifications for the different months and elements in Debrecen (T, S and P, respectively)

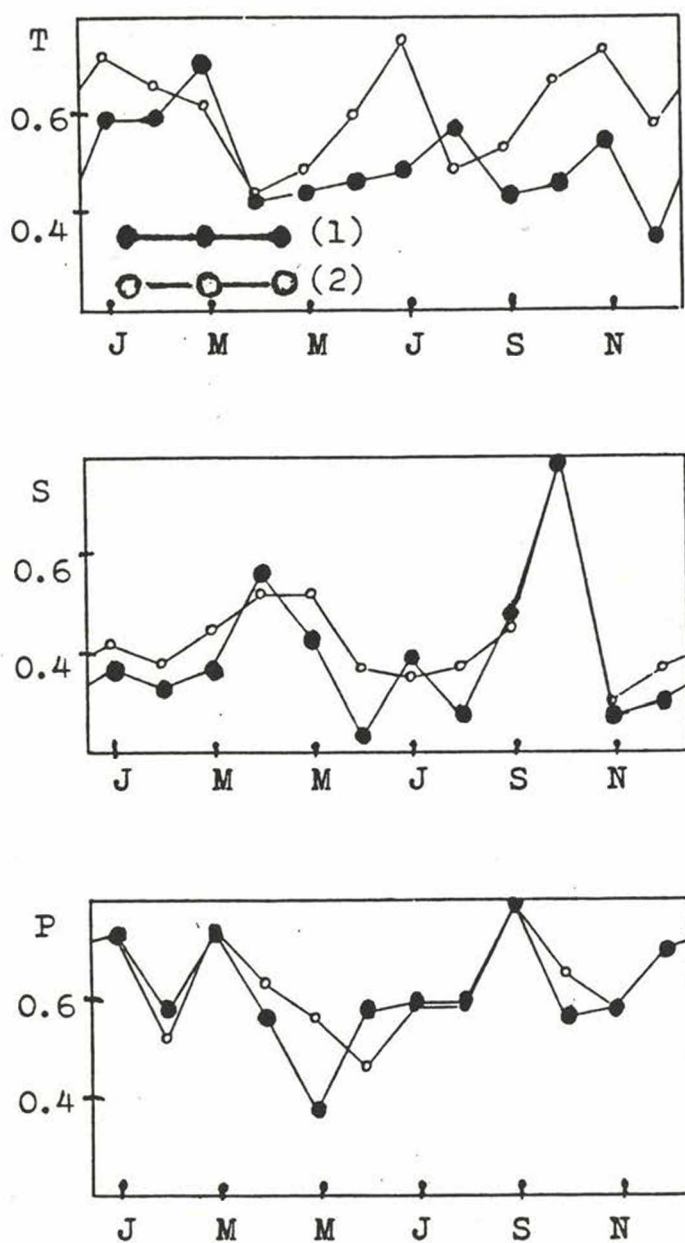


Fig. 4. Proportion of days with more than 10 % narrowing the uncertainty in the original (1) and newly derived (2) classifications for the different months and elements in Debreceen (T, S and P, respectively)

**Table 1.** Frequency distribution of similarity "scores" for larger-scale macrotypes (Ambrózy et al. 1984) that occur significantly frequently parallel with the original Péczely's macrotypes.

Season/Score	1	2	3	4	5	6	7	8	Total
Winter	—	—	—	4	36	21	7	—	68
Spring	—	—	6	16	41	53	13	—	129
Summer	—	—	—	—	—	—	12	—	12
Autumn	—	—	2	11	25	8	7	—	53
Annual	—	—	8	31	102	82	39	—	262

**Table 2.** Split of 7 macrotypes as determined by the previous ones:

1 – zonal (high index) 2 – meridional (low index) realization of the original types. (Results of the first iteration are set bold)

To/From:	mCc	AB	CMc	mCw	Ae	CMw	zC	Aw	As	An	AF	A	C
AB	<b>1</b>	—	<b>1</b>	<b>1</b>	<b>2</b>	<b>1</b>	<b>1</b>	<b>1</b>	<b>1</b>	<b>2</b>	<b>2</b>	<b>2</b>	<b>1</b>
mCw	<b>1</b>	<b>1</b>	<b>1</b>	—	<b>2</b>	<b>2</b>	<b>1</b>	<b>1</b>	<b>1</b>	<b>2</b>	<b>2</b>	<b>1</b>	<b>1</b>
Ae	<b>1</b>	<b>2</b>	<b>1</b>	<b>1</b>	—	<b>1</b>	<b>1</b>	<b>2</b>	<b>1</b>	<b>2</b>	<b>2</b>	<b>1</b>	<b>1</b>
zC	<b>1</b>	<b>1</b>	<b>2</b>	<b>1</b>	<b>1</b>	<b>1</b>	—	<b>1</b>	<b>1</b>	<b>2</b>	<b>2</b>	<b>1</b>	<b>1</b>
Aw	<b>1</b>	<b>2</b>	<b>1</b>	<b>1</b>	<b>2</b>	<b>1</b>	<b>1</b>	—	<b>1</b>	<b>2</b>	<b>2</b>	<b>2</b>	<b>1</b>
An	<b>1</b>	<b>2</b>	<b>1</b>	<b>1</b>	<b>2</b>	<b>1</b>	<b>1</b>	<b>1</b>	<b>1</b>	—	<b>2</b>	<b>2</b>	<b>1</b>
A	<b>1</b>	<b>2</b>	<b>1</b>	<b>2</b>	<b>2</b>	<b>1</b>	<b>1</b>	<b>1</b>	<b>1</b>	<b>2</b>	<b>2</b>	—	<b>1</b>

**Table 3.** Frequency (per mille) of the 13 original Péczely's macrotypes (in bold setting) and the splitting 7 types, 1961–1990

	Jan	Feb	Mar	Apr	May	Jun	Jul	Aug	Sep	Oct	Nov	Dec
mCc	<b>61</b>	<b>66</b>	<b>59</b>	<b>97</b>	<b>98</b>	<b>116</b>	<b>97</b>	<b>76</b>	<b>42</b>	<b>33</b>	<b>46</b>	<b>46</b>
AB/1	17	45	27	37	49	46	52	43	58	34	23	29
AB/2	14	18	11	41	14	42	48	24	24	15	29	19
AB	<b>31</b>	<b>63</b>	<b>38</b>	<b>78</b>	<b>63</b>	<b>88</b>	<b>100</b>	<b>67</b>	<b>82</b>	<b>49</b>	<b>52</b>	<b>48</b>
CMc	29	45	27	70	39	32	22	17	23	19	29	33
mCw/1	44	60	52	70	60	66	43	47	23	41	58	62
mCw/2	45	33	56	44	68	23	15	29	46	46	38	48
mCw	<b>89</b>	<b>93</b>	<b>108</b>	<b>114</b>	<b>128</b>	<b>89</b>	<b>58</b>	<b>76</b>	<b>69</b>	<b>87</b>	<b>96</b>	<b>111</b>
Ae/1	70	61	88	57	44	30	26	55	86	124	84	74
Ae/2	118	81	78	42	34	36	34	46	58	88	72	55
Ae	<b>188</b>	<b>143</b>	<b>167</b>	<b>99</b>	<b>78</b>	<b>66</b>	<b>60</b>	<b>101</b>	<b>143</b>	<b>212</b>	<b>157</b>	<b>129</b>
CMw	69	112	110	111	74	60	28	43	69	68	127	76
zC/1	40	41	51	30	39	31	42	24	22	15	53	66
zC/2	0	1	4	6	3	1	0	4	6	1	2	1
zC	<b>40</b>	<b>43</b>	<b>55</b>	<b>36</b>	<b>42</b>	<b>32</b>	<b>42</b>	<b>28</b>	<b>28</b>	<b>16</b>	<b>56</b>	<b>67</b>
Aw/1	91	47	109	73	77	137	166	99	83	88	61	97
Aw/2	61	53	31	32	42	64	101	98	93	66	61	65
Aw	<b>153</b>	<b>100</b>	<b>140</b>	<b>106</b>	<b>119</b>	<b>201</b>	<b>267</b>	<b>197</b>	<b>177</b>	<b>154</b>	<b>122</b>	<b>161</b>
As	69	55	48	41	34	24	31	26	57	54	78	71
An/1	87	90	60	51	75	48	34	69	51	37	41	48
An/2	45	72	60	62	69	69	85	78	67	95	31	51
An	<b>132</b>	<b>162</b>	<b>120</b>	<b>113</b>	<b>144</b>	<b>117</b>	<b>119</b>	<b>147</b>	<b>118</b>	<b>131</b>	<b>72</b>	<b>99</b>
AF	26	27	41	29	73	32	43	26	26	19	20	26
A/1	68	38	37	29	40	72	91	102	104	74	51	73
A/2	33	41	32	30	19	31	26	37	53	76	72	49
A	<b>101</b>	<b>79</b>	<b>69</b>	<b>59</b>	<b>59</b>	<b>103</b>	<b>122</b>	<b>139</b>	<b>158</b>	<b>151</b>	<b>123</b>	<b>123</b>
C	12	12	19	48	47	40	12	18	9	6	23	10



**Table 4.** Annual mean deviation of the conditional average anomalies from zero, expressed in percentage of the appropriate interdiurnal standard deviations (see in Fig. 2), applying linear ( $|M|$ ) and squared ( $M^2$ ) averaging from the absolute values related to the individual macrotypes and months

	Temperature		Sunshine duration		Precipitation	
	$ M $	$M^2$	$ M $	$M^2$	$ M $	$M^2$
20 types	43.2	52.8	37.1	45.3	29.1	35.0
13 types	39.7	46.5	37.8	45.3	30.5	37.8

**Table 5.** Conditional standard deviations of temperature within the original (13) and new splitted macrotypes, as expressed in percentage of the standard deviations (presented in Fig. 2). Values, higher in the 7 original classes being splitted, than both in their 1 and 2 versions, separately are underlined.

	Jan	Feb	Mar	Apr	May	Jun	Jul	Aug	Sep	Oct	Nov	Dec
mCc	99	96	82	95	101	88	102	98	110	102	67	97
AB	<u>114</u>	88	88	82	<u>81</u>	101	104	96	87	77	99	73
AB/1	<u>111</u>	81	95	84	74	95	109	87	90	71	111	62
AB/2	78	101	60	75	72	104	87	104	68	84	87	81
CMc	91	85	98	123	90	108	113	112	100	91	88	108
mCw	81	96	105	<u>91</u>	97	88	80	89	98	<u>94</u>	110	98
mCw/1	87	84	90	91	102	91	84	94	110	86	115	106
mCw/2	68	117	117	88	91	61	55	66	89	74	101	87
Ae	96	94	86	86	<u>84</u>	51	85	79	71	<u>92</u>	<u>94</u>	94
Ae/1	114	110	82	88	83	54	105	77	73	90	85	91
Ae/2	85	80	88	84	63	49	68	80	68	89	86	93
CMw	88	90	90	102	104	85	86	123	94	113	92	95
zC	65	43	89	<u>87</u>	94	94	83	96	80	78	74	94
zC/1	65	43	92	85	97	90	83	95	83	80	73	90
zC/2	—	—	50	76	69	—	—	108	75	—	—	—
Aw	81	<u>56</u>	90	80	86	<u>95</u>	<u>93</u>	99	82	<u>77</u>	75	76
Aw/1	75	52	84	74	76	87	88	85	78	77	81	81
Aw/2	84	56	109	88	89	91	88	103	86	76	70	66
As	77	83	80	94	105	74	96	88	95	89	83	92
An	75	87	100	98	<u>85</u>	91	<u>70</u>	90	93	<u>100</u>	<u>89</u>	88
An/1	66	94	100	103	84	93	70	85	90	94	88	89
An/2	80	77	101	92	85	84	68	94	95	98	86	78
AF	74	104	104	97	97	103	75	81	127	87	79	63
A	<u>118</u>	<u>108</u>	85	87	93	87	90	89	98	84	<u>73</u>	<u>91</u>
A/1	99	81	80	59	90	84	80	92	91	75	70	80
A/2	115	101	92	108	100	93	106	78	111	92	68	73
C	64	53	83	90	96	109	85	80	100	86	99	77

Table 6. The same as Table 5 for the relative sunshine duration

	Jan	Feb	Mar	Apr	May	Jun	Jul	Aug	Sep	Oct	Nov	Dec
mCc	85	86	84	86	93	95	105	116	104	88	96	111
AB	95	<u>108</u>	93	96	91	95	99	92	87	98	99	129
AB/1	71	106	87	100	95	87	102	95	87	96	88	130
AB/2	116	107	102	91	73	100	96	88	89	104	107	131
CMc	68	85	82	87	87	103	93	119	109	71	68	74
mCw	<u>75</u>	71	85	90	88	96	88	111	97	88	<u>84</u>	70
mCw/1	74	65	85	90	89	95	91	116	92	82	84	74
mCw/2	75	82	87	90	89	97	75	100	101	90	83	66
Ae	107	105	89	89	79	88	77	79	77	89	104	105
Ae/1	109	99	88	88	70	62	72	75	75	85	100	105
Ae/2	105	108	91	91	86	98	81	84	80	95	109	107
CMw	50	65	80	96	97	97	91	104	106	87	61	34
zC	80	94	91	92	88	87	101	94	88	86	98	78
zC/1	80	91	88	97	87	89	101	97	94	89	99	79
zC/2	—	—	102	73	124	—	—	64	61	—	—	—
Aw	99	100	92	95	99	94	94	99	102	86	106	99
Aw/1	93	109	91	93	88	100	96	103	107	89	109	101
Aw/2	107	90	96	98	117	81	91	95	99	82	101	98
As	73	105	82	82	88	71	47	60	82	83	97	91
An	<u>127</u>	114	<u>104</u>	101	98	94	85	93	<u>100</u>	96	114	130
An/1	125	116	102	104	95	95	89	106	100	101	118	111
An/2	126	111	102	97	102	88	84	75	98	90	112	140
AF	123	100	101	88	97	97	98	102	93	102	114	118
A	100	103	101	83	51	<u>71</u>	65	65	71	86	<u>111</u>	97
A/1	108	106	96	87	53	71	68	63	70	86	107	90
A/2	79	101	107	80	47	70	51	73	72	86	100	106
C	72	2	62	75	88	98	97	95	72	117	42	11

Table 7. The same as Table 5, for the precipitation

	Jan	Feb	Mar	Apr	May	Jun	Jul	Aug	Sep	Oct	Nov	Dec
mCc	167	133	88	138	139	112	151	127	197	126	163	81
AB	38	34	98	51	117	57	115	75	65	82	40	70
AB/1	21	40	105	65	86	61	94	91	74	98	56	69
AB/2	52	8	80	35	193	52	134	31	39	6	12	73
CMc	88	109	72	154	58	72	94	86c	138	182	88	132
mCw	116	130	196	132	93	136	106	136	109	93	152	146
mCw/1	124	121	138	88	83	139	104	121	119	59	141	164
mCW/2	107	146	237	180	102	127	112	161	105	113	168	121
Ae	66	71	52	21	44	121	123	47	72	119	52	82
Ae/1	64	76	58	26	46	35	42	51	64	154	51	851
Ae/2	68	67	45	9	41	160	158	42	83	28	54	79
CMw	176	141	143	135	111	98	230	145	247	174	123	158
zC	108	123	50	32	37	107	43	44	47	186	117	120
zC/1	108	125	51	31	39	108	43	29	50	191	119	121
zC/2	-	-	41	38	11	-	-	90	26	-	-	-
Aw	53	77	57	53	43	87	75	127	36	70	48	49
Aw/1	51	32	63	51	23	79	72	61	40	86	43	51
Aw/2	56	99	32	58	64	102	79	169	32	37	53	46
As	86	108	42	44	42	73	19	46	49	18	40	46
An	53	29	48	33	108	87	86	85	46	42	95	61
An/1	55	31	54	23	85	77	127	119	14	49	95	81
An/2	50	26	41	39	129	94	63	33	60	39	97	31
AF	56	19	37	34	112	163	95	89	12	44	78	45
A	22	30	18	38	60	48	22	14	25	19	27	52
A/1	22	40	17	53	73	56	24	12	31	25	14	30
A/2	22	16	20	5	0	20	12	19	2	9	33	74
C	262	152	146	114	152	126	54	147	115	211	144	103

Table 8. Annual mean proportion of macrosynoptic types (%) with poor (&gt; 100 %) and fairly good (&lt; 71 %) performance in narrowing the standard deviation of the investigated element within the macrotypes, as compared to their unconditional values.

	Temperature		Sunshine duration		Precipitation	
	s > 100 %	s < 71 %	s > 100 %	s < 71 %	s > 100 %	s < 71 %
20 types	19.6	13.3	29.4	12.1	32.5	51.2
13 types	17.9	5.8	25.0	13.5	40.4	42.3

## References

- Ambrózy P., Bartholy J., Gulyás O. 1984; A system of seasonal macrocirculation patterns for the Atlantic-European region. *Időjárás* 88, 121–133
- Barry R. G., Perry A. H., 1973; *Synoptic Climatology*. Methuen & Co. Ltd, London
- Bartholy J., Gulyás O. 1980; A method of analysing macrosynoptic types using analogy indices. *Acta Climatologica, Acta Universitatis Szegediensis*, 16/17, 1–4, 11–17
- Giorgi F., Marinucci M. R., Visconti G. 1990; Use of a limited area model nested in a general circulation model for regional climate simulation over Europe. *J. Geophys. Res.* 95, 18413–18431
- Hess P., Brezowsky H. 1969; Katalog der Grosswetterlagen Europas. *Berichte des Deutschen Wetterdienstes*. 15, 113, Offenbach
- Kapitány E., Maller A. 1989; Hungarian experiences in the use of NWP products from the ECMWF and WMC Washington. *Hungarian Meteorological Service, Budapest*, p. 16
- Károssy Cs. 1987; Péczely's catalogue of macrosynoptic types (1983–1987). *Légtér* 32, 3, 28–30 (in Hungarian)
- Kiss Á., Károssy Cs. 1973; Charakteristiken der Tagesschwankung der Temperatur auf dem südlichen Teil der ungarischen Tiefebene. *Acta Climatologica, Acta Universitatis Szegediensis*, 12, 1–4, 19–46
- Koppány G., Kiss Á. 1958; Variability of temperature and wind direction in Péczely's macrosynoptic situations in Szeged. *Időjárás* 89, 269–277
- Lakatos M., Ferenczi Z. 1993; Investigation of background air pollution in connection with circulation conditions over Hungary. In: *Proceeding of the Geophysics and Environment: Background Air Pollution Meeting*, 16–18 June 1992, Rome, Italy
- Makra L. 1980; Large scale weather situations in Hungary and the periodical components of their time array. *Acta Climatologica, Acta Universitatis Szegediensis* 16/17, 1–4, 19–43
- Maller A., Németh E., Rimek I., Török L., Varga L. 1990; Areal precipitation distributions in several circulation patterns and medium range probabilistic precipitation forecasts. *Időjárás* 94, 108–123 (in Hungarian)
- Mika J. 1993; Effects of the large-scale circulation on local climate anomalies in relation to GCM-outputs. *Időjárás*, 97, 21–34
- Mika J., Szentimrey T., Domonkos P., Rimóczi-Paál A., Károssy C. 1994; Approximating climatic representativity for satellite samples of limited length. *Advances in Space Research* 14, (1) 125–(1)128
- Péczely G. 1957; *Grosswetterlagen in Ungarn*. Kleinere Veröffentlichungen der Zentralanstalt für Meteorologie, Budapest, 30



- Péczely G. 1961; Climatological description of macrosynoptic situation for Hungary. Minor Contributions of the Hungarian Meteorological Service, Budapest, 32 (in Hungarian)
- Péczely G. 1983; Catalogue of the macrosynoptic types for Hungary (1881–1983). Publications of the Hungarian Meteorological Service, Budapest, 53
- van Bebber W. J., Köppen W. 1895; Die Isobartypen des Nordatlantischen Ozeans und Westeuropas, ihre Beziehung zur Lage und Bewegung der Barometrischen Maxima und Minima. Arch. dtsch. Seewarte (Hamburg) 18 (4), 27 pp.



## COMMUNICATIONS

### Academic doctor in meteorology

The title *Doctor of Earth Sciences* has been awarded to **Dr. Géza Tóth**, retired director of the Meteorological Institute of Hungary. He defended his thesis in the presence of an invited jury at the Academy of Sciences, on September 23, 1993. The subject of his dissertation: *Development of the aerological research in Hungary – technical basis for modern weather-forecast*. The jury acknowledged his scientific achievements and pioneering work in this field by a unanimous 100 percent vote for his nomination as academic doctor.

### Dr. Univ. dissertation

P. SZÜCS

Department of Geophysics, University of Miskolc  
H-3515 Miskolc-Egyetemváros, Hungary

### Investigation of, water saturation of shaly sand hydrocarbon reservoirs according to the most frequent value inverse procedure

From economic aspect the knowledge of accurate water (or hydrocarbon) saturation is one of the most important points of hydrocarbon prospecting. Geophysical interpretation of well logs can supply very important parameters (porosity, saturation, thickness, lithology, clay content etc) for the exploration, but the exact determination of water saturation of reservoirs has not been solved satisfactorily. For the interpretation of measured data we use the response equations of different logs. First of all we have to concentrate on resistivity logs when we would like to calculate the saturations. Resistivity logs are the so-called saturation logs. Several resistivity response equations (VHS models, Waxman-Smiths, dual-water, ...) have been improved to explain the electrical properties of shaly sand reservoirs. On the other hand, we have to apply modern (robust) statistical procedures for data analyses and inversion, because the real datasets are rarely from Gaussian distributions. In this case we have the chance to make more accurate interpretation of well logs.

Nowadays the main statistical interpretation systems (Schlumberger-GLOBAL; Gearhart-ULTRA; Dresser Atlas-OPTIMA) make the interpretation separately for each depth level. In the dissertation new type interpretation system was

improved (first of all for water saturation) which uses not only the well log data of one depth level but also the well log data of longer section. In this case we can utilize the well known fact as valuable information that the adjoining (neighbouring) points in a geological layer are seldom independent from each other. For the computation an inverse algorithm was developed based on the most frequent value procedure. This robust statistical algorithm was introduced by his supervisor, Prof. F. Steiner. When this new system is applied, the results can be more accurate and reliable than the results of industry.

CS. NEMES

Department of Meteorology, Eötvös University  
H-1083 Budapest, Ludovika tér 2., Hungary

### **Drought and its impact on the corn crop yield**

#### **Drought**

Drought is a recurrent phenomenon of our climate, however, devastating droughts occurred very seldom due to the favorable climatic conditions of this area for the cultivation of certain crops, vegetables, fruits. For some of these species, one of the most significant limiting factors of production is the climatic water shortage, which just appears in the form of mild-to-severe drought episodes besides of being expressed in terms of overall agroclimatic potential. The limited severity of this climate hazard means that it leads to crop anomalies, which usually do not exceed one tenth of its expected amounts (taking also into account the effects of technological improvements). Apart from the agricultural consequences, effects on the water management or other impacts, meteorological droughts are characterized by their intensity, persistence and frequency by means of various drought parameters. In these term, the recent decade in Hungary is extraordinary: perhaps there were only two exception, namely in 1987 and 1988 when the precipitation amounts, their temporal and spatial distributions were adequate for the most part of the country. In some areas, the whole decade is considered drought with repeated crops failures. The meteorological literature is rich in works on the various aspects of the drought: synoptic situations leading to this phenomenon, phenomenological description of concrete drought incidences in form of case-studies, historical perspectives of prolonged drought events and their impacts, problems of predictability and many other sides of this subject have been addressed. Analyzing drought periods helps us to better understand and predict them, and to decrease our vulnerability to them. The drought periods are regularly investigated from these points of view.



Drought is a rather special hazard, partially because of its relatively slow emergence as compared to many other natural hazards. Drought also expresses some sort of imbalance, arising from either extraordinary climatic variations or human activities (overconsumption of water e.g. irrigation and/or public water; overgrazing and soil erosion etc.). In some cases an inappropriate government response to drought (or no response) may have more adverse consequences than the drought itself. Analysis of specific drought episodes can facilitate understanding of appropriate government responses.

One of the greatest problem in coping with drought is in defining the phenomenon. The broadly used definitions of drought are meteorological, agricultural and hydrological:

Meteorological Drought (MD) is the state of atmosphere for a longer period of time with considerably less than average precipitation amounts, which may influence agricultural and/or other socioeconomic activities; the precipitation anomaly is considered in its absolute value or it is contrasted to the water (moisture) demand for evaporation (evapotranspiration) and refill of the upper soil layers. Sometimes, the term of the precipitation deficit, the lasting negative anomaly of the humidity in the air.

Agricultural Drought (AD) occurs when the available soil moisture is inadequate to meet the evaporation demand by crops; it results in considerable crops yield losses (e.g., more than 10 percent of the expected average yield).

Hydrological Drought (HD) refers to a period of below-normal streamflow, depleted reservoir storage or runoff, which is caused by below-normal precipitation, intense evaporation and/or snow accumulation.

It is clear that, by using the principal drought definitions and the related indices, taking into account the areal scale, and analyzing the gradual extension/propagation of different types of droughts can be made monitoring and/or assessments of an actual drought episode (i.e., the way how a persistent precipitation anomaly can lead to HD and/or AD) and in this way its may open possibility to assess the possible and/or actual impact of the drought events.

In practice, are very useful the following indices: precipitation anomaly ( $P - \mu(P)$ ); relative precipitation anomaly ( $(P/\mu(P) * 100\%)$ ); potential water deficit ( $PE/P$ ); moisture anomaly index ( $MAI: P/PE$ ); relative evapotranspiration ( $ET/PE * 100\%$ ) etc...

#### *Drought events in the last 40 years*

##### MD - AD

1952: summer; country wide; high intensity

1962: summer halfyear; country wide; high intensity

1967: summer; country wide; high intensity

- 1968: winter-spring; West part of Hungary; high/moderate  
1973: winter-spring; country wide; high/moderate  
1974: winter-spring; East part of Hungary high intensity  
1976: summer; country wide; "cold-drought"; intensive  
1983: summer; country wide; high intensity  
1984: summer; country wide; "cold-drought"; intensive  
1986: August-September; county wide; high/moderate

#### MD - AD - HD

- 1968: winter halfyear, spring; country wide; high intensity  
1973: winter halfyear, spring; country wide; high intensity  
1975/76: from October to June; country wide High intensity  
1989/90: from October to August; country wide; one of the highest intensity in this century in Hungary  
1991/92: from December to August; country wide; one of the highest intensity in this century in Hungary

#### *Drought frequency and climatic change*

Several climate change scenarios indicate that with the global warming considerable decrease in the summer rainfall is expectable in our region. This would lead to increased drought hazard, however, the potential damaging effects on the plant cultivation is unclear (or at least, their assessment is rather complicated) because of many other factors, but could be very dangerous at all. That is why, are important the appropriate scientific analysis of the drought estimations and yield climate models. According to some results of trend analysis of long term Hungarian monthly precipitation and temperature sample demonstrate that there are significant decreasing sign of the estimated trend of precipitation and the relative soil moisture content. This process may lead to an increasing tendency in the occurrence of drought events in Hungary.

#### **Drought impacts on the corn crop yield**

Instead of the "natural" meteorological characteristics (averaged or cumulative values of such meteorological elements as, e.g., the temperature, precipitation or the photosynthetically available radiation), complex variables are developed and used in the yield-climate models, which models can estimate the extreme meteorological impacts (e.g. the drought impact). The most informative meteorological variables are specific for particular regions and crop species. Frequently, only a single parameter is used which expresses the natural (atmospheric) moisture supply because this is usually the most severe limiting (in Hungary) factor of the crop production (e.g. especially for corn crop yield). Dryness or wetness indices are used more often for such purposes.



*Trend estimation of the yield data series*

The basic Hungarian data comprise of the average corn yields for the period of 1921–1990. First of all, simple technological trend was fitted prior to the consideration of climatic effect. Linear, quadratic and piece-wise linear curves are chosen for the corn yield data. The 'break-point' (1960 for the Hungarian series, respectively) was found by means of minimizing standard error of the two-stage linear regression model.

It is expected that when the technological trend is properly filtered out from the sample series, the remaining values fluctuate more or less in the vicinity of a base line and these fluctuations are primarily governed by the meteorological factors.

*Drought impact estimation*

There were used some simple drought indices (e.g. relative soil moisture contents (RSM), potential water deficit (PE-P), BMDI and the moisture anomaly index (P/PE:MAI)) for the estimation of the wet/dry conditions of the Hungarian climate data series (1921–1990).

There was used a linear regression scheme for the estimation of the relation between the estimated corn yield trend ratio and the drought indices. There are found some high significant results for the mentioned relation.

There was an unsolved issue, that the above mentioned results are not sufficient for extreme events of the climate-yield relations. The main question is, how can we estimate the appropriate connections – between corn crop yield and weather/climate –, the process in the case of drought events.

That is the reason why, we made different subsets by the help of the climatic long time series and trend ratio of the estimated corn crop trend. There were selected different subsets which contain such elements, which have anomalies from different given thresholds. The thresholds could be composed on the one hand (in the case of climate factors) by statistically determined factors (e.g. standard deviation, lower/upper quartile etc.) and on the other hand (in the case of the crop yield series) by estimated trend ratio series (which sign the crop yield anomalies governed by the climate factors).

The results show, that the most useful subsets are composed by the trend ratio, where the ratio at least 20 % and 30 %. By these subsets may give the best estimation to the corn crop yield deficit in the case of drought impact.

By the help of the above mentioned method, we have got a sufficient estimation to the corn crops yield deficit for the drought impact on the crop yield in the year of 1990. and 1992., which are the following:

- 1990: the estimated corn crop yield deficit was 30 percent, the real deficit was 37 percent

- 1992: the estimated corn crop yield deficit was 42 percent, the real deficit was 40 percent

However, if we made the estimation by the original, whole sample, we would get the estimated crop yield deficit about above 20 percent than the real deficit.

## I. SZUNYOGH

Department of Meteorology Eötvös University,  
H-1083 Budapest, Ludovika tér 2., Hungary

### **Application of Hamiltonian mechanics to the investigation of numerical weather prediction models**

Numerical techniques have a long history of use in the theoretical investigation of non-linear problems since the appearance of digital computers. One of the most important strongly non-linear problems is the turbulence which governs atmospheric motion at different scales. However, the main problem is that only a finite group of the infinite number of acting interactions can be taken into consideration by numerical models. In addition, models not only restrict the number of interactions due to the reduction in the number of degrees of freedom, but they may also deform their structure. A frequently-asked question concerns the correct connection between the results of model computations and the real atmosphere. In other words, it seems reasonable to ask whether the models can be identified with a real physical system. If the answer is "yes", then what is the connection between this system and the real atmosphere?

A simple systematic method has been developed to investigate the laws of conservation for approximating model equations. The main purpose of this work is to identify these model equations as approximations of continuous Hamiltonian systems. If this identification is possible, the laws of conservation of the model system can be investigated as for a finite dimensional Hamiltonian system.

It has been shown that if the mathematical approximation is energy conservative, the discretized equations are formally equivalent to a finite dimensional Hamiltonian system in symplectic notation, even if the symplectic operator does not satisfy the Jacobi condition. Taking into account this fact the denomination of quasi-Hamiltonian system has been introduced for the energy conserving numerical approximations. The applicability of the general method has been verified by using five well-known (finite-difference and spectral) schemes as examples.

One of the most important consequences of the general theory described above is that the preservation the Casimir invariants for the quasi-Hamiltonian (energy con-



serving) discretized equations can be investigated as if it were a finite-dimensional Hamiltonian system.

Conservative quantities play an important role in the statistical mechanical behaviour of dynamical systems, and this statement is especially valid for the Casimir invariants. As a straightforward application of the quasi-Hamiltonian approach, it has been shown that if a numerical approximation to the shallow-water system of equations conserves the total energy and the potential enstrophy, the purely rotational interactions will satisfy the Liouville theory of statistical physics. It means that in the absence of divergent vorticity forcing (energy flow from the divergent part to the rotational part of the kinetic energy), the rotational kinetic energy evolves toward a two-dimensional equilibrium. The divergent forcing is controlled by the conservation of potential enstrophy, thus the two-dimensional approximation well describes the temporary spectral distribution of the rotational kinetic energy. In order to examine the acting processes, numerical experiments were carried out by a well-known kinetic energy and potential enstrophy conserving scheme, which takes into consideration the effect of the bottom topography.

### **In memoriam László Erdős**

László Erdős was born 22 October 1926 in Soltvadkert. He completed his university studies in 1951 in Eötvös Loránd University and got a university diplom in geography and history. He had been working for the Department of Meteorology in Eötvös Loránd University since 1951. He prepared his dissertation with the title of "Analyses of agrometeorological water-budget" and C. Sc was received in 1966.

His educational and scientific activity of high level was carried out in the field of agrometeorology, he was an acknowledged expert of heat- and water balance on a European level.

In 1972 a summarizing study had been made with the title of "Chapters of agrometeorology", which is widely used in both education and researches.

He had been guiding work of Agrometeorological Laboratory in Martonvásár-Erdőhátpuszta by making a use of his professional knowledge.

In 1992 he retired as associate professor of Department of Meteorology, however he kept on working and guiding agrometeorological activities carried out in the department till the day of his death 7 October 1993.

His memory will never fade.

**F. Rákóczi**